Title

Lysophosphatidylcholine acyltransferase 3-dependent phospholipid remodeling regulates lipid homeostasis and inflammation

Author

Rong, Xin

Publication Date

2015

Peer reviewed|Thesis/dissertation

UNIVERSITY OF CALIFORNIA

Los Angeles

Lysophosphatidylcholine acyltransferase 3-dependent phospholipid remodeling regulates lipid homeostasis and inflammation

A dissertation submitted in partial satisfaction of

the requirements for the degree Doctor of Philosophy

in Cellular and Molecular Pathology

by

Xin Rong

2015

ABSTRACT OF THE DISSERTATION

Lysophosphatidylcholine acyltransferase 3-dependent phospholipid remodeling regulates lipid homeostasis and inflammation

by

Xin Rong

Doctor of Philosophy in Cellular and Molecular Pathology

University of California, Los Angeles 2015

Professor Peter John Tontonoz, Chair

Phospholipids (PLs) are important structural components of biological membranes and precursors of numerous signaling molecules. The fatty acyl composition of PLs determines the biophysical characteristics of membranes. Multiple lines of evidence demonstrated that changes in fatty acyl composition could potentially affect the properties of proteins associated with membranes and influence the biological processes that occur on membranes. However, there is little understanding of how regulatory pathways control PL fatty acyl composition *in vivo* or how such regulation dictates physiological responses. In this work, we investigated the regulation of membrane fatty acyl composition by the Liver X Receptor (LXR)-Lysophosphatidylcholine Acyltranferase 3 (Lpcat3) pathway and its physiological or pathological relevance in lipid homeostasis and metabolic diseases.

In chapter 2, we define a nuclear receptor pathway for the dynamic modulation of membrane composition in response to changes in cellular lipid metabolism. Ligand activation of LXR preferentially drives the incorporation of polyunsaturated fatty acids into PLs through induction of the remodeling enzyme Lpcat3. Promotion of Lpcat3 activity decreases endoplasmic reticulum (ER) stress induced by saturated free fatty acids *in vitro* or by obesity and hepatic lipid accumulation *in vivo*. Conversely, Lpcat3 knockdown in liver exacerbates ER stress and inflammation. Mechanistically, Lpcat3 modulates inflammation both by regulating c-Src (Proto-oncogene tyrosine-protein kinase Src) and JNK (c-Jun N-terminal kinases) activation through changes in membrane composition and by affecting substrate availability for inflammatory mediator production. These results outline an endogenous mechanism for the preservation of membrane homeostasis during lipid stress and identify Lpcat3 as an important mediator of LXRs effects on metabolism.

In chapter 3, we show that Lpcat3 is a critical determinant of triglyceride secretion due to its unique ability to catalyze the incorporation of arachidonate into membranes. Mice lacking Lpcat3 in the intestine fail to thrive during weaning and exhibit massive enterocyte lipid accumulation and reduced plasma triglycerides. Mice lacking Lpcat3 in the liver show reduced plasma triglycerides, hepatosteatosis, and secrete lipid-poor very low density lipoprotein (VLDL) lacking arachidonoyl PLs. Mechanistic studies indicate that Lpcat3 activity controls membrane lipid mobility in living cells, suggesting a biophysical basis for the requirement of arachidonoyl PLs in lipidating lipoprotein particles. These data identify Lpcat3 as a key factor in lipoprotein production and illustrate how manipulation of membrane composition can be used as a regulatory mechanism to control metabolic pathways.

The dissertation of Xin Rong is approved.

Peter A Edwards

Tomas Ganz

Samuel W French

Steven J Bensinger

Peter John Tontonoz, Committee Chair

University of California, Los Angeles

2015

Table of Contents

Acknowledgements

Through the course of my Ph.D. study, I have been fortunate to have a number of people to guide me through the trails and hardships. Foremost, I would like to express my sincere gratitude to my advisor, Dr. Peter Tontonoz, for his continuous support and guidance through my graduate study and research, and for his patience, motivation, enthusiasm, and immense knowledge. Peter has always given me unprecedented freedom to explore my intellectual curiosity and fostered my capacity as an independent researcher. I have profoundly benefited from my association with him over the past 5 years, and will carry with me throughout my career.

I would also like to express my deep gratitude to the members of my dissertation committee, Drs. Peter Edwards, Steven Bensinger, Tomas Ganz and Samuel French, for their invaluable discussion, exceptional guidance, critiques and timely help. They have always offered me thorough and excellent feedback on my research and kept me on the right track in my career.

I would like to extent my heartfelt thanks to my fellow labmates, past and present, who made this lab such a wonderful place to work. Many of them spent countless hours to teach me the basic skills to survive in a biology lab when I was a fresh graduate student. More importantly, without their cheerful and compassionate support this work would have been much harder and taken much longer. In particular, I want to especially thank my "lab partner" Bo Wang who contributed significantly to the work presented here. Without his valuable input and persistent endeavor, this work would not have been possible. In addition, I would like to give my gratitude to Jie Gao, a diligent scientist and intimate friend, who has helped me a lot in the lab as well as in life. I also would like to thank Li Zhang, Cynthia Hong, Ito Ayaka, Elizabeth Tarling and Thomas Vallim for their countless support throughout my graduate study.

My thesis would not be possible without all the collaborators: Dr. David Ford, who helped us with the lipidomics analysis; Dr. Steven Young, who provided us many insightful advices on the research of lipoprotein biology; Dr. Enrico Gratton, who performed the biophysics studies; and all other collaborators who made contributions to the projects discussed here.

Finally, I would like to thank my parents and my girlfriend. It is their unconditional love that makes all of this possible and meaningful.

This work is support by the pre-doctoral fellowship from the American Heart Association.

Chapter 2 is a modified reprint of Xin Rong, Carolyn J. Albert, Cynthia Hong, Mark A. Duerr, Brian T. Chamberlain, Elizabeth J. Tarling, Ayaka Ito, Jie Gao, Bo Wang, Peter A. Edwards, Michael E. Jung, David A. Ford, and Peter Tontonoz, LXRs regulate ER stress and inflammation through dynamic modulation of membrane phospholipid composition. Cell Metab. 2013 Nov 5;18(5):685-97. doi: 10.1016/j.cmet.2013.10.002 and appears with the permission of Elsevier Inc.

Chapter 3 is a modified reprint of Xin Rong, Bo Wang, Merlow M Dunham, Per Niklas Hedde, Jinny S Wong, Enrico Gratton, Stephen G Young, David A Ford, Peter Tontonoz, Lpcat3-dependent production of arachidonoyl phospholipids is a key determinant of triglyceride secretion. Elife. 2015 Mar 25;4. doi: 10.7554/eLife.06557 and appears with the permission of Creative Commons Attribution License.

Biographical Sketch/Bibliography

Institution & Location	Date Attended	Degree	Conferred	Field of study
University of California, Los Angeles (Los Angeles, CA)	2009-present	(Ph.D. Candidate)		Cellular and Molecular Pathology
Tsinghua University (Beijing, China)	2005-2009	BSc	2009	Biological Science

A. Positions and Honors

Position and members

2009 to present Graduate Student Researcher; PI: Peter Tontonoz Ph.D. M.D.; Department of Pathology and Laboratory Medicine, School of Medicine, UCLA
2013 to 2014 Teaching Assistant, Life Science, UCLA
2011 to 2012 Teaching Assistant, Department of Molecular, Cellular, and Developmental Biology, UCLA

Honors & Awards

2013 to present American Heart Association Pre-doctoral Fellowship
2015 eLife Lectureship at 2015 DEUEL conference
2014 National Heart, Lung and Blood Scholarship at Keystone Symposia on Innate Immunity, Metabolism and Vascular Injury
2014 Poster Award at 2014 DEUEL conference
2012 Poster Award at 2012 DEUEL conference
2012 UCLA Nonresident Training Award
2008 International Genetically Engineered Machine Competition Winner
2006-2009 National Endeavor Fellowship

B. Peer Reviewed Publications

1. **Rong X**, Wang B, Dunham MM, Hedde PN, Wong JS, Gratton E, Young SG, Ford DA, Tontonoz P. Lpcat3-dependent production of arachidonoyl phospholipids is a key determinant of triglyceride secretion. Elife. 2015 Mar 25;4.

2. Warrier M, Shih DM, Burrows AC, Ferguson D, Gromovsky AD, Brown AL, Marshall S, McDaniel A, Schugar RC, Wang Z, Sacks J, **Rong X**, de Aguiar Vallim T, Chou J, Ivanova PT, Myers DS, Brown HA, Lee RG, Crooke RM, Graham MJ, Liu X, Parini P, Tontonoz P, Lusis AJ, Hazen SL, Temel RE, Brown JM. The TMAO Generating Enzyme Flavin

Monooxygenase 3 is a Central Regulator of Cholesterol Balance. Cell Rep. Cell Rep. 2015 Jan 14. pii: S2211-1247(14)01065-1

3. Sallam T, Ito A, **Rong X**, Kim J, van Stijn C, Chamberlain BT, Jung ME, Chao LC, Jones M, Gilliland T, Wu X, Su GL, Tangirala RK, Tontonoz P, Hong C. The macrophage lipopolysaccharide binding protein gene is an LXR target that promotes macrophage survival and atherosclerosis. J Lipid Res. 2014 Mar 26;55(6):1120-1130

4. **Rong X**, Albert CJ, Hong C, Duerr MA, Chamberlain BT, Tarling EJ, Ito A, Gao J, Wang B, Edwards PA, Jung ME, Ford DA, Tontonoz P. LXRs regulate ER stress and inflammation through dynamic modulation of membrane phospholipid composition. Cell Metab. 2013 Nov 5;18(5):685-97

5. Hong C, Bradley MN, **Rong X**, Wang X, Wagner A, Grijalva V, Castellani LW, Salazar J, Realegeno S, Boyadjian R, Fogelman AM, Van Lenten BJ, Reddy ST, Lusis AJ, Tangirala RK, Tontonoz P. LXRα is uniquely required for maximal reverse cholesterol transport and atheroprotection in ApoE-deficient mice. J Lipid Res. 2012 Jun;53(6):1126-33

6. Hong C, Kidani Y, A-Gonzalez N, Phung T, Ito A, **Rong X**, Ericson K, Mikkola H, Beaven SW, Miller LS, Shao WH, Cohen PL, Castrillo A, Tontonoz P, Bensinger SJ. Coordinate regulation of neutrophil homeostasis by liver X receptors in mice. J Clin Invest. 2012 Jan 3;122(1):337-47

Chapter 1: Introduction

Background

Phospholipids (PLs) are major structural components of biological membranes and precursors of numerous signaling molecules. In most cellular organisms, PLs form lipid bilayers to compartmentalize living cells, form intracellular organelles, and provide platforms for a wide variety of physiological processes. PLs can also act as substrates for the generation of diverse bioactive signaling molecules.

PLs in eukaryotic cellular membranes have remarkable diversity. Hundreds of PLs has been detected in eukaryotic cells (Dowhan, 1997; Wenk, 2005). The identity of a PL is determined by its backbone (either glycerol or sphingosine), the polar head group and the fatty acyl chains linked to it. The PL composition and its ratio to sterols determine the biophysical properties of membranes (Holthuis and Menon, 2014; Spector and Yorek, 1985). Of particular interest here is the PL fatty acyl composition in cellular membranes. Membrane fatty acyl composition among tissues, cells or intracellular organelles is not only significantly different but also tightly maintained (Antonny et al., 2015; Holthuis and Menon, 2014). Previous *in vitro* biochemical and biophysical studies have demonstrated that changes in PLs fatty acyl composition could affect the function of proteins associated with membranes and impact the biological processes that occur on them, which suggests that the tightly regulated membrane fatty acyl composition may serve specific biological functions.

The work presented here dissects the endogenous regulatory mechanisms by which membrane fatty acyl composition is regulated and elucidates its physiological functions *in vivo*. The relevant background material is introduced in this chapter.

Phospholipid

Phospholipid diversity and membrane properties

A PL consists of a polar or charged phosphate head group and two hydrophobic fatty acyl chains linked to a glycerol or a spingosine backbone. This bipolar structure enables PLs to spontaneous associate into lipid bilayers in aqueous solution, which is the basis for biological membranes. PLs are classified into phosphatidylcholine (PC), phosphatidylethanolamine (PE), phosphatidylserine (PS), phosphatidic acid (PA), phosphatidylinositol (PI), cardiolipin, and sphingophospholipids. Furthermore, each PL class contains a variety of molecular species defined by the length and the degree of saturation of their fatty acyl chains.

Both head group and fatty acyl chain composition determine the biophysical properties of membranes (de Kroon et al., 2013) (Fig. 1-1). Previous studies have focused more on the function of PL head group in cellular membranes. PL polar head groups affect the electric charge of the membrane and also serve as the binding dock for many signaling proteins (Lemmon, 2008). The function of fatty acyl chain composition, especially physiological function, is less well understood. PL fatty acyl chain composition determines various membrane biophysical properties, including bilayer thickness, lipid packaging density and fluidity, capability of membrane bending, etc (Bigay and Antonny, 2012; Sharpe et al., 2010) (Fig. 1-1). In general, membranes containing more unsaturated PLs show lower packing density and higher fluidity, due to the conformational plasticity of their unsaturated fatty acyl chain (Koynova and Caffrey, 1998), whereas membranes composed of long chain saturated PLs have a thicker bilayer with more ordered and rigid structure (Slotte, 2013; van Meer et al., 2008). Membrane curvature is strongly affected by PL shape (Bigay and Antonny, 2012). PLs with a small area ratio of polar head to acyl chain induce negative curvature, such as polyunsaturated PE, whereas lipids with a

bigger head to chain ratio induce positive curvature, such as lysophosphatidylcholine (Lyso-PC) (Frolov et al., 2011) (Fig. 1-1).

Thanks to the advances in lipidomics analytical technologies, scientists now are able to profile PL fatty acyl composition of various biological membranes (Brugger, 2014). These studies showed a remarkable diversity of membrane PLs in eukaryotic cells. Hundreds of PL species have been identified in eukaryotic cell membranes at different abundance (Dowhan, 1997; Wenk, 2005). Among these PLs, PC is the most commonly used building block for eukaryotic cellular membranes, which accounts for more than 50% of the PLs. In addition, the PL fatty acyl composition among different organisms, tissues, cells and organelles varies significantly (Keenan and Morre, 1970; Salem et al., 2001; Schneiter et al., 1999). For example, in eukaryotic cells, the fatty acyl chain saturation gradually increases along the endoplasmic reticulum (ER), Golgi and plasma membrane secretory pathway (Keenan and Morre, 1970; Schneiter et al., 1999). Neurons contain more of arachidonoyl and docosahexaenoyl phospholipids in their synaptic membranes, whereas the cell body membranes are composed of less unsaturated linoleic PLs (Salem et al., 2001).

The PL fatty acyl composition also changes during development or under different physiological/pathological conditions (Sampaio et al., 2011). It has long been known that the embryonic development of brain is accompanied by the enrichment of ω-6 and ω-3 polyunsaturated PLs (Martinez, 1992). Defects in this process can seriously impair the formation of blood brain barrier (Ben-Zvi et al., 2014; Nguyen et al., 2014). A recent study implicates that the amount of arachidonoyl-PC oscillates during the cell cycle (Koeberle et al., 2013). Last but not least, membrane PL saturation increases in several cancer cells and tissues (Guo et al., 2014; Naguib et al., 2015).

The distinct spatiotemporal membrane PL composition strongly suggests that membrane lipid composition is subjected to complicated regulatory mechanisms. However, the metabolic network that controls these processes is not entirely clear, and we do not know how the unique membrane composition contributes to precise biological functions. Nevertheless, the preservation of distinctive membrane lipid composition among different intracellular organelles or cell types *in vivo* suggests that membrane lipid composition may serve a profound role in defining cell/organelle identity and function.

Phospholipid biogenesis and remodeling

The fatty acyl groups in PL are not only highly diverse but also distributed in an asymmetric manner. Saturated fatty acids are normally found at the sn-1 site, whereas monounsaturated and polyunsaturated fatty acids are usually linked to the sn-2 site. After being activated by acyl-CoA synthetases (ACSLs), fatty acids from diet or de novo lipogenesis are esterified to PLs via two major pathways. One is the de novo synthesis pathway (also known as Kennedy pathway) (Kennedy and Weiss, 1956) (Fig. 1-2), where PA is synthesized from glycerol-1-phosphate by GPAT and LPAAT. PA is then converted to two intermediate molecules, diacylglycerol (DAG) which is precursor for the synthesis of PC, PE and PS, and cytidine diphospho-DAG which is responsible for the biogenesis of PI and cardiolipin (Kent, 1995). The other pathway is the PL remodeling pathway (also known as Land's cycle) (Lands, 1958) (Fig. 1-2), where the fatty acyl chain at the sn-2 site is substituted by a new acyl group through the coordinated actions of phospholipase A2 (PLA2) and lysophospholipid acyltransferase (LPLAT). In this process, the fatty acyl group at the sn-2 site is first hydrolyzed by PLA2 to generate a lysophospholipid. Then, LPLAT transfers another fatty acyl CoA to the sn-2 site and generates a

PL with a new set of fatty acyl groups. It is acknowledged that there is another minor PL remodeling pathway, which is catalyzed by a group of enzymes named transacylase (Yamashita et al., 2014). Biochemical studies suggest that the diversity and asymmetric distribution of fatty acyl groups in PL (except PA) cannot be fully explained by the PL de novo synthesis pathway, probably because many enzymes in the de novo synthesis pathway lack the specificity for fatty acyl substrates. For example, radioactive labeling pulse and chase experiments showed that the fatty acyl composition of newly synthesized PCs in the rat heart was different from that of endogenous PC (Arthur and Choy, 1984). In contrast, the LPLATs mainly involved in the remodeling pathways (with the exception of LPAATs, which also participate in de novo synthesis pathway) have high substrate specificity and are believed to play a major role in the determination of the acyl chain composition of PLs (Shindou et al., 2013).

Although the PL remodeling process was proposed more than 50 years ago and the LPLAT activity has been discovered in different tissues through biochemical analyses, the molecular identity of the acyltransferases involved in this process were discovered only recently (Shindou et al., 2013). Acyltransferases in PL remodeling process mainly belong to two protein families: the AGPAT family and the MBOAT family. There are more than 10 LPLATs cloned from mouse genome (Shindou et al., 2013). Different enzymes have different substrate preference and expression pattern (Chen et al., 2006; Harayama et al., 2008; Hishikawa et al., 2008; Nakanishi et al., 2006; Zhao et al., 2008). However, the physiological relevance of these enzymes for endogenous fatty acyl composition and biological function are largely unknown.

LPCAT

Several acyltransferases cloned recently posses LPCAT activities, including LPCAT1, LPCAT2, LPCAT3, and LPCAT4. LPCAT1 and LPCAT2 belong to the AGPAT family, and LPCAT3 and LPCAT4 belong to the MBOAT family. Initial characterization of these enzymes showed that they have different substrate preference and tissue expression pattern, suggesting their different biological function *in vivo* (Shindou et al., 2013).

LPCAT1 prefers saturated fatty acyl-CoA as substrates and the major lipid product is dipalmitoyl-PC, which is the essential component of pulmonary surfactant in lung. Consistent with its enzymatic function, LPCAT1 is mainly expressed in lung, especially in alveolar type II cells (Chen et al., 2006; Nakanishi et al., 2006). A genetic knockout mouse model demonstrated that LPCAT1 is required for the production of surfactant in lung *in vivo* and loss-of-LPCAT1 could cause the early onset of acute lung injury (Harayama et al., 2014).

LPCAT2 is a lyso-PAF and lyso-PC acetyltransferase. It is highly expressed in inflammatory cells and induced by immune stimuli, such as lipopolysaccharide (LPS) (Shindou et al., 2007). It was reported that LPCAT2 is also regulated at post-translational level through phosphorylation by p38 MAP kinase in response to inflammatory stimulation (Shindou et al., 2005). Phosphorylation of LPCAT2 activates its enzymatic activity and induces the production of PAF.

LPCAT3 is ubiquitously expressed in various tissues, with especially high expression in intestine, liver, fat, and kidney. *In vitro* biochemical analysis suggests that LPCAT3 prefers polyunsaturated fatty acyl-CoA (18:2 CoA and 20:4 CoA) and saturated lyso-PC as substrates. Besides the LPCAT activity, LPCAT3 also shows minor LPEAT and LPSAT activities. In cells, LPCAT3 is primarily located on the ER membrane, which is the major site for PL remodeling

(Hishikawa et al., 2008; Zhao et al., 2008). It has been reported that LPCAT3 is involved in the arachidonic acid metabolism in immune cells (Perez-Chacon et al., 2010). However, all of the studies regarding the function of LPCAT3 were performed in *in vitro* cell culture systems. The endogenous function of this enzyme remains unknown.

Preliminary characterization of LPCAT4 showed that it is highly expressed in epididymis, brain, testis and ovary, and prefers 18:1-CoA as a substrate (Hishikawa et al., 2008). Very little data has been shown about the physiological relevance and the regulation of these enzymes *in vivo*.

Influence of PL fatty acyl chain composition on protein functions

Ever since the fluid mosaic model of membrane structure was proposed in 1972 by Singer and Nicolson (Singer and Nicolson, 1972), scientists have been asking a basic question: do lipids in the membrane affect the function of membrane proteins? Using *in vitro* biochemical or biophysical systems, researchers have demonstrated that modification of membrane PL fatty acyl composition does affect the function of membrane proteins (Spector and Yorek, 1985). For example, studies have shown that enrichments of 18:2 and 20:4 in the plasma membrane phospholipids increase the Na^++K^+-ATPase activity in several cell types (Solomonson et al., 1976; Szamel and Resch, 1981). Furthermore, recent biochemical study suggests that increased ER membrane saturation could directly activate the dimerization of the membrane-span ER stress sensors, IRE1a and PERK, independent of the accumulation of unfolded proteins in the lumen of ER (Volmer et al., 2013). Interestingly, unsaturated fatty acid treatment prevents the activation of ER stress by membrane saturation (Wei et al., 2006).

PL fatty acyl composition not only affects membrane protein activity, but also regulates biological processes associated with membranes. A recent biophysical study showed that polyunsaturated PLs facilitate endocytosis through reducing the energy required by membrane deformation and fission (Pinot et al., 2014). PL fatty acyl composition also affects the assembly of membrane subdomains. Incorporation of saturated fatty acids into plasma membrane PL helps to recruit c-Src kinase to lipid raft domains and contributes to the activation of JNK signaling cascades in adipocytes (Holzer et al., 2011).

To date, most studies of the effects of PL fatty acyl composition on biological systems have utilized *in vitro* biochemical assays or treated cells with large amount of exogenous lipids, due to the difficulty of directing specific changes in membrane composition in living animals. While these studies implicated that changes in PL fatty acyl composition could affect membrane protein function, they provided no information as to whether such effects actually occurred in animal *in vivo*. Therefore, there are critical questions to be answered: is membrane fatty acyl composition dynamically regulated *in vivo?* Does the dynamical modulation of the fatty acyl composition dictate physiology *in vivo*? These questions will be discussed in this study.

Phospholipid derived lipid-signaling molecules

PLs are not only structural components of biological membranes, but also serve as the precursors of numerous bioactive lipid mediators, including eicosanoids, lysophosphatidic acid (LPA), and DAG. Arachidonic acid is the precursor of most eicosanoids, such as prostaglandin, thromboxane and leukotriene. In cells, the majority of arachidonic acids are stored at the sn-2 site in PLs (Brash, 2001). In response to intracellular or extracellular stimuli, arachidonic acids are released by PLA_2, and enter into the eicosanoid synthesis cascades (Leslie, 2004). Therefore,

the availability of arachidonic acid in membrane PLs will impact the generation of eicosanoids. While PLA_2 hydrolyzes the sn-2 acyl chain, it also generates a Lyso-PL, which is another bioactive lipid mediator. For instance, Lyso-PC can act as a chemokine to recruit immune cells to inflammatory sites. Lyso-PA is well-known for its roles in cell proliferation and immunity (Sevastou et al., 2013). The biogenesis of these molecules has been intensely studied. However, how membrane PL composition impacts these signaling pathways is not entirely clear.

Liver X Receptors

Nuclear receptors are ligand activated transcription factors that exert diverse effects on cellular and physiological functions through regulation of target gene expression (Chawla et al., 2001). The first member of this superfamily is estrogen receptor, discovered in 1958 (Chambon, 2004). However, the rapid growth of the field came in the mid-1980s, when the steroid receptors were cloned and found to exhibit extensive sequence similarity. Based on the sequence homology, many other nuclear receptors were subsequently cloned from human genome (Maglich et al., 2001). There are a large number of nuclear receptors that were initially cloned without knowing their endogenous ligands, and therefore named orphan nuclear receptors. Several of them became "adopted" after their physiologic ligands were identified in the past 30 years. Today, 48 nuclear receptors have been reported in human genome (Maglich et al., 2001). They regulate a wide variety of biological processes including reproduction, development, immunology, and of particular interest here lipid metabolism (Evans, 2004). A group of adopted orphan nuclear receptors have been show to dictate a feedback regulatory loop to maintain lipid homeostasis in cells and animals (Chawla et al., 2001). This group includes the fatty acid sensor

peroxisome proliferator-activated receptors (PPARs), the sterol sensor liver X receptors (LXRs), and the bile acid sensor farnasoid X receptors (FXRs).

Mammalian cells contain two isoforms of LXRs encoded by the genes NR1H3 (LXRα) and NR1H2 (LXRβ) (Lu et al., 2001; Willy et al., 1995). The two isoforms share high protein sequence homology. Both of them contain an NH_2-terminal region that harbors a ligand-independent transcriptional activation domain (AF-1); a core DNA-binding domain that recognizes a conserved DR4 motif 'AGGTCAnnnnAGGTCA' (where 'n' refers to any nucleotide); a ligand-binding domain and a ligand-dependent transcriptional activation domain (AF-2) at the COOH-terminus (Chawla et al., 2001). The physiological ligands for LXRs are oxysterols and certain intermediates in cholesterol synthetic pathway, such as desmosterol (Lehmann et al., 1997; Yang et al., 2006). Strong pharmacological activation can also be achieved with synthetic agonists, such as GW3965 (Collins et al., 2002). The transcriptional activity of LXRs requires the formation of heterodimers with retinoid X receptors (RXRs). In the absence of a bound ligand, the LXR-RXR heterodimer is believed to remain bound to the promoter region of its target genes in complex with co-repressors, thus inhibiting target gene activation. Upon ligand binding, the conformation of the LXR-RXR complex is altered, leading to the substitution of nuclear receptor co-repressors with the co-activators (Glass and Rosenfeld, 2000; Tontonoz, 2011). Due to the high structural similarity, LXRα and LXRβ also share most of their target genes. The differential physiological function of the two isoforms is attributed to their distinct expression patterns *in vivo*. LXRα is selectively expressed in metabolically active tissues and cell types such as liver, intestine, adipose, adrenals, kidney and macrophages, whereas LXRβ is ubiquitously expressed in most tissues (Annicotte et al., 2004). Activation of

LXRs exerts diverse effects on cellular and physiological functions, including cholesterol homeostasis, lipogenesis and immunology (Fig. 1-3).

Regulation of reverse cholesterol transport

The fact that oxysterols act as endogenous ligands for LXRs suggests that these nuclear receptors may play a role in cholesterol homeostasis. Research in the past two decades demonstrated that LXRs are the major regulators in reverse cholesterol transportation through promoting cholesterol efflux, transportation, catabolism and extraction (Zelcer and Tontonoz, 2006). These functions are achieved by coordinated regulation of target gene expression in different tissues. LXRs promote cholesterol efflux from peripheral cells through induction of the expression of members of the ABC membrane transporter protein family, such as ABCA1 and ABCG1 (Cavelier et al., 2006). ABCA1 is a plasma membrane protein that facilitates the transport of cholesterol from plasma membrane to receptor proteins, including ApoAI. Lack of ABCA1 activity has been shown to cause Tangiers disease in human, which is characterized by the absence of HDL and premature coronary artery disease (Aiello et al., 2002; Bodzioch et al., 1999). ABCG1 is an intracellular sterol transporter that forms homo-dimers on the surface of endosomes and facilitates the redistribution of sterols away from the endoplasmic reticulum (Kennedy et al., 2005). In contrast to ABCA1, ABCG1 mediates cholesterol efflux to HDL rather than ApoAI (Kennedy et al., 2005; Wang et al., 2004). LXRs also promote the excretion of cholesterol from hepatocytes and enterocytes by inducing the expression of ABCG5 and ABCG8 (Yu et al., 2002a; Yu et al., 2002b). This process is also reinforced by the induction of the major bile acid synthetic enzyme Cyp7A1 by LXRs (Zelcer and Tontonoz, 2006).

In addition to promoting cholesterol efflux, LXRs also prevent the uptake of cholesterol through the induction of an E3 ubiquitin ligase IDOL (inducible degrader of the LDLR). LXR activation induces the expression of IDOL, which in turn ubiquitinates the LDLR, thereby targeting it for degradation and limiting cholesterol uptake (Zelcer et al., 2009).

In complement to their role in reverse cholesterol transport, LXRs induce the expression of many apolipoproteins that may serve as cholesterol acceptors, including APOE, APOC1, APOC2 and APOC4 (Mak et al., 2002) and lipoprotein-remodeling enzymes, including phospholipid transfer protein (PLTP) and cholesteryl ester transfer protein (CETP), which facilitates the transportation of PLs and cholesterol from triglycerides rich lipoproteins to HDL (Laffitte et al., 2003b).

Regulation of fatty acid synthesis and glucose metabolism

Besides the central role in cholesterol homeostasis, LXRs also regulate lipogenesis *in vivo*. Activation of LXRs upregulates a powerful lipogenesis regulator SREBP1c, which drives the expression of multiple enzymes involved in hepatic lipogenesis biochemical pathway (Repa et al., 2000). LXRs also directly activate several genes involved in fatty acid synthesis, including fatty acid synthase and stearoyl-CoA desaturase 1 (Joseph et al., 2002a). Consistent with the transcription regulation, treatment of mice with synthetic LXR agonists promotes triglyceride synthesis in liver, stimulates very-low-density lipoprotein (VLDL) production and, at least transiently, raises plasma triglyceride levels (Schultz et al., 2000).

Glucose metabolism is also impacted by LXR activity. Recent work suggests that loss of LXR activity benefits diabetes in a genetic engineered mouse model. Deletion of both LXRα and LXRβ on the *ob/ob* mouse background increases hepatic insulin sensitivity due to the reduced

steatosis and adipocyte insulin sensitivity probably due to the activation of PPARγ (Beaven et al., 2013). Paradoxically, the short-term treatment of diet-induced obese mice with an LXR agonist has also been reported to improve glucose tolerance through suppression of hepatic gluconeogenesis and increase in glucose uptake into adipose tissues through GLUT4 (Laffitte et al., 2003a). However, long-term agonist treatment causes sever hepatic steatosis and leads to liver damage.

Anti-inflammatory effects of LXRs

In addition to the essential role in lipid metabolism, LXRs have profound anti-inflammatory effects. Activation of LXRs antagonizes inflammatory gene expression triggered by stimuli such as LPS or cytokines (Joseph et al., 2003). It was postulated that the anti-inflammatory effects are mediated by a mechanism termed "trans-repression". According to this mechanism, LXRs become SUMOylated in response to LXR agonists and SUMOylated LXR monomer stabilizes repressive nuclear complexes on the promoters of inflammatory genes (Ghisletti et al., 2007). However, the "trans-repression" model was established with an overexpression cell model, which renders its physiological relevance to be tested. Given that LXRs are master regulators of lipid metabolism and studies in various systems have shown the link between lipid overload and inflammatory response, it would be reasonable to hypothesize that there might be a connection between the function of LXRs in lipid metabolism and anti-inflammation. Unpublished data from our lab suggest that the anti-inflammatory properties of LXRs can be directly tied to changes in the cholesterol content of lipid bilayers and consequently are mediated by actions of target genes, such as ABCA1. Whether other mechanisms are also employed by LXRs to suppress inflammation needs further study.

Interestingly, LXRs are also involved in other aspects of immune responses. Our lab has shown that LXRs are required for the appropriate response to microbial pathogen infections through regulation of macrophage apoptosis (Joseph et al., 2004). We also showed that LXRs impact the proliferation of T cells and neutrophils homeostasis (Bensinger et al., 2008).

LXRs and Human Disease

The important roles of LXRs in cholesterol homeostasis and anti-inflammation have attracted considerable attention for pharmacologic manipulation. One of the major focuses is atherosclerosis, which is driven by hypercholesterolemia and inflammation in the artery lesion. A number of studies have proved the protective effects on atherosclerosis by LXR activation (Bradley et al., 2007; Joseph et al., 2002b). The beneficial effects of LXR agonists were observed even without the change of serum cholesterol level, suggesting that the beneficial effects are at least partially due to the action of LXRs on artery (Teupser et al., 2008). Another potential therapeutic application of LXR agonists is Alzheimer's disease. The etiology of Alzheimer's disease is postulated to be related to dysregulation of lipid metabolism and inflammatory pathways in brain. Observations that ABCA1, APOE and LDLR influenced the development of Alzheimer's disease in mouse models suggest a potential role of LXRs in Alzheimer's disease pathogenesis and therapy (Kim et al., 2009; Wahrle et al., 2005). Treatment of LXR agonist in mice reduced amyloid-β load and improved memory capacity (Zelcer et al., 2007). In addition, LXR signaling has been proposed to influence diverse disease processes including asthma, liver fibrosis and steatosis, diabetes, and cancer.

However, the major obstacle in the clinical development of LXR-based therapy is the undesired pleotropic effects caused by the LXR agonists, such as hypertriglyceridemia and hepatic steatosis. Several approaches have been proposed to address these complications. One is to develop LXRβ-selective agonists, based on the observation that LXRα is the predominant isoform in liver and drives the lipogenesis and hypertriglyceridemia upon ligand activation. However, due to high homology between LXRα and LXRβ, very few LXRβ-selective agonists have been discovered and they showed poor tolerability in clinical trials despite bypassing hepatic lipogenesis. Another strategy for pharmacologically intervening LXR signaling is to directly target LXR downstream genes, since it provides an opportunity to only targeting a single aspect of the LXR signaling program (Hong and Tontonoz, 2014).

Figure legend

Figure 1-1. Membranes lipid composition determines its biophysical properties

Physical membrane properties are influenced by lipid composition. Fluidity is promoted by lipids with short, unsaturated fatty acids. The double bonds introduce kinks that lower the packing density of the acyl chains and inhibit transition of the membrane from a fluid to a solid gel phase. Phospholipids typically pair a saturated with an unsaturated fatty acid, which is an elegant means to prevent the two types of acyl chains from phase separating when the temperature drops. Thickness is promoted by acyl-chain length and sterols, which order and stretch the acyl chains. High levels of packing defects are found in lipids with unsaturated acyl chains and small head groups. Surface charge is determined by the presence of anionic lipids such as PS and PI. Curvature is determined by lipid shape. Lipids with a small area ratio of polar head to acyl chain (creating a cone shape) induce negative curvature, lipids with an equal head to chain ratio (creating a cylinder shape) are neutral, and those with a much larger head compared with the acyl chain area (creating an inverted cone shape) induce a positive curvature. PtdCho, phosphatidylcholine; PtdEtn, phosphatidylethanolamine; SM, sphingomyelin. (Reprinted by permission from Macmillan Publishers Ltd: Nature (Holthuis and Menon, 2014), copyright (2014), license: 3621000880907)

Figure 1-2. Phospholipid synthesis and remodeling pathways in mammals

Biosynthetic pathways of glycerophospholipids. Upper panel shows the de novo synthesis (green lines) and the fatty acid remodeling (magenta lines) of glycerophospholipids. LPLATs involved in each reacylation of the lysophospholipids are indicated. Lower panel shows an example of the fatty acid remodeling of PC. In this reaction, PLA2s release fatty acid (arachidonic acid) from

the sn-2 position of PC, while LPCATs catalyze the reacylation at the sn-2 position of LPC using acyl-CoA (arachidonoyl-CoA). PGP, phosphatidylglycerolphosphate. (Reprinted by permission from The Journal of Biological Chemistry (Hishikawa et al., 2014) license: CC-BY license)

Figure 1-3. Coordinated effects of LXRs on metabolism

Liver X receptors (LXRs) mediate effects on multiple metabolic pathways in a tissue-specific manner. In peripheral cells such as macrophages, LXR induces expression of IDOL (inducible degrader of the low-density lipoprotein receptor (LDLR)), which promotes the proteasome-mediated degradation of LDLR and thus results in reduced LDL uptake into the cell. In peripheral cells, LXR also increases ARL7 (ADP-ribosylation factor-like 7), ABCA1 (ATP-binding cassette transporter A1) and ABCG1 expression, promoting the movement of cholesterol to the plasma membrane and cholesterol efflux and transfer to lipid-poor molecules such as apolipoprotein AI (APOAI) and pre-β high-density lipoprotein (HDL), thus increasing plasma HDL levels. APOE promotes the return of HDL to the liver. Furthermore, in the liver, LXR promotes cholesterol conversion to bile acids by cytochrome P450 7A1 (CYP7A1). It also promotes fatty acid synthesis via induction of sterol-regulatory element-binding protein 1C (SREBP1C) and its targets, fatty acid synthase (FAS), acetyl CoA carboxylase (ACC) and steroyl CoA desaturase 1 (SCD1). Secretion of triglyceride-rich very low-density lipoproteins (VLDLs) by the liver transports lipids to peripheral tissues, including adipose tissue, where the action of lipoprotein lipase (LPL) liberates fatty acids from VLDL. In adipose tissue, LXR regulates the expression of lipid-binding and metabolic proteins such as APOD and SPOT14 and may promote the breakdown of fatty acids through their β-oxidation (which occurs in mitochondria). LXR also promotes glucose uptake via induction of glucose transporter type 4

(GLUT4). Finally, in the intestine, LXR inhibits cholesterol absorption by inducing the expression of the ABC transporters ABCG5 and ABCG8 and possibly ABCA1. (Reprinted by permission from Macmillan Publishers Ltd: Nature Reviews Molecular Cell Biology, copyright (2012), license: 3621071505638)

Figure 1-1. Membranes lipid composition determines its biophysical properties

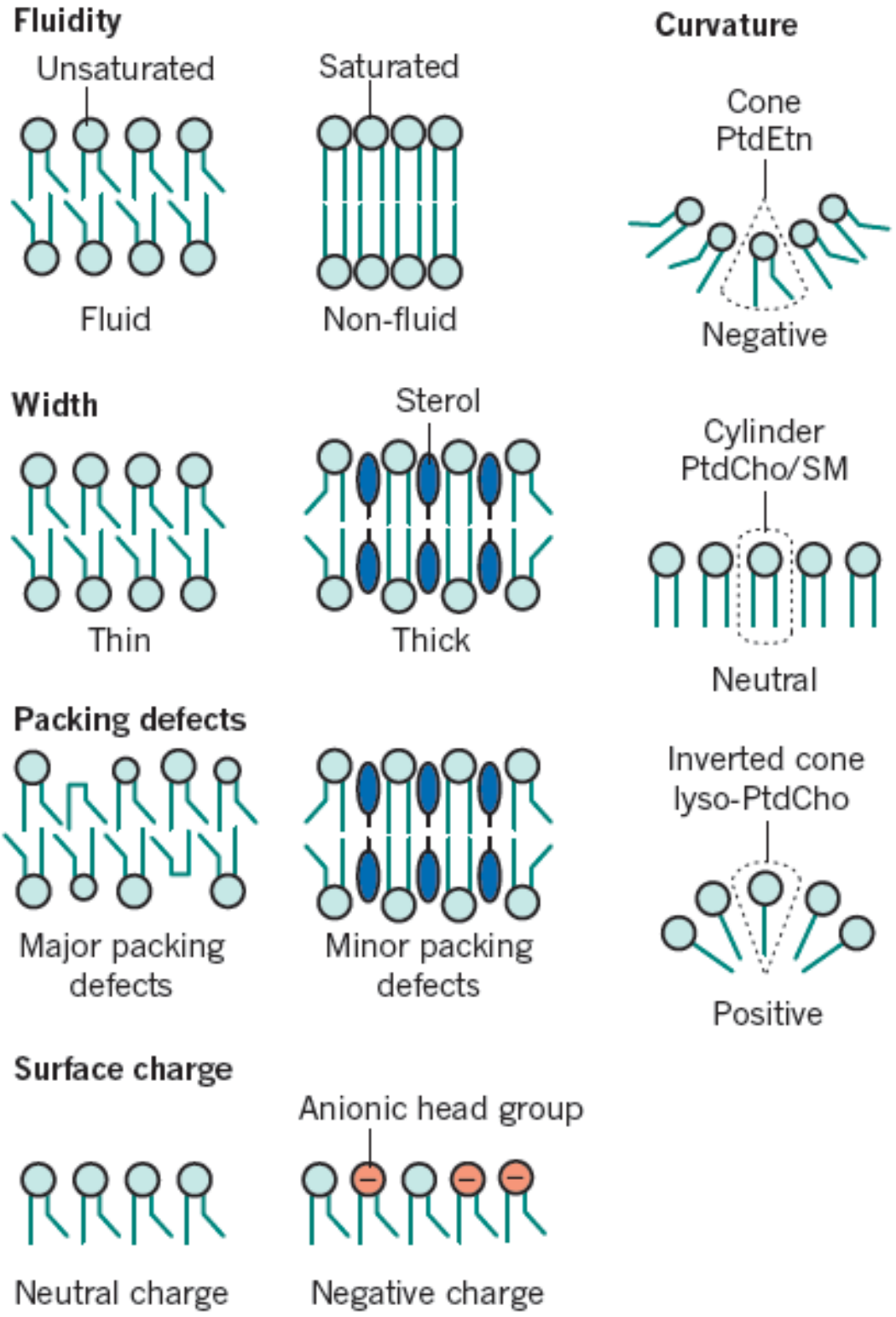

Figure 1-2. Phospholipid synthesis and remodeling pathways in mammals

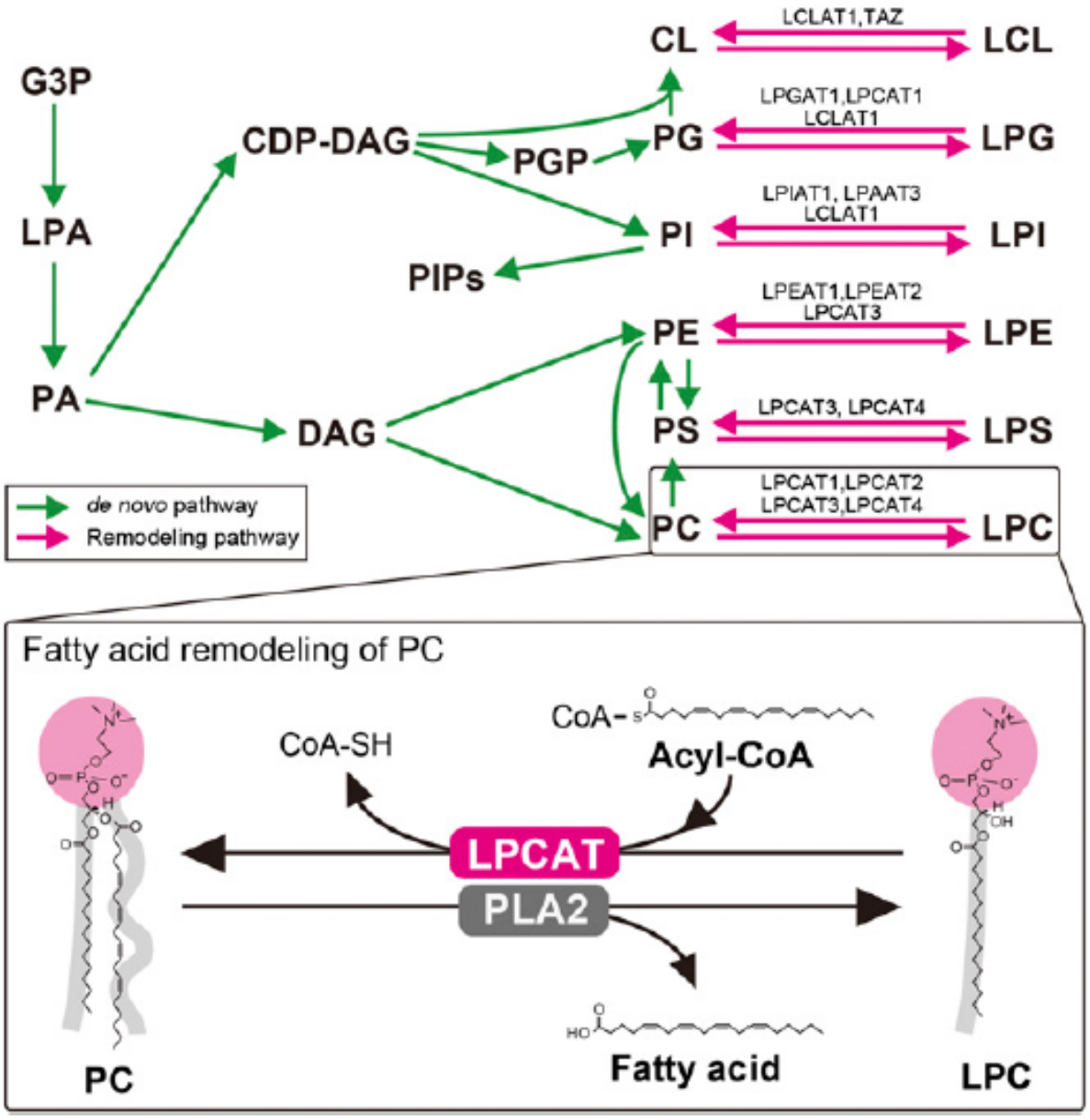

Figure 1-3. Coordinated effects of LXR on metabolism

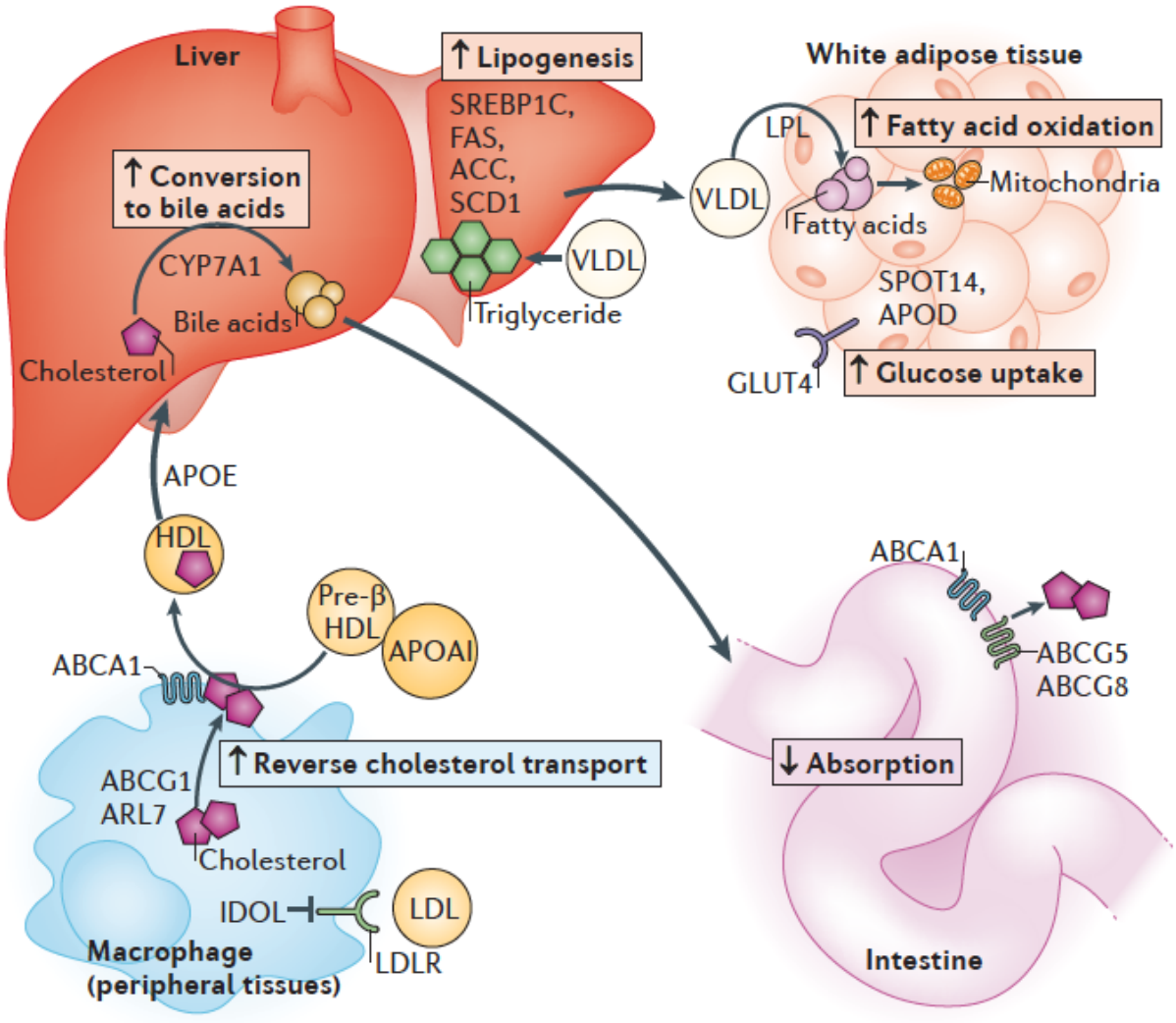

Reference

Aiello, R.J., Brees, D., Bourassa, P.A., Royer, L., Lindsey, S., Coskran, T., Haghpassand, M., and Francone, O.L. (2002). Increased atherosclerosis in hyperlipidemic mice with inactivation of ABCA1 in macrophages. Arterioscler Thromb Vasc Biol *22*, 630-637.

Annicotte, J.S., Schoonjans, K., and Auwerx, J. (2004). Expression of the liver X receptor alpha and beta in embryonic and adult mice. Anat Rec A Discov Mol Cell Evol Biol *277*, 312-316.

Antonny, B., Vanni, S., Shindou, H., and Ferreira, T. (2015). From zero to six double bonds: phospholipid unsaturation and organelle function. Trends Cell Biol.

Arthur, G., and Choy, P.C. (1984). Acyl specificity of hamster heart CDP-choline 1,2-diacylglycerol phosphocholine transferase in phosphatidylcholine biosynthesis. Biochim Biophys Acta *795*, 221-229.

Beaven, S.W., Matveyenko, A., Wroblewski, K., Chao, L., Wilpitz, D., Hsu, T.W., Lentz, J., Drew, B., Hevener, A.L., and Tontonoz, P. (2013). Reciprocal regulation of hepatic and adipose lipogenesis by liver X receptors in obesity and insulin resistance. Cell Metab *18*, 106-117.

Ben-Zvi, A., Lacoste, B., Kur, E., Andreone, B.J., Mayshar, Y., Yan, H., and Gu, C. (2014). Mfsd2a is critical for the formation and function of the blood-brain barrier. Nature *509*, 507-511.

Bensinger, S.J., Bradley, M.N., Joseph, S.B., Zelcer, N., Janssen, E.M., Hausner, M.A., Shih, R., Parks, J.S., Edwards, P.A., Jamieson, B.D., et al. (2008). LXR signaling couples sterol metabolism to proliferation in the acquired immune response. Cell *134*, 97-111.

Bigay, J., and Antonny, B. (2012). Curvature, lipid packing, and electrostatics of membrane organelles: defining cellular territories in determining specificity. Dev Cell *23*, 886-895.

Bodzioch, M., Orso, E., Klucken, J., Langmann, T., Bottcher, A., Diederich, W., Drobnik, W., Barlage, S., Buchler, C., Porsch-Ozcurumez, M., et al. (1999). The gene encoding ATP-binding cassette transporter 1 is mutated in Tangier disease. Nat Genet *22*, 347-351.

Bradley, M.N., Hong, C., Chen, M., Joseph, S.B., Wilpitz, D.C., Wang, X., Lusis, A.J., Collins, A., Hseuh, W.A., Collins, J.L., et al. (2007). Ligand activation of LXR beta reverses atherosclerosis and cellular cholesterol overload in mice lacking LXR alpha and apoE. J Clin Invest *117*, 2337-2346.

Brash, A.R. (2001). Arachidonic acid as a bioactive molecule. J Clin Invest *107*, 1339-1345.

Brugger, B. (2014). Lipidomics: analysis of the lipid composition of cells and subcellular organelles by electrospray ionization mass spectrometry. Annu Rev Biochem *83*, 79-98.

Cavelier, C., Lorenzi, I., Rohrer, L., and von Eckardstein, A. (2006). Lipid efflux by the ATP-binding cassette transporters ABCA1 and ABCG1. Biochim Biophys Acta *1761*, 655-666.

Chambon, P. (2004). How I became one of the fathers of a superfamily. Nat Med *10*, 1027-1031.

Chawla, A., Repa, J.J., Evans, R.M., and Mangelsdorf, D.J. (2001). Nuclear receptors and lipid physiology: opening the X-files. Science *294*, 1866-1870.

Chen, X., Hyatt, B.A., Mucenski, M.L., Mason, R.J., and Shannon, J.M. (2006). Identification and characterization of a lysophosphatidylcholine acyltransferase in alveolar type II cells. Proc Natl Acad Sci U S A *103*, 11724-11729.

Collins, J.L., Fivush, A.M., Watson, M.A., Galardi, C.M., Lewis, M.C., Moore, L.B., Parks, D.J., Wilson, J.G., Tippin, T.K., Binz, J.G., et al. (2002). Identification of a nonsteroidal liver X receptor agonist through parallel array synthesis of tertiary amines. J Med Chem *45*, 1963-1966.

de Kroon, A.I., Rijken, P.J., and De Smet, C.H. (2013). Checks and balances in membrane phospholipid class and acyl chain homeostasis, the yeast perspective. Prog Lipid Res *52*, 374-394.

Dowhan, W. (1997). Molecular basis for membrane phospholipid diversity: why are there so many lipids? Annu Rev Biochem *66*, 199-232.

Evans, R. (2004). A transcriptional basis for physiology. Nat Med *10*, 1022-1026.

Frolov, V.A., Shnyrova, A.V., and Zimmerberg, J. (2011). Lipid polymorphisms and membrane shape. Cold Spring Harb Perspect Biol *3*, a004747.

Ghisletti, S., Huang, W., Ogawa, S., Pascual, G., Lin, M.E., Willson, T.M., Rosenfeld, M.G., and Glass, C.K. (2007). Parallel SUMOylation-dependent pathways mediate gene- and signal-specific transrepression by LXRs and PPARgamma. Mol Cell *25*, 57-70.

Glass, C.K., and Rosenfeld, M.G. (2000). The coregulator exchange in transcriptional functions of nuclear receptors. Genes Dev *14*, 121-141.

Guo, S., Wang, Y., Zhou, D., and Li, Z. (2014). Significantly increased monounsaturated lipids relative to polyunsaturated lipids in six types of cancer microenvironment are observed by mass spectrometry imaging. Sci. Rep. *4*.

Harayama, T., Eto, M., Shindou, H., Kita, Y., Otsubo, E., Hishikawa, D., Ishii, S., Sakimura, K., Mishina, M., and Shimizu, T. (2014). Lysophospholipid acyltransferases mediate phosphatidylcholine diversification to achieve the physical properties required in vivo. Cell Metab *20*, 295-305.

Harayama, T., Shindou, H., Ogasawara, R., Suwabe, A., and Shimizu, T. (2008). Identification of a novel noninflammatory biosynthetic pathway of platelet-activating factor. J Biol Chem *283*, 11097-11106.

Hishikawa, D., Hashidate, T., Shimizu, T., and Shindou, H. (2014). Diversity and function of membrane glycerophospholipids generated by the remodeling pathway in mammalian cells. J Lipid Res *55*, 799-807.

Hishikawa, D., Shindou, H., Kobayashi, S., Nakanishi, H., Taguchi, R., and Shimizu, T. (2008). Discovery of a lysophospholipid acyltransferase family essential for membrane asymmetry and diversity. Proc Natl Acad Sci U S A *105*, 2830-2835.

Holthuis, J.C., and Menon, A.K. (2014). Lipid landscapes and pipelines in membrane homeostasis. Nature *510*, 48-57.

Holzer, R.G., Park, E.J., Li, N., Tran, H., Chen, M., Choi, C., Solinas, G., and Karin, M. (2011). Saturated fatty acids induce c-Src clustering within membrane subdomains, leading to JNK activation. Cell *147*, 173-184.

Hong, C., and Tontonoz, P. (2014). Liver X receptors in lipid metabolism: opportunities for drug discovery. Nat Rev Drug Discov *13*, 433-444.

Joseph, S.B., Bradley, M.N., Castrillo, A., Bruhn, K.W., Mak, P.A., Pei, L., Hogenesch, J., O'Connell R, M., Cheng, G., Saez, E., et al. (2004). LXR-dependent gene expression is important for macrophage survival and the innate immune response. Cell *119*, 299-309.

Joseph, S.B., Castrillo, A., Laffitte, B.A., Mangelsdorf, D.J., and Tontonoz, P. (2003). Reciprocal regulation of inflammation and lipid metabolism by liver X receptors. Nat Med *9*, 213-219.

Joseph, S.B., Laffitte, B.A., Patel, P.H., Watson, M.A., Matsukuma, K.E., Walczak, R., Collins, J.L., Osborne, T.F., and Tontonoz, P. (2002a). Direct and indirect mechanisms for regulation of fatty acid synthase gene expression by liver X receptors. J Biol Chem *277*, 11019-11025.

Joseph, S.B., McKilligin, E., Pei, L., Watson, M.A., Collins, A.R., Laffitte, B.A., Chen, M., Noh, G., Goodman, J., Hagger, G.N., et al. (2002b). Synthetic LXR ligand inhibits the development of atherosclerosis in mice. Proc Natl Acad Sci U S A *99*, 7604-7609.

Keenan, T.W., and Morre, D.J. (1970). Phospholipid class and fatty acid composition of golgi apparatus isolated from rat liver and comparison with other cell fractions. Biochemistry *9*, 19-25.

Kennedy, E.P., and Weiss, S.B. (1956). The function of cytidine coenzymes in the biosynthesis of phospholipides. J Biol Chem *222*, 193-214.

Kennedy, M.A., Barrera, G.C., Nakamura, K., Baldan, A., Tarr, P., Fishbein, M.C., Frank, J., Francone, O.L., and Edwards, P.A. (2005). ABCG1 has a critical role in mediating cholesterol efflux to HDL and preventing cellular lipid accumulation. Cell Metab *1*, 121-131.

Kent, C. (1995). Eukaryotic phospholipid biosynthesis. Annu Rev Biochem *64*, 315-343.

Kim, J., Basak, J.M., and Holtzman, D.M. (2009). The role of apolipoprotein E in Alzheimer's disease. Neuron *63*, 287-303.

Koeberle, A., Shindou, H., Koeberle, S.C., Laufer, S.A., Shimizu, T., and Werz, O. (2013). Arachidonoyl-phosphatidylcholine oscillates during the cell cycle and counteracts proliferation by suppressing Akt membrane binding. Proc Natl Acad Sci U S A *110*, 2546-2551.

Koynova, R., and Caffrey, M. (1998). Phases and phase transitions of the phosphatidylcholines. Biochim Biophys Acta *1376*, 91-145.

Laffitte, B.A., Chao, L.C., Li, J., Walczak, R., Hummasti, S., Joseph, S.B., Castrillo, A., Wilpitz, D.C., Mangelsdorf, D.J., Collins, J.L., et al. (2003a). Activation of liver X receptor improves glucose tolerance through coordinate regulation of glucose metabolism in liver and adipose tissue. Proc Natl Acad Sci U S A *100*, 5419-5424.

Laffitte, B.A., Joseph, S.B., Chen, M., Castrillo, A., Repa, J., Wilpitz, D., Mangelsdorf, D., and Tontonoz, P. (2003b). The phospholipid transfer protein gene is a liver X receptor target expressed by macrophages in atherosclerotic lesions. Mol Cell Biol *23*, 2182-2191.

Lands, W.E. (1958). Metabolism of glycerolipides; a comparison of lecithin and triglyceride synthesis. J Biol Chem *231*, 883-888.

Lehmann, J.M., Kliewer, S.A., Moore, L.B., Smith-Oliver, T.A., Oliver, B.B., Su, J.L., Sundseth, S.S., Winegar, D.A., Blanchard, D.E., Spencer, T.A., et al. (1997). Activation of the nuclear receptor LXR by oxysterols defines a new hormone response pathway. J Biol Chem *272*, 3137-3140.

Lemmon, M.A. (2008). Membrane recognition by phospholipid-binding domains. Nat Rev Mol Cell Biol *9*, 99-111.

Leslie, C.C. (2004). Regulation of the specific release of arachidonic acid by cytosolic phospholipase A2. Prostaglandins Leukot Essent Fatty Acids *70*, 373-376.

Lu, T.T., Repa, J.J., and Mangelsdorf, D.J. (2001). Orphan nuclear receptors as eLiXiRs and FiXeRs of sterol metabolism. J Biol Chem *276*, 37735-37738.

Maglich, J.M., Sluder, A., Guan, X., Shi, Y., McKee, D.D., Carrick, K., Kamdar, K., Willson, T.M., and Moore, J.T. (2001). Comparison of complete nuclear receptor sets from the human, Caenorhabditis elegans and Drosophila genomes. Genome Biol *2*, RESEARCH0029.

Mak, P.A., Laffitte, B.A., Desrumaux, C., Joseph, S.B., Curtiss, L.K., Mangelsdorf, D.J., Tontonoz, P., and Edwards, P.A. (2002). Regulated expression of the apolipoprotein E/C-I/C-IV/C-II gene cluster in murine and human macrophages. A critical role for nuclear liver X receptors alpha and beta. J Biol Chem *277*, 31900-31908.

Martinez, M. (1992). Tissue levels of polyunsaturated fatty acids during early human development. J Pediatr *120*, S129-138.

Naguib, A., Bencze, G., Engle, D.D., Chio, II, Herzka, T., Watrud, K., Bencze, S., Tuveson, D.A., Pappin, D.J., and Trotman, L.C. (2015). p53 mutations change phosphatidylinositol acyl chain composition. Cell Rep *10*, 8-19.

Nakanishi, H., Shindou, H., Hishikawa, D., Harayama, T., Ogasawara, R., Suwabe, A., Taguchi, R., and Shimizu, T. (2006). Cloning and characterization of mouse lung-type acyl-CoA:lysophosphatidylcholine acyltransferase 1 (LPCAT1). Expression in alveolar type II cells and possible involvement in surfactant production. J Biol Chem *281*, 20140-20147.

Nguyen, L.N., Ma, D., Shui, G., Wong, P., Cazenave-Gassiot, A., Zhang, X., Wenk, M.R., Goh, E.L., and Silver, D.L. (2014). Mfsd2a is a transporter for the essential omega-3 fatty acid docosahexaenoic acid. Nature *509*, 503-506.

Perez-Chacon, G., Astudillo, A.M., Ruiperez, V., Balboa, M.A., and Balsinde, J. (2010). Signaling role for lysophosphatidylcholine acyltransferase 3 in receptor-regulated arachidonic acid reacylation reactions in human monocytes. J Immunol *184*, 1071-1078.

Pinot, M., Vanni, S., Pagnotta, S., Lacas-Gervais, S., Payet, L.A., Ferreira, T., Gautier, R., Goud, B., Antonny, B., and Barelli, H. (2014). Lipid cell biology. Polyunsaturated phospholipids facilitate membrane deformation and fission by endocytic proteins. Science *345*, 693-697.

Repa, J.J., Liang, G., Ou, J., Bashmakov, Y., Lobaccaro, J.M., Shimomura, I., Shan, B., Brown, M.S., Goldstein, J.L., and Mangelsdorf, D.J. (2000). Regulation of mouse sterol regulatory element-binding protein-1c gene (SREBP-1c) by oxysterol receptors, LXRalpha and LXRbeta. Genes Dev *14*, 2819-2830.

Salem, N., Jr., Litman, B., Kim, H.Y., and Gawrisch, K. (2001). Mechanisms of action of docosahexaenoic acid in the nervous system. Lipids *36*, 945-959.

Sampaio, J.L., Gerl, M.J., Klose, C., Ejsing, C.S., Beug, H., Simons, K., and Shevchenko, A. (2011). Membrane lipidome of an epithelial cell line. Proc Natl Acad Sci U S A *108*, 1903-1907.

Schneiter, R., Brugger, B., Sandhoff, R., Zellnig, G., Leber, A., Lampl, M., Athenstaedt, K., Hrastnik, C., Eder, S., Daum, G., et al. (1999). Electrospray ionization tandem mass spectrometry (ESI-MS/MS) analysis of the lipid molecular species composition of yeast subcellular membranes reveals acyl chain-based sorting/remodeling of distinct molecular species en route to the plasma membrane. J Cell Biol *146*, 741-754.

Schultz, J.R., Tu, H., Luk, A., Repa, J.J., Medina, J.C., Li, L., Schwendner, S., Wang, S., Thoolen, M., Mangelsdorf, D.J., et al. (2000). Role of LXRs in control of lipogenesis. Genes Dev *14*, 2831-2838.

Sevastou, I., Kaffe, E., Mouratis, M.A., and Aidinis, V. (2013). Lysoglycerophospholipids in chronic inflammatory disorders: the PLA(2)/LPC and ATX/LPA axes. Biochim Biophys Acta *1831*, 42-60.

Sharpe, H.J., Stevens, T.J., and Munro, S. (2010). A comprehensive comparison of transmembrane domains reveals organelle-specific properties. Cell *142*, 158-169.

Shindou, H., Hishikawa, D., Harayama, T., Eto, M., and Shimizu, T. (2013). Generation of membrane diversity by lysophospholipid acyltransferases. J Biochem *154*, 21-28.

Shindou, H., Hishikawa, D., Nakanishi, H., Harayama, T., Ishii, S., Taguchi, R., and Shimizu, T. (2007). A single enzyme catalyzes both platelet-activating factor production and membrane biogenesis of inflammatory cells. Cloning and characterization of acetyl-CoA:LYSO-PAF acetyltransferase. J Biol Chem *282*, 6532-6539.

Shindou, H., Ishii, S., Yamamoto, M., Takeda, K., Akira, S., and Shimizu, T. (2005). Priming effect of lipopolysaccharide on acetyl-coenzyme A:lyso-platelet-activating factor acetyltransferase is MyD88 and TRIF independent. J Immunol *175*, 1177-1183.

Singer, S.J., and Nicolson, G.L. (1972). The fluid mosaic model of the structure of cell membranes. Science *175*, 720-731.

Slotte, J.P. (2013). Biological functions of sphingomyelins. Prog Lipid Res *52*, 424-437.

Solomonson, L.P., Liepkalns, V.A., and Spector, A.A. (1976). Changes in (Na+ + K+)-ATPase activity of Ehrlich ascites tumor cells produced by alteration of membrane fatty acid composition. Biochemistry *15*, 892-897.

Spector, A.A., and Yorek, M.A. (1985). Membrane lipid composition and cellular function. J Lipid Res *26*, 1015-1035.

Szamel, M., and Resch, K. (1981). Modulation of enzyme activities in isolated lymphocyte plasma membranes by enzymatic modification of phospholipid fatty acids. J Biol Chem *256*, 11618-11623.

Teupser, D., Kretzschmar, D., Tennert, C., Burkhardt, R., Wilfert, W., Fengler, D., Naumann, R., Sippel, A.E., and Thiery, J. (2008). Effect of macrophage overexpression of murine liver X receptor-alpha (LXR-alpha) on atherosclerosis in LDL-receptor deficient mice. Arterioscler Thromb Vasc Biol *28*, 2009-2015.

Tontonoz, P. (2011). Transcriptional and posttranscriptional control of cholesterol homeostasis by liver X receptors. Cold Spring Harb Symp Quant Biol *76*, 129-137.

van Meer, G., Voelker, D.R., and Feigenson, G.W. (2008). Membrane lipids: where they are and how they behave. Nat Rev Mol Cell Biol *9*, 112-124.

Volmer, R., van der Ploeg, K., and Ron, D. (2013). Membrane lipid saturation activates endoplasmic reticulum unfolded protein response transducers through their transmembrane domains. Proc Natl Acad Sci U S A *110*, 4628-4633.

Wahrle, S.E., Jiang, H., Parsadanian, M., Hartman, R.E., Bales, K.R., Paul, S.M., and Holtzman, D.M. (2005). Deletion of Abca1 increases Abeta deposition in the PDAPP transgenic mouse model of Alzheimer disease. J Biol Chem *280*, 43236-43242.

Wang, N., Lan, D., Chen, W., Matsuura, F., and Tall, A.R. (2004). ATP-binding cassette transporters G1 and G4 mediate cellular cholesterol efflux to high-density lipoproteins. Proc Natl Acad Sci U S A *101*, 9774-9779.

Wei, Y., Wang, D., Topczewski, F., and Pagliassotti, M.J. (2006). Saturated fatty acids induce endoplasmic reticulum stress and apoptosis independently of ceramide in liver cells. Am J Physiol Endocrinol Metab *291*, E275-281.

Wenk, M.R. (2005). The emerging field of lipidomics. Nat Rev Drug Discov *4*, 594-610.

Willy, P.J., Umesono, K., Ong, E.S., Evans, R.M., Heyman, R.A., and Mangelsdorf, D.J. (1995). LXR, a nuclear receptor that defines a distinct retinoid response pathway. Genes Dev *9*, 1033-1045.

Yamashita, A., Hayashi, Y., Nemoto-Sasaki, Y., Ito, M., Oka, S., Tanikawa, T., Waku, K., and Sugiura, T. (2014). Acyltransferases and transacylases that determine the fatty acid composition

of glycerolipids and the metabolism of bioactive lipid mediators in mammalian cells and model organisms. Prog Lipid Res *53*, 18-81.

Yang, C., McDonald, J.G., Patel, A., Zhang, Y., Umetani, M., Xu, F., Westover, E.J., Covey, D.F., Mangelsdorf, D.J., Cohen, J.C., et al. (2006). Sterol intermediates from cholesterol biosynthetic pathway as liver X receptor ligands. J Biol Chem *281*, 27816-27826.

Yu, L., Hammer, R.E., Li-Hawkins, J., Von Bergmann, K., Lutjohann, D., Cohen, J.C., and Hobbs, H.H. (2002a). Disruption of Abcg5 and Abcg8 in mice reveals their crucial role in biliary cholesterol secretion. Proc Natl Acad Sci U S A *99*, 16237-16242.

Yu, L., Li-Hawkins, J., Hammer, R.E., Berge, K.E., Horton, J.D., Cohen, J.C., and Hobbs, H.H. (2002b). Overexpression of ABCG5 and ABCG8 promotes biliary cholesterol secretion and reduces fractional absorption of dietary cholesterol. J Clin Invest *110*, 671-680.

Zelcer, N., Hong, C., Boyadjian, R., and Tontonoz, P. (2009). LXR regulates cholesterol uptake through Idol-dependent ubiquitination of the LDL receptor. Science *325*, 100-104.

Zelcer, N., Khanlou, N., Clare, R., Jiang, Q., Reed-Geaghan, E.G., Landreth, G.E., Vinters, H.V., and Tontonoz, P. (2007). Attenuation of neuroinflammation and Alzheimer's disease pathology by liver x receptors. Proc Natl Acad Sci U S A *104*, 10601-10606.

Zelcer, N., and Tontonoz, P. (2006). Liver X receptors as integrators of metabolic and inflammatory signaling. J Clin Invest *116*, 607-614.

Zhao, Y., Chen, Y.Q., Bonacci, T.M., Bredt, D.S., Li, S., Bensch, W.R., Moller, D.E., Kowala, M., Konrad, R.J., and Cao, G. (2008). Identification and characterization of a major liver lysophosphatidylcholine acyltransferase. J Biol Chem *283*, 8258-8265.

Chapter 2: LXRs regulate ER stress and inflammation through dynamic modulation of membrane phospholipid composition

Abstract

The fatty acyl composition of phospholipids determines the biophysical character of membranes and impacts the function of membrane proteins. Here we define a nuclear receptor pathway for the dynamic modulation of membrane composition in response to changes in cellular lipid metabolism. Ligand activation of LXR preferentially drives the incorporation of polyunsaturated fatty acids into phospholipids through induction of the remodeling enzyme Lpcat3. Promotion of Lpcat3 activity ameliorates ER stress induced by saturated free fatty acids *in vitro* or by obesity and hepatic lipid accumulation *in vivo*. Conversely, Lpcat3 knockdown in liver exacerbates ER stress and inflammation. Mechanistically, Lpcat3 modulates inflammation both by regulating c-Src and JNK kinase activation through changes in membrane composition and by affecting substrate availability for inflammatory mediator production. These results outline an endogenous mechanism for the preservation of membrane homeostasis during lipid stress and identify Lpcat3 as an important mediator of LXRs effects on metabolism.

Introduction

Phospholipids (PLs) are important structural components of biological membranes and precursors of numerous signaling molecules. PL membranes compartmentalize living cells, form intracellular organelles and provide platforms for a wide variety of important physiological processes, such as vesicle trafficking, signal transduction, molecular transport, and biosynthesis. PLs also act as substrates for the generation of diverse bioactive molecules involved in signal transduction, including eicosanoids, LPA and diacyl glycerol (Holzer et al., 2011; Spector and Yorek, 1985).

The fatty acyl composition of PLs determines the biophysical characteristics of membranes, including membrane fluidity and the assembly of specific membrane subdomains (Holzer et al., 2011; Spector and Yorek, 1985). Therefore, changes in fatty acyl composition can potentially affect the properties of proteins associated with membranes and influence the biological processes that occur on membranes. It has been reported that modifications of the fatty acyl composition of cell membranes influences a range of cell processes, most importantly, the activity of membrane-bound enzymes and transporters and the localization of acylated proteins in membrane subdomains (Cornelius, 2001; Fu et al., 2011; Holzer et al., 2011). For example, membrane fatty acyl composition affects the activity of the Na+/K+-ATPase and the sarcoplasmic-endoplasmic reticulum calcium ATPase-2b (*SERCA2b*) (Cornelius, 2001; Li et al., 2004). It is also known that incorporation of saturated fatty acids into plasma membrane recruits c-Src kinase to lipid raft domains and increases its activity (Holzer et al., 2011).

In mammalian cells, PLs are first synthesized by the *de novo* pathway and subsequently undergo further remodeling through fatty acyl deacylation and reacylation, a pathway referred to as the Lands cycle (Lands, 1958). As a result, saturated fatty acids are preferably linked at the

sn-1 position and unsaturated fatty acids are primarily found at the *sn*-2 position. This diversity and asymmetric distribution is largely established by the remodeling process, since the *de novo* PL synthesis process appears to have very little fatty acyl-CoA substrate specificity. In the liver, a major enzyme that catalyzes the formation of phosphatidylcholine (PC) from saturated lysophosphatidylcholines (LysoPC) and unsaturated fatty acyl-CoAs is lysophosphatidyl acyltransferase 3 (Lpcat3) (Hishikawa et al., 2008; Li et al., 2012). Lpcat3 preferentially synthesizes PC containing unsaturated fatty acids, particularly arachidonic acid (20:4) and linoleic acid (18:2), at the *sn*-2 position.

To date, most of the studies regarding the effects of PL fatty acyl composition on biological systems have utilized *in vitro* biochemical assays, due to the difficulty of directing specific changes in membrane composition in living cells. Therefore, there is little understanding of how regulatory pathways control PL fatty acyl composition or how such regulatory pathways could dictate cell responses. It is known that increased levels of saturated fatty acids can cause ER stress, and this has been postulated to involve charges in ER membrane composition (Borradaile et al., 2006). It is also been shown that inhibition of SCD-1 or Lpcat3 activity increases membrane saturation, secondary to changes in fatty acid production (Miyazaki et al., 2000) or phospholipid remodeling (Ariyama et al., 2010), respectively. Loss of either SCD-1 or Lpcat3 activity has been shown to enhance ER stress in cultured cells (Ariyama et al., 2010). But are there regulatory pathways that modify membrane lipid composition in response to extracellular or intracellular cues *in vivo*? Furthermore, could such pathways be targeted pharmacologically to manipulate ER membrane composition? Finally, what is the contribution of PL remodeling to ER stress responses *in vivo* in the setting of metabolic disease?

The Liver X receptors (LXRs) are important regulators of cholesterol and fatty acid homeostasis and potent inhibitors of inflammatory gene expression (Hong and Tontonoz, 2008). However, the impact of LXRs on the major constituents of membranes–phospholipids–has not been rigorously investigated. Here we show that LXRs are major regulators of membrane phospholipid composition and that this previously unappreciated action underlies the ability of LXRs to influence ER stress and inflammation. *Lpcat3*, a key enzyme in the PL remodeling pathway, is a direct LXR target gene in mice and humans. Ligand activation of LXR promotes the incorporation of unsaturated fatty acids into phospholipids through Lpcat3, and thereby reduces hepatic ER stress and inflammation in the context of genetic obesity. These studies identify the LXR-Lpcat3 pathway as an important modulator of PL metabolism, metabolic stress responses and inflammation.

Results

Lpcat3 is a direct target of LXR in mice and humans

We previously identified *Lpcat3* (also known as MBOAT5) as an LXR-responsive gene through transcriptional profiling studies of BV-2 microglia cells (Zelcer et al., 2007). *Lpcat3* was also reported to be responsive to synthetic LXR agonists in other cell lines (Demeure et al., 2011). However, the dependence of Lpcat3 on the genetic expression of LXRα and LXRβ has not been examined. Lpcat3 is widely expressed in mice *in vivo*, with especially prominent expression in metabolic tissues (**Fig. 2-2A**). Exposure of primary mouse hepatocytes to the synthetic LXR agonists GW3965 or T1317 induced the expression of *Lpcat3* as well as the established targets *Idol* and *Abca1* (**Fig. 2-1A**). The combination of LXR and RXR ligands further boosted *Lpcat3* expression (**Fig. 2-1B**). Importantly, the ability of LXR agonist to promote *Lpcat3* expression was lost in *Lxrαβ*-/- cells. Furthermore, both LXRα and LXRβ are competent to regulate Lpcat3, as the response to ligands was comparable between *Lxrα*-/- and *Lxrβ*-/- cells (**Fig. 2-1B and Fig. 2-2B**). We also observed regulation of *Lpcat3* by LXR agonists in several other cell types, including primary macrophages, RAW264.7 cells and Hep3B cells (**Fig. 2-2C, D and G**). Regulation of *Lpcat3* by LXR was not sensitive to cycloheximide, suggesting that it was a direct transcriptional effect (**Fig. 2-2E**). It was also not secondary to the induction of SREBP-1c, because oxysterols that block SREBP processing still induced *Lpcat3* expression (**Fig. 2-2F, G**). Finally, administration of GW3965 (40 mg/kg/day) for 3 days to C57Bl/6 mice induced the expression of *Lpcat3* in multiple tissues *in vivo*, including liver, fat, muscle and kidney (**Fig. 2-1C and H**).

Given that Lpcat3 is a lysophosphatidylcholine acyltransferase, we reasoned that activation of LXR might regulate PL fatty acyl composition in cells. Using an *in vitro* acyltransferase

assay with radiolabeled fatty acyl-CoA and LysoPL, we found that LXR agonist increased lysophosphatidylcholine acyltransferase activity and drove the formation of PC from labeled substrates (**Fig. 2-1D**). Furthermore, ESI-MS/MS analysis of whole cell lipid extracts showed that LXR ligand treatment markedly increased the abundance of polyunsaturated PC, especially arachidonoyl (20:4) and linoleoyl (18:2)-containing PC, in RAW 264.7 cells (**Fig. 2-1E**). The abundance of monounsaturated PC and saturated PC was not affected or even reduced by LXR ligand treatment (**Fig. 2-1E**). On the other hand, stable knockdown Lpcat3 expression in RAW 264.7 cells with shRNA constructs reduced Lpcat3 expression and activity (**Fig. 2-2I**), as well as the amount of 20:4 and 18:2-containing PC (**Fig. 2-1F)**. The regulation of phospholipid metabolism by LXR was also evident *in vivo*. Treatment of C57BL/6 mice with GW3965 for 2 days led to a change in the abundance of several polyunsaturated PC species in total liver extracts (**Fig. 2-1G**), including those containing linoleic acid (18:2), one of the preferred substrates of Lpcat3 (Hishikawa et al., 2008).

LXR suppresses saturated fatty acid-induced endoplasmic reticulum stress

High levels of saturated fatty acids such as palmitic acid (PA) are postulated to trigger ER stress pathways by altering membrane dynamics and integrity (Borradaile et al., 2006). The observation that LXR activation increased levels of unsaturated PLs in cells led us to explore whether LXR was able to protect cells from saturated fatty acid-induced ER stress. We first assessed the unfolded protein response (UPR)–signaling pathways activated by the accumulation of unfolded proteins commonly used as indicators of ER stress. Pretreatment of Hep3B hepatoma cells with GW3965 blunted the induction of the downstream UPR target genes CHOP and ATF3 by PA in a dose-dependent manner (**Fig. 2-3A and 2-4A**). Similar effects were also

observed in primary mouse hepatocytes and macrophages (**Fig. 2-4B, C**). Interestingly, however, LXR ligand had no effect on the induction of ER stress by thapsigargin (**Fig. 2-3A**), suggesting that LXR specifically modulates lipid-induced ER stress. The protective effects of LXR agonist were observed in wild-type but not in *Lxrαβ*-/- primary hepatocytes, indicating that they are indeed mediated by LXRs (**Fig. 2-3B**). The absence of LXRs also sensitized the hepatocytes to PA-induced ER stress markers. In addition, we found that LXR agonist treatment decreased the formation of spliced *Xbp1* mRNA and reduced the phosphorylation of PERK and EIF2α (**Fig. 2-3C, D**).

The accumulation of excess free cholesterol in macrophages is also known to trigger the activation of ER stress pathways (Feng et al., 2003). Treatment of primary mouse macrophages with LXR agonist blunted the induction of UPR target genes induced by loading the cells with acetylated LDL in the presence of an ACAT inhibitor (**Fig. 2-3E**).

Chronic ER stress induced by lipotoxicity eventually causes cell apoptosis. Therefore, we addressed whether LXR activation could also protect cells from lipotoxicity-induced apoptosis. As predicted, Hep3B cells pretreated with LXR ligand were protected from saturated fatty acid-induced apoptosis as assessed by caspase-3 activity (**Fig. 2-4D, E**). Together, these data demonstrate that LXR activation attenuates UPR signaling initiated by fatty acid or cholesterol lipotoxicity and protects cells from chronic ER stress-induced apoptosis.

Lpcat3 contributes to LXR-dependent suppression of ER stress signaling

Next we addressed the mechanism by which LXR protects cells from lipid-induced ER stress. Prior biochemical studies have shown that unsaturated PLs increase membrane dynamics, an effect that might potentially reverse deleterious effects of saturated fatty acids on membrane

structure. We therefore hypothesized that LXRs might reduce ER stress by increasing the proportion of polyunsaturated PLs in membranes through *Lpcat3* induction. Consistent with the observation that knockdown of *Lpcat3* decreased membrane PL unsaturation (**Fig. 2-1F**), loss of Lpcat3 also affected fatty acid-induced ER stress. siRNA-mediated knockdown of *Lpcat3* in Hep3B cells markedly enhanced the expression of CHOP and ATF3 (**Fig. 2-3F**), as well as the phosphorylation of eIF2a in response to PA (**Fig. 2-3G**).

To address whether Lpcat3 activity mediated protective effects of LXR on ER stress, we treated primary hepatocytes with LXR agonist in the presence or absence of Lpcat3 knockdown. LXR agonist strongly suppressed the expression of sXBP-1, ATF3 and ATF-4 in response to PA (**Fig. 2-5A**). The magnitude of suppression by LXR agonist was reduced but not abolished by shRNA-mediated knockdown of Lpcat3. The residual effect of LXR agonist on ER stress is consistent with prior studies showing that SCD-1 also inhibits ER stress (Erbay et al., 2009).

To establish that the effects of LXR on cellular phospholipid composition were dependent on Lpcat3, we examined primary mouse hepatocytes deficient in either LXR or Lpcat3 expression. Treatment of wild-type hepatocytes with GW3965 increased the abundance of PC species containing 20:4 or 18:2 acyl chains, and this effect was completely abrogated in hepatocytes from mice lacking both LXRα and LXRβ (DKO; **Fig. 2-5B**). Furthermore, shRNA-mediated knockdown of *Lpcat3* expression in primary hepatocytes blunted the ability of LXR agonist to induce levels of these same unsaturated PC species (**Fig. 2-5C**). Thus, the ability of GW3965 to modulate cellular phospholipid composition is dependent on both LXR and Lpcat3 expression.

The primary function of Lpcat3 is to catalyze the formation of polyunsaturated PL. Therefore, we reasoned that polyunsaturated PLs produced by Lpcat3 are the bioactive

molecules that mediate the effects of the LXR pathway on ER stress. If this hypothesis is correct, then treatment of cells with arachidonoyl-containing PC should mimic the protection effects of the LXR-Lpcat3 pathway. Indeed, pretreatment of cells with liposomes made with 16:0, 20:4 PC but not saturated 16:0, 18:0 PC inhibited PA-induced ER stress in a dose-dependent manner (**Fig. 2-5D**). Since polyunsaturated fatty acids are known to reduce ER stress, we considered the possibility that the protective effects of arachidonoyl-containing PC were secondary to the enzymatic release of arachidonic acid from the PC. To rule out this possibility, we used the phospholipase A2 inhibitor bromoenol lactone (BEL), to prevent the release of arachidonic acid from PC. 16:0, 20:4 PC retained its protective effects even in the presence of BEL treatment (**Fig. 2-5E**), strongly suggesting that the arachidonoyl-containing PC itself is the active molecule. In sum, these results demonstrate that LXR activation protects cells from lipid-induced ER stress, at least in part, by promoting Lpcat3-mediated formation of unsaturated PC species.

The LXR-Lpcat3 pathway regulates metabolic ER stress in vivo

ER stress has been observed in a number of metabolic diseases and has been postulated to be a key pathogenic factor in their development. Therefore, we investigated the physiological impact of the LXR-Lpcat3 pathway on ER stress in mouse models of metabolic disease. To test whether endogenous LXR signaling influenced the development of hepatic ER stress induced by lipid-rich diet, we fed *Lxr$\alpha\beta$*-/- (DKO) mice and wild-type littermates a Western diet for 12 weeks. DKO mice exhibited increased expression of ER stress markers, including ATF3 and CHOP (**Fig. 2-6A**). Furthermore, increased ER stress pathway activation correlated with reduced *Lpcat3* expression in the livers of DKO mice (**Fig. 2-6A**). To address whether *Lpcat3* deficiency would exacerbate metabolic ER stress *in vivo*, we used adenoviral vectors to deliver

an shRNA construct targeting *Lpcat3* to the livers of *ob/ob* mice–a genetic model of obesity known to exhibit hepatic ER stress (Ozcan et al., 2004). shRNA-mediated knockdown of Lpcat3 induced the expression of a panel of genes linked to ER stress (sXBP1, CHOP, ATF3, BIP; **Fig. 2-6B**) compared to shRNA control. This was also accompanied by increased phosphorylation of PERK and eIF2a (**Fig. 2-6C**), consistent with enhanced ER stress pathway activation.

Since the ability of Lpcat3 to ameliorate ER stress *in vitro* correlated with production of unsaturated PC (**Figs. 2-1 and 2-3**), we analyzed the effect of Lpcat3 expression on PL fatty acyl composition *in vivo*. ESI-MS/MS analysis of total lipids revealed clear changes in PC fatty acyl composition in mouse liver transduced with shLpcat3 adenovirus compared to control, and these changes were largely consistent with our results in cultured cells. The amount of arachidonoyl- and linoloyl-containing PC species was reduced by shRNA-mediated knockdown of Lpcat3, while the amounts of saturated or mono-unsaturated PC were not changed or even increased by Lpcat3 knockdown (**Fig. 2-6D**). Similar trends were observed for PE fatty acyl composition, in line with prior reports that PE is also a substrate for Lpcat3-dependent remodeling (**Fig. 2-7A**).

After 7 days of transduction with shLpcat3, *ob/ob* mice exhibited a modest decrease in blood glucose levels and no significant change in plasma insulin, suggesting that there was minimal effect on the insulin resistance phenotype of the mice over this time frame (**Fig. 2-7B**). Plasma TG levels were modestly increased and liver TG levels were decreased (**Fig. 2-7B**). These observations are consistent with prior reports that Lpcat3 and ER stress affect VLDL secretion from the liver (Li et al., 2012; Wang et al., 2012).

We transduced adenoviral vectors expressing EGFP control or Lpcat3 into *ob/ob* mice to ask whether increased Lpcat3 activity in the liver might ameliorate lipid-induced ER stress. Adenoviral expression of Lpcat3 in *ob/ob* livers reduced expression of ATF3 and there was a

trend towards decreased spliced XBP-1 (**Fig. 2-8A**). Interestingly, Lpcat3 expression in this model was also associated with an improvement in glucose homeostasis. Mice expressing Lpcat3 had reduced blood glucose levels, plasma insulin levels, and insulin resistance index compared to control-transduced mice (**Fig. 2-8B**). There was no difference in liver or plasma TG levels or plasma free fatty acids. Lpcat3-transduced *ob/ob* mice also showed modest improvement in glucose tolerance compared to controls (**Fig. 2-8C**).

We employed *db/db* mice as an additional model of lipid-induced hepatic ER stress. These mice exhibit more severe insulin resistance, hepatic steatosis and inflammation compared to *ob/ob* mice. Expression of Lpcat3 in *db/db* mice reduced the expression of ER stress-associated genes, including CHOP, ATF3 and sXBP-1 (**Fig. 2-8D**). Collectively, these data implicate the LXR-Lpcat3 pathway as a physiological regulator of PL fatty acyl composition in mouse liver that affects hepatic UPR signaling in the setting of metabolic stress. Although we observed relatively modest changes in lipid and glucose metabolism in response to Lpcat3-dependent perturbations in ER stress over the 7-day time frame of these studies, we cannot exclude the possibility that more chronic changes in Lpcat3 activity might have more robust metabolic effects.

Lpcat3 activity modulates inflammatory responses in vivo

Since alteration of membrane lipid composition has previously been shown to affect inflammatory signaling, we further investigated the influence of Lpcat3 activity on hepatic inflammation. Histological analysis of livers from wild-type C57BL/6 mice transduced with shLpcat3 adenovirus revealed marked infiltration of F4/80+ macrophages, consistent with ongoing inflammation (**Fig. 2-9A**). Macrophage infiltration in Lpcat3-knockdown livers was

confirmed by qPCR analysis of F4/80 gene expression (**Fig. 2-10A**). Furthermore, the mRNA expression of pro-inflammatory cytokines (MCP-1, TNFα and IL-1β) was elevated in shLpcat3-transduced livers compared to controls, indicative of enhanced inflammatory signaling (**Fig. 2-10B**). To comprehensively analyze the impact of Lpcat3 knockdown on hepatic gene expression, we performed transcriptional profiling. This analysis revealed that a large number of pro-inflammatory genes were induced in response to Lpcat3 knockdown, including pro-inflammatory cytokines and chemokines, cytokine and chemokine receptors, and complement components (**Fig. 2-9B**).

Next, we investigated whether Lpcat3 activity could also modulate hepatic inflammatory responses in the setting of metabolic disease and hepatic steatosis. Indeed, knockdown of Lpcat3 expression with an adenoviral shRNA vector in *ob/ob* mouse liver exacerbated the expression of a panel of pro-inflammatory cytokines and chemokines, including Cox-2, MCP-1,and MIP-2. (**Fig. 2-9C**). Consistent with increased hepatic inflammation, plasma ALT and AST levels were also increased in mice transduced with Lpcat3 knockdown adenoviral vector (**Fig. 2-10C**).

We further tested the effect of increased Lpcat3 activity on hepatic inflammatory signaling in both wild-type and genetically obese mice. Adenovirus-mediated Lpcat3 expression in wild-type livers reduced the basal expression of a panel of inflammatory cytokines (**Fig. 2-9D**). In fact, many of the same genes increased by Lpcat3 knockdown were reduced by Lpcat3 expression. Interestingly, we did not observe any difference in ER stress markers in wild-type mice overexpressing Lpcat3 (**Fig. 2-10D**), suggesting that the effects of Lpcat3 on inflammation may be independent of those on ER stress. We also employed *ob/ob* mice as a model of lipid-induced hepatic inflammation. Remarkably, expression of Lpcat3 in livers of these mice ameliorated hepatic inflammation, evidenced by a marked reduction in the expression of

inflammatory chemokines and cytokines (**Fig. 2-9E**). Similar results on inflammatory markers and plasma AST and ALT levels were also observed in *db/db* mice (**Fig. 2-10E, F**). These data suggest that Lpcat3 is a regulator of hepatic inflammation and that enhanced Lpcat3 activity has beneficial effects on inflammation in the setting of metabolic disease.

Lpcat3 activity affects the production of lipid inflammatory mediators

To address whether the effects of Lpcat3 activity on inflammation were cell-autonomous, we analyzed inflammatory signaling in cultured primary hepatocytes and macrophages. shRNA-mediated knockdown of Lpcat3 in primary mouse hepatocytes with an adenoviral vector led to increased expression of well-established hepatic inflammatory mediators, including CXCL10 and MIP-2 (**Fig. 2-11A**). Furthermore, knockdown of Lpcat3 ameliorated the suppressive effect of LXR agonist on the expression of these genes. Similarly, siRNA-mediated knockdown of Lpcat3 expression in murine peritoneal macrophages augmented the induction of inflammatory genes in response to LPS (**Fig. 2-12A**). Lpcat3 knockdown in macrophages blunted the ability of LXR agonist to repress MCP-1, and to a lesser extent, TNF-α expression. This observation suggests that Lpcat3 induction by LXR may contribute to the repressive effects of LXR agonists on some inflammatory genes.

Products of arachidonic acid and lysoPCs are well-known pro-inflammatory lipid mediators. Arachidonic acid-derived eicosanoids play multiple roles in local and systemic inflammation, including leukocyte chemotaxis and vasodilation; lysoPCs facilitate the activation of different immune cells and are key lipid mediators involved in the development of atherosclerosis (Funk, 2001; Kabarowski, 2009). Since activation of LXR-Lpcat3 pathway converts the bioactive free arachidonic acid and lysoPCs into PLs, we hypothesized that

increased activity of this pathway may serve to limit inflammatory mediator production by limiting substrate availability. In support of this idea, acute induction of Lpcat3 activity by treatment with LXR agonist (GW3965) strongly reduced the levels of multiple LysoPC species (**Fig. 2-11B**). This effect was completely abolished by Lpcat3 knockdown. Although we did not observe changes in lysoPC levels between shCtrl- and shLpcat3-treated WT mice after 8 d, this may reflect compensatory responses in LysoPC metabolism in the setting of chronic alteration of Lpcat3 activity. Furthermore, GC-MS analysis revealed greatly increased levels of free arachidonic acid in livers of wild-type mice in which Lpcat3 expression was knocked down (**Fig. 2-11C**). Conversely, ectopic expression of Lpcat3 in livers of wild-type mice markedly decreased levels of free arachidonate (**Fig. 2-11D**). We also analyzed PGE2 production by LPS-stimulated macrophages *in vitro*. Consistent with our hypothesis that Lpcat3 activity limits arachidonic acid availability for eicosanoid synthesis, ligand activation of LXR in these cells repressed PGE_2 secretion (**Fig. 2-12B**). Collectively, these findings suggest that Lpcat3 activity affects inflammation, at least in part, through modulation of lipid inflammatory mediator production.

Lpcat3 activity modulates c-Src activation in membrane microdomains

Increasing membrane saturation has been shown to affect the compartmentalization and activity of membrane-bound c-Src kinase by recruiting the protein to membrane microdomains, sometimes referred to as lipid rafts (Holzer et al., 2011). Activated c-Src initiates the downstream JNK signaling pathway, a central regulator of inflammation (Wellen and Hotamisligil, 2005). Given that activation of Lpcat3 reduces membrane saturation, we hypothesized that the LXR-Lpcat3 pathway might regulate the activity of the c-Src-JNK pathway

through modulation of membrane lipid composition. In support of this idea, treatment of primary macrophages with LXR agonist decreased LPS-stimulated phosphorylation of membrane-bound c-Src kinase (**Fig. 2-11E**). Induction of ABCA1, a canonical LXR target, served as a positive control for LXR activation. On the contrary, knockdown of Lpcat3 expression with an adenoviral shRNA vector in *ob/ob* mouse liver increased the phosphorylation of c-Src and JNK (**Fig. 2-11F**). To examine whether Lpcat3 activity altered the compartmentalization and activation of c-Src in membranes microdomains, Hep3B cells were treated with Lpcat3 siRNA followed by PA stimulation. Detergent-resistant membrane (DRM) was isolated through density gradient centrifugation. DRM and its associated proteins were enriched in fraction 2, as indicated by Flot1, a DRM marker; while soluble protein and cell debris were enriched in fraction 3 and 4, as shown by TfR, a membrane protein excluded from DRM. In Lpcat3-knockdown cells, phospho-c-Src abundance was greatly increased in the DRM fraction, although the amount of total c-Src protein in DRM was unchanged (**Fig. 2-11G**). This observation strongly suggests that a reduction in the abundance of Lpcat3 PL products alters the structure of membrane microdomains in a way that favors the activation of c-Src. Thus, in addition to modulation of lipid inflammatory mediators, Lpcat3 activity also regulates the activation of the c-Src-JNK pathway. Collectively, our results define mechanisms whereby LXR signaling modulates ER and inflammatory homeostasis in response to changing cellular lipid levels through Lpcat3.

Discussion

Given the difficulty of manipulating fatty acyl composition in living cells, few studies have addressed the physiological impact of dynamic changes in PL fatty acyl composition. We have shown here that LXR regulates PL fatty acyl composition through transcriptional induction of Lpcat3. Activation of the LXR-Lpcat3 pathway with synthetic LXR agonists promotes the formation of polyunsaturated PLs and decreases membrane saturation. This membrane remodeling counteracts saturated fatty acid-induced ER stress in hepatocytes and mouse liver. Furthermore, the LXR-Lpcat3 pathway ameliorates hepatic inflammation by modulating c-Src kinase activation and controlling the availability of lipid inflammatory mediators, including arachidonic acid and lysoPC. These observations identify Lpcat3 regulation as an important mechanism by which LXR signaling modulates lipid homeostasis in both physiology and disease.

Studies of *in vitro* biochemical systems have demonstrated that changes in PL fatty acyl composition strongly affect membrane protein function. Whether membrane fatty acyl composition is actively regulated by endogenous signaling pathway has not been intensively studied. The SREBP pathway functions as an important determinant of membrane lipid composition through the regulation of cholesterol and phospholipid synthesis (Brown and Goldstein, 1999; Dobrosotskaya et al., 2002; Walker et al., 2011). Our study has identified the LXR-Lpcat3 pathway as a physiological regulator of membrane fatty acyl composition. This function fits well with LXRs' previously defined roles as coordinators of cholesterol and fatty acid metabolism. The fatty acyl chain of polyunsaturated PL assumes a flexible and bent conformation, resulting in decreased membrane order and increased membrane fluidity. Notably, cellular levels of cholesterol, another important cellular membrane structural component, are also regulated by LXR signaling. Activation of LXRs reduces cholesterol levels by promoting

cholesterol efflux and inhibiting cholesterol uptake (Calkin and Tontonoz, 2012), an effect that would be expected to impact membrane order and fluidity. LXR is also an important regulator of SCD-1 expression (Chu et al., 2006; Repa et al., 2000). Increased desaturation of newly synthesized fatty acids would be expected to increase substrate availability for synthesis of unsaturated PC. Indeed, increased SCD-1 expression has been proposed to alleviate ER stress in atherosclerosis through a mechanism involving the lipid chaperone aP2 (Erbay et al., 2009). Thus, LXR signaling alters membrane lipid composition and modifies membrane physical properties through multiple mechanisms.

ER stress has been postulated to be an important contributor to metabolic disease, as it is observed in livers of obese mice and humans. In our study, we observed modest changes in systemic metabolism in response to short-term alterations in Lpcat3 activity. In particular, adenoviral expression of Lpcat3 in the livers of *ob/ob* mice lowered blood glucose and insulin levels. However, we believe that more chronic models (e.g. transgenics or knockouts) are better suited to test the ability of Lpcat3 to affect the development or progression of metabolic disease. Such models are currently under development.

The exact mechanisms by which obesity activates ER stress are incompletely understood, but saturated free fatty acids are believed to induce ER stress through the alteration of ER membrane structure (Borradaile et al., 2006; Volmer et al., 2013). Excess saturated fatty acids in cells are rapidly incorporated into PLs in ER membranes, resulting in increased membrane order and reduced membrane fluidity. Although the nature of the link between membrane fluidity and ER stress is not entirely clear, a growing body of evidence suggests that altered lipid composition affects the function of ER membrane proteins. For instance, enrichment of ER membrane with saturated PLs *in vitro* has been reported to inhibit the activity of the calcium pump SERCA2b (Li

et al., 2004), leading to ER Ca^{2+} depletion and the activation of ER stress. Recently, increased ER membrane saturation has been shown to enhance the activation of IRE1α and PERK directly (Volmer et al., 2013). We have shown here that the LXR-Lpcat3 pathway promotes the formation of polyunsaturated PC, and that this is itself is a potent ameliorator of ER stress. Our results support a biophysical model in which the LXR-Lpcat3 pathway alters membrane fatty acyl composition and fluidity, thereby counteracting the membrane-toxic effects of saturated fatty acid and alleviating ER stress.

Activated LXRs strongly suppress the expression of pro-inflammatory cytokines and chemokines in response to inflammatory stimuli (Hong and Tontonoz, 2008). However, the precise mechanisms underlying LXR's anti-inflammatory effects are not clear. In particular, potential connections between LXR's effects on lipid metabolism and inflammatory gene expression remain to be investigated. In this study, we have shown that *Lpcat3*, a direct transcriptional target of LXR, strongly modulates inflammatory responses *in vitro* and *in vivo*. Knockdown of *Lpcat3* in mouse liver induced a series of inflammatory responses, including macrophage infiltration, increased serum ASL and ALT, and upregulation of pro-inflammatory cytokines and chemokines. Conversely, overexpression of Lpcat3 had opposite effects, indicating that Lpcat3 enzyme activity is a potent modifier of inflammatory responses.

How does Lpcat3-medated modulation of PL composition influence inflammatory responses in hepatocytes? JNK is a pro-inflammatory kinase whose downstream signaling cascade controls various inflammatory responses, including the production of cytokines and chemokines (Solinas et al., 2007; Tuncman et al., 2006). Recently, Holzer et al. reported that changes in membrane lipid composition affect JNK activation by altering the compartmentalization and activation of c-Src kinase in cell membranes (Holzer et al., 2011). Treatment of cells with PA increases the

partitioning and activation of c-Src in membrane subdomains with higher order and rigidity, which in turn phosphorylates JNK and initiates the JNK signaling cascade. We found that knockdown of Lpcat3, which reduces membrane fluidity, also increased the activation of c-Src and JNK in livers of obese mice. Moreover, knockdown of Lpcat3 in hepatocytes enhanced the activation of c-Src in DRMs in response to PA stimulation, directly implicating c-Src and JNK signaling in the inflammatory effects of Lpcat3. These data suggest that modulation of membrane lipid composition is a key mechanism by which Lpcat3 activity affects inflammatory signaling in hepatocytes.

Our data also reveal a second mechanism of Lpcat3 action in inflammation. In addition to affecting membrane physical properties, modulation of Lpcat3 activity alters the availability of the two substrates in the enzymatic reaction, LysoPC and free arachidonic acid, both of which have been demonstrated to be involved in inflammatory responses. The reduction in LysoPC and arachidonic acid availability may be an additional mechanism by which Lpcat3 activity influences inflammatory signaling in mouse livers. In support of this possibility, LXR agonists inhibit the production of PGE2 by macrophages in culture. However, further studies are needed to elucidate the precise signaling pathways that connect LysoPC and arachidonic acid with hepatic inflammatory responses. Recently, another study reported that the LXR-Lpcat3 pathway also regulates phospholipid metabolism in human primary (Ishibashi et al., 2013). But in contrast to our work, that study suggested that LXR ligands stimulate eicosanoid secretion and pro-inflammatory effects. Such effects are difficult to reconcile with the large body of literature supporting the net anti-inflammatory actions of endogenous LXR signaling *in vitro* and *in vivo*. We find LXR signaling to be strongly anti-inflammatory in macrophages, although synthetic LXR agonists can have non-specific anti-inflammatory effects.

Abnormal cellular membrane lipid composition and fluidity have been observed in several metabolic diseases. For example, cellular membranes from atherosclerotic and obese individuals show decreased fluidity (Chen et al., 1995; Faloia et al., 1999; Gillies and Robinson, 1988). Although direct *in vivo* evidence is still needed to establish the pathogenic effects of abnormal membrane lipid composition, multiple *in vitro* studies have demonstrated that alterations in membrane lipid composition affect cellular ion balance, inflammation, and ER stress, all of which are involved in the development of chronic metabolic diseases. Our data indicate that increased Lpcat3 activity is able to modulate membrane lipid composition, increase membrane fluidity, and most importantly, reduce inflammation and ER stress in liver. These findings suggest that regulation of phospholipid remodeling might represent a novel strategy for intervention in chronic metabolic diseases.

Acknowledgements

We thank Kevin Wroblewski, Simon Beaven and Brian Parks for discussions and technical support. This work was supported by NIH grants HL030568 and DK063491 (to P.T.) and HL074214 and HL111906 (to D.A.F.). P.T. is an Investigator of the Howard Hughes Medical Institute.

Methods

Reagents and Plasmids–The synthetic LXR ligands GW3965 and T0901317 were synthesized according to published methods (Collins et al., 2002a; Collins et al., 2002b; Li et al., 2000). Thapsigargin and oxysterols were from Sigma (St. Louis, MO). Sequences of shRNA targeting mouse Lpcat3 were designed using BLOCK-iT RNAi designer tool (Invitrogen). Sense and antisense oligos were annealed and cloned into pENTR/U6 vector using the BLOCK-iT U6 RNAi Entry Vector Kit (Invitrogen). The shRNA constructs were further cloned into a gateway adapted pBabe-puro plasmids through LR recombination (Invitrogen). The following shRNA oligos were used: lacZ shRNA CACCGGGCCAGCTGTATAGACATCTCGAA AGATGTCTATACAGCTGGCCC; Lpcat3 shRNA CACCGCAGGTCAGCAGTCTAATTCGTTCAAGAGACGAATTAGACTGCTGACCTGC. Only sense strands are shown.

Generation and Amplification of Adenoviral Particles–Ad-Lpcat3 and Ad-shLpcat3 adenoviral vectors were generated by LR recombination of pEntr-Lpcat3 or pEntr/U6-shLpcat3 and pAd/CMV/V5-DEST (Invitrogen). The crude virus lysates were made by transfecting 293A cells with pAd/CMV/V5-DEST plasmids following the manufacturer's manual (Invitrogen). Viruses were amplified, purified and titred by Viraquest Inc.

Cell Culture–HEK293T, HEK293A, Huh7, and Raw264.7 cells were cultured in DMEM with 10% fetal bovine serum (FBS) and antibiotics at 37ºC and 5% CO2. Hep3B cells were cultured in EMEM. Mouse primary hepatocytes were isolated from 2- to 3-month-old male C57BL/6 mice, *Lxrα*$^{-/-}$, *Lxrβ*$^{-/-}$ or *Lxrαβ*$^{-/-}$ mice as described in (Pei et al., 2006) and cultured in William E

medium with 5% FBS. Bone marrow-derived macrophages and thioglycollate-elicited or concanavalin A-elicited peritoneal macrophages were isolated as described (Castrillo et al., 2003; Feng et al., 2003). Raw 264.7 stable cell lines were made by pBabe retro-viral vectors as described (Venkateswaran et al., 2000).

Gene Expression and Microarray Analysis–Total RNA was isolated from cells and tissues with Trizol (Invitrogen). cDNA was synthesized with the iScript cDNA synthesis kit (Bio-Rad, Hercules, CA) and quantified by real-time PCR using SYBR Green (Diagenode, Denville, NJ) and an ABI 7900 instrument. Gene expression levels were determined by using a standard curve. Each gene was normalized to 36B4 or GAPDH. Primer sequences are available upon request. For microarray experiments, liver tissues were harvested after 8 days post adenovirus injection. RNA was pooled from n≥5 biological replicates and processed in the UCLA Microarray Core Facility using Gene-Chip Mouse Gene 430.2 Arrays (Affymetrix, Santa Clara, CA). Data analysis was performed using software GenespringGX (Agilent, Santa Clara, CA).

Animal Studies–8-12 week old male C57BL/6, *ob/ob*, and *db/db* mice were acquired from Jackson Laboratory (Sacramento, CA). *Lxrα*$^{-/-}$, *Lxrβ*$^{-/-}$ and *Lxrαβ*$^{-/-}$ mice were originally gifts of David Mangelsdorf. Mice were fed a standard chow diet and housed in a temperature-controlled environment under a 12-hour light-dark cycle under pathogen-free conditions. For adenoviral infections, 8-10 week old male mice were injected with 2 x 10^9 or 3 x 10^9 PFU by tail-vein. Mice were sacrificed 7-9 d later following a 6 h fast. Fasting blood glucose was measured before sacrifice. Liver tissues were collected and immediately frozen in liquid nitrogen and stored at -80°C or fixed in 10% formalin for histochemical staining. Blood was collected by direct cardiac

puncture with plasma separated by centrifugation. ALT and AST were determined at the UCLA core facilities. Plasma lipids were measured using Wako L-Type TG M kit and Wako HR series NEFA-HR(2) kit (Wako, Richmond, VA). Liver triglycerides were extracted using Bligh-Dyer lipid extraction (Bligh and Dyer, 1959) and measured by Wako L-Type TG M kit (Wako, Richmond, VA). Animal experiments were conducted in accordance with the UCLA Animal Research Committee.

Lipid Analyses–Cells or liver tissue were snap frozen in liquid nitrogen. Cellb suspensions or liver homogenates were subsequently subjected to a modified Bligh-Dyer lipid extraction (Bligh and Dyer, 1959) in the presence of lipid class internal standards including eicosanoic acid, 1-0-heptadecanoyl-sn-glycero-3-phosphocholine, 1,2-dieicosanoyl-sn-glycero-3-phosphocholine, and 1,2-ditetradecanoyl-sn-glycero-3-phosphoethanolamine (Demarco et al., 2013). Fatty acids were converted to their pentafluorobenzyl esters and then were subsequently quantified using GC-MS with negative ion chemical ionization with methane as the reactant gas (Quehenberger et al., 2008). For phospholipids, lipid extracts were diluted in methanol/chloroform (4/1, v/v) and molecular species were quantified using electrospray ionization mass spectrometry on a triple quadrupole instrument (Themo Fisher Quantum Ultra) employing shotgun lipidomics methodologies (Han and Gross, 2005). Both phosphatidylcholine and lysophosphatidylcholine molecular species were quantified as lithiated adducts in the positive ion mode using neutral loss scanning for 59.1 amu (collision energy = -28eV).

Phosphatidylethanolamine molecular species were quantified in the negative ion survey scan mode. Individual molecular species were quantified by comparing the ion intensities of the

individual molecular species to that of the lipid class internal standard with additional corrections for type I and type II 13C isotope effects (Han and Gross, 2005).

Protein Analysis–Cells were lysed in RIPA buffer (Tris-HCL, pH 7.4 50 mM, NaCL 150 mM, NP-40 1%, Sodium deoxycholate 0.5%, SDS 0.1%) supplemented with protease and phosphatase inhibitors (Roche Molecular Biochemicals). Tissues were homogenized with a dounce in the same lysis buffer. Non-dissolved components in the lysate were cleared through centrifugation. Supernatants were run on 4%–12% Bis-Tris Gel (Invitrogen), transferred to hybond ECL membrane (GE Healthcare, Piscataway, NJ) and analyzed with anti-phospho-eIF2a (9721, Cell Signaling, Danvers, MA), anti-eIF2a (5324S, Cell Signaling), anti-phospho-PERK (3179S, Cell Signaling), anti-CHOP (sc-575, Santa Cruz Biotechnology, Santa Cruz, CA), anti-phospho-JNK (9251, Cell signaling), or anti-JNK (sc-7345, Santa Cruz Biotechnology). Goat anti-mouse and Goat anti-rabbit secondary antibodies were visualized with chemiluminescence (ECL, Amersham Pharmacia Biotech).

Membrane Preparation and in vitro Acyltransferase Activity Assay–The membranepreparation and in vitro acyltransferase activity assay were performed as described (Zhao et al., 2008). For membrane preparation, cells were harvested into ice-cold buffer (20 mM Tris-HCl pH 7.4, 250 mM sucrose, 1mM EDTA, and protease inhibitors), and lysed by passing through a 25 gauge needle. Total cell lysates were subjected to an initial centrifugation at 10,000g for 10 min at 4 °C. Supernatants were then centrifuged at 100,000g for 1 hour at 4°C to obtain a membrane fraction, which was suspended in the same buffer and stored at -80 °C. For activity assay, 200μM 16:0 lysophosphatidylcholine, 10 μCi H3 arachidonate-CoA and 5ug of

membrane protein were mixed in the reaction buffer (5 mM Tris-HCl pH 7.4, 1 mg/ml fatty acid-free bovine serum albumin) and incubated for 30 min. Reactions were stopped by adding 1 ml of chloroform/methanol (2:1, v/v). Lipids were extracted from the reaction mixture and separated by thin layer chromatography (chloroform:ethanol:water:triethylamine 30:35:7:35). Acyltransferase activity was determined by the formation of radiolabeled PC.

Fatty Acid and Phospholipid Treatment–Fatty acid free, low endotoxin BSA was purchased from Sigma (Sigma-Aldrich, St. Louis, MO) and dissolved in 1X phosphate buffered saline. Palmitic acids were dissolved in ethanol at 70°C and added to BSA solution at 37°C slowly with vortexing to make the final concentration of 10mM PA and 6:1 PA/BSA mole ratio. BSA-conjugated PA was filtered and added to cells at a final concentration of 500μM PA for 6 hours, unless otherwise indicated. Phospholipids dissolved in chloroform were purchased from Avanti Polar Lipids (Avanti Polar Lipids, Alabaster, AL). 1 μmol phospholipids solutions were evaporated under a stream of nitrogen gas and thoroughly dried by rotary vacuum dryer. Dry phospholipids were then hydrated in 1ml PBS at 55 °C for 16:0 18:0 PC and 25 °C for 16:0 20:4 PC with rigorous shaking, followed by sonication until the mixture became almost clear. PLs were added to cells at the indicated concentration(s).

Glucose tolerance tests (GTTs)–Mice were fasted for 6 hr prior to an i.p. injection of glucose (1 g/kg of body weight). Blood glucose was measured by tail vein bleeding and analyzed by Bayer Contour next EZ blood glucose monitoring system at 0, 15, 30, 60, 90 and 120 min after glucose injection.

Detergent-Resistant Membrane Isolation–The method for the isolation of detergentresistant lipid rafts has been described (Lingwood and Simons, 2007). Briefly, cells were washed and harvested in TNE buffer (150 mM NaCl, 2 mM EDTA, 50 mM Tris-HCl, pH7.4), lysed by passing through a 25 gauge needle, and solubilized with 1% TritonX-100 at 4ºC for 30 min. Lysates were mixed with Optiprep to form a 40% iodixanol bottom layer in the centrifuge tube, overlaid with a 30% iodixanol layer and a 0% (TNE buffer) layer, and centrifuged for 2 hours at 260,000 g in TLA100.2 rotor. Four fractions were collected from the top of the gradient and subjected to immunoblot analysis.

Prostaglandin E2 secretion–Primary mouse macrophages were treated with the LXR ligand GW3965 (1 μM) overnight. Then cells were washed with cold PBS twice and incubated in serum-free DMEM medium with 10 ng/ml LPS and GW3965 (1 μM). Culture medium was harvested after 8 hours and centrifuged to remove cellular debris. PGE2 concentration in the medium was measured by Prostaglandin E2 EIA Kit Cayman Chemical, Ann Arbor).

Statistical analysis–Statistics were performed using Student's t test (2 groups) or ANOVA (>2 groups), with post hoc tests to compare to the control group. Data are presented as means ± SEM or means ± SD as indicated and considered statistically significant at $p < 0.05$.

Figure Legends

Figure 2-1. LXRs regulate Lpcat3 expression and activity

(A) Primary mouse hepatocytes were treated with GW3965 (GW, 1 μM) and T0901317 (T, 1 μM) overnight. Gene expression in this and all subsequent figures was analyzed by real-time PCR. Results are representative of three independent experiments. Values are means ± SD.

(B) LXR-dependent regulation of Lpcat3 in primary mouse hepatocytes after overnight treatment with GW (1μM) or T (1 μM), and/or the RXR ligand LG268 (LG, 50 nM). Results are representative of two independent experiments. Values are means ± SD.

(C) Induction of Lpcat3 mRNA expression in livers of mice treated with 40 mg/kg/day GW3956 by oral gavage for 3 days (N=5 per group). Values are means ± SEM.

(D) Stable Raw 264.7-LXRα cells were treated with the LXR agonist GW (1 μM). Microsomal Lpcat3 activity was measured by radiolabeled acyltransferase assay. Thin-layer chromatogram is shown (upper panel); radioactivity in excised bands was quantified by scintillation counter (low left). Induction of Lpcat3 mRNA was measured by real-time PCR (lower right). Results are representative of two independent experiments. Values are means ± SD.

(E) ESI-MS/MS analysis of the abundance of PC species in Raw 264.6 cells treated with GW3965 (1 μM) for 48 h. N=3 per group. Values are means ± SEM.

(F) ESI-MS/MS analysis of the abundance of PC species in Raw 264.6 cells stably expressing shRNA targeting Lpcat3 (shLpcat3) or LacZ (shCtrl). N=3 per group. Values are means ± SEM.

(G) ESI-MS/MS analysis of the abundance of PC species in livers from C57BL/6 mice treated with 20 mg/kg GW3965 by oral gavage, 2 doses/day for 2 days (N=5 per group). Values are means ± SEM.

Statistical analysis was performed using student's t-test (C, E, F and G). *$p < 0.05$; **$p < 0.01$.

Figure 2-2. Transcription of Lpcat3 is directly activated by LXRs

(A) Tissue expression of Lpcat3 mRNA in mice determined by real-time PCR. Samples were pooled from 3 C57BL/6 mice. Values are means ± SD.

(B) Thioglycollate-elicited peritoneal macrophages from wild-type, LXRα-/-, LXRβ-/- and LXRαβ-/- mice were treated with the LXR agonist GW3965 (1 μM) or T0901317 (1 μM) overnight, followed by gene expression analysis by real-time PCR. Results are representative of two independent experiments. Values are means ± SD.

(C) Thioglycollate-elicited peritoneal macrophages from wild-type and LXRαβ-/- mice were treated with the LXR agonists GW (1 μM) or T (1 μM) and the RXR ligand LG268 (50 nM), followed by gene expression analysis by real-time PCR. Results are representative of two independent experiments. Values are means ± SD.

(D) Hep3B cells were treated with GW3965 overnight at the indicated concentration. Lpcat3 expression was analyzed by real-time PCR. Results are representative of two independent experiments. Values are means ± SD.

(E) Thioglycollate-elicited peritoneal macrophages were treated with the LXR agonists GW (1 μM) or T (1 μM), the RXR ligand LG268 (50 nM), and/or cycloheximide (CHX,10 μg/ml). Lpcat3 expression was analyzed by real-time PCR. Results represent independent replicate experiments. Values are means ± SD.

(F) Thioglycollate-elicited peritoneal macrophages from wild-type mice and LXRαβ-/- mice were treated with the LXR synthetic ligand GW (1 μM) or endogenous ligand 22(R)-hydroxycholesterol (2.5 μM). Lpcat3 expression was analyzed by real-time PCR. Results represent independent replicate experiments. Values are means ± SD.

(G) RAW264.7 macrophages were treated with vehicle, GW (1 μM) or 25-hydroxycholesterol (2.5μM) for 24 h. Gene expression was analyzed by real-time PCR. Results are representative of two independent experiments. Values are means ± SD.

(H) Induction of Lpcat3 mRNA expression in tissues of mice treated with 40 mg/kg/day GW3956 by oral gavage for 3 days (n=5 per group). Gene expression was measured by real-time PCR. Values are means ± SEM. *$p<0.05$ **$p<0.01$ by Student's t-test.

(I) Lpcat3 activity in RAW 264.7 cells stably expressing control shRNA (shCtrl), or two Lpcat3-targeting shRNAs (sh2-1 and sh4-1) were quantified by acyltransferase activity assay. Thin layer chromoatogram is shown at top and Lpcat3 mRNA expression was quantified by real-time PCR (bottom). Values are means ± SD.

Figure 2-3. LXRs and Lpcat3 attenuate lipid-induced ER stress

(A) Hep3B cells were pretreated with GW3965 (1 μM) for 24 h, followed by stimulation with BSA-conjugated palmitic acid (PA), BSA-conjugated oleic acid (OA) or thapsigargin (Tg) at the indicated concentration for 6 h. Induction of CHOP and ATF3 mRNA was analyzed by real-time PCR. Values are means ± SD.

(B) Primary hepatocytes from wild-type and *LXRαβ*$^{-/-}$ mice were pre-treated with GW3965 (1 μM) for 24 h and then stimulated with 500 μM BSA-conjugated palmitic acid (PA). Values are means ± SD.

(C) Hep3B cells were pretreated with GW3965 (GW) 1 μM for 24 h, followed by stimulation with a gradient concentration of BSA-conjugated palmitic acid (PA). Induction of Xbp-1 splicing was analyzed by PCR and gel electrophoresis.

(D) Hep3B cells were pre-treated with GW3965 (1 μM) for 24 h and stimulated with BSA-conjugated palmitic acid (PA) at the indicated concentrations. Activation of UPR signaling was analyzed by Immunoblotting.

(E) Concanavalin A-elicited peritoneal macrophages were treated with GW3965 (1 μM) and loaded with cholesterol by incubating with acetylated-LDL (ac-LDL) alone or acylated-LDL and ACAT inhibitor to induce ER stress. Values are means ± SD.

(F) Hep3B cells were transfected with siRNA targeting Lpcat3 (siLpcat3) or scramble (siCtrl) for 48 h, followed by stimulation with BSA-conjugated palmitic acid (PA). Values are means ± SD.

(G) Hep3B cells were transfected as in F. Phosphorylation of eIF2α was analyzed by immunoblot. t-EIF2α, total EIF2α; p-EIF2α, phospho-EIF2α.

Statistical analysis was by two-way ANOVA with Bonferroni post hoc tests (A, B, E and F): *$p < 0.05$; **$p < 0.01$; n.s., not significant.

Figure 2-4. LXR agonist attenuates saturated fatty acid-induced ER stress and apoptosis

(A) Hep3B cells were treated with the LXR ligand GW3965 at indicated concentration, followed by stimulation with 500 μM BSA-conjugated palmitic acid (PA). Gene expression was analyzed by real-time PCR. Results are representative of two independent experiments. Values are means ± SD.

(B) Primary mouse hepatocytes were treated with the LXR ligand GW3965 (1 μM), followed by treatment of 500 μM BSA-conjugated palmitic acid to induce ER stress. Expression of ER stress marker genes was analyzed by real-time PCR. Results are representative of two independent experiments. Values are means ± SD.

(C) Thioglycollate-elicited peritoneal macrophages were treated with the LXR ligand GW3965 (1 μM), followed by treatment of 500 μM BSA-conjugated palmitic acid to induce ER stress. Expression of ER stress marker genes was analyzed by real-time PCR. Results are representative of two independent experiments. Values are means ± SD.

(D) Microscopic images of Hep3B cells treated with GW3965 (1 μM), followed by palmitic acid (500 μM) stimulation for 18 h.

(E) Hep3B and Huh7 cells were treated with GW3965 (1 μM) for 24 h and stimulated with BSA-conjugated palmitic acid for 18 h. Caspase-3 activity was measured by colorimetric assay. Values are means ± SD. *$p<0.05$ by one way ANOVA with Bonferroni post hoc tests over veh+PA.

Figure 2-5. Lpcat3 contributes to LXR-dependent phospholipid remodeling and suppression of ER stress signaling

(A) Primary mouse hepatocytes were transfected with adenoviral shRNA targeting Lpcat3 (shLpcat3) or control (shCtrl) for 48 h, with GW3965 (1 μM) treatment for the last 24 h, followed by stimulation with 500 μM BSA-conjugated palmitic acid. Gene expression was analyzed by real-time PCR. The % repression of PA-induced gene expression by GW is indicated for control versus Lpcat3 knockdown. Values are means ± SEM.

(B) ESI-MS/MS analysis of the abundance of PC species in primary hepatocytes from wild-type or *LXRαβ*$^{-/-}$ (DKO) mice treated with the LXR agonist GW3965 (1 μM) for 48h. N=3 per group. Values are means ± SEM.

(C) ESI-MS/MS analysis of the abundance of PC species in wild-type primary hepatocytes transfected with adenoviral shRNA targeting Lpcat3 (shLpcat3) or control (shCtrl) for 48 h and treated with GW3965 (1 μM) for the last 24 h. N=3 per group. Values are means ± SEM.

(D) Hep3B cells were treated with increasing concentrations of liposomes composed of different species of PC, followed by stimulation with BSA-conjugated palmitic acid (PA) at 500 μM. Values are means ± SD.

(E) Hep3B cells were treated with vehicle or 1 μM bromoenol lactone (BEL) and then incubated with liposomes made with 16:0 20:4 PC or vehicle (veh). 500 μM BSA-conjugated palmitic acid (PA) was used to stimulated ER stress. Values are means ± SD.

Statistical analysis was by student's t-test (A, over the % repression in shCtrl), one-way ANOVA with Bonferroni post hoc tests (D) or two-way ANOVA with Bonferroni post hoc tests (B, C and E): *$p < 0.05$; **$p < 0.01$; N.S., not significant.

Figure 2-6. Inhibition of the LXR-Lpcat3 pathway increases ER stress *in vivo*

(A) Wild-type and *LXRαβ*$^{-/-}$ (DKO) mice were fed a western diet for 12 weeks. Liver gene expression was analyzed by real-time PCR. N=4-5 per group. Values are means ± SEM.

(B) *ob/ob* mice were transduced with adenoviral-expressed shRNA targeting Lpcat3 (shLpcat3) or control (shCtrl) for 7 days. UPR signaling in livers was analyzed by real-time PCR on day 7, normalized to Gapdh and shown as fold change over shCtrl. N=6 per group. Values are means ± SEM.

(C) Immunoblot analysis of protein expression in livers of *ob/ob* mice transduced with adenoviral shcontrol (shCtrl) or shLpcat3 for 7 days.

(D) ESI-MS/MS analysis of liver PC species from *ob/ob* mice transduced with shcontrol (shCtrl) or shLpcat3 for 7 days. N=6 per group. Values are means ± SEM.

Statistical analysis was performed using student's t-test. *p < 0.05; **p < 0.01.

Figure 2-7. Lpcat3 activity modulates phosphatidylethanolamine (PE) profiles *in vivo*

(A) ob/ob mice were transduced with adenoviral-expressed shRNA target Lpcat3 (shLpcat3) or control (shCtrl) for 7 days. Liver PE profile was quantified by ESI-MS/MS. N=6 per group. Values are means ± SEM.

(B) Metabolic parameters in ob/ob mice transduced with adenoviral-expressed shRNA targeting Lpcat3 (shLpcat3) or control (shCtrl) for 7 days. N=6 per group. Values are means ± SEM.

Statistical analysis was performed using student's t-test. *p < 0.05; **p < 0.01.

Figure 2-8. Expression of Lpcat3 in mouse liver affects metabolism and reduces ER stress

(A) *ob/ob* mice were transduced with adenovirus expressing Lpcat3 (Ad-Lpcat3) or control EGFP (Ad-Ctrl) for 7 days. Liver gene expression was determined by real-time PCR, normalized to 36B4, and presented as fold change over Ad-Ctrl. N=6 per group. Values are means ± SEM.

(B) Metabolic parameters in *ob/ob* mice transduced with control EGFP (Ctrl) or Lpcat3 (Lpcat3) adenovirus for 7 days. N=6 per group. Values are means ± SEM.

(C) Glucose tolerance test performed on *ob/ob* mice transduced with control EGFP or Lpcat3 adenovirus 4 days after infection. N=6 per group. Values are means ± SEM.

(D) *db/db* mice were transduced with adenovirus expressing Lpcat3 (Ad-Lpcat3) or control EGFP (Ad-Ctrl) for 7 days. Gene expression was determined by real-time PCR, normalized to 36B4 and shown as fold change over Ad-Ctrl. N=5 per group. Values are means ± SEM.

Statistical analysis was performed using student's t-test compared to control. *p < 0.05; **p < 0.01.

Figure 2-9. Lpcat3 activity modulates hepatic inflammation *in vivo*

(A) Immunostaining with F4/80 antibody of liver sections from C57BL/6 mice transduced with adenoviral-expressed shRNA targeting Lpcat3 (shLpcat3) or control (shCtrl) for 8.

(B) C57BL/6 mice were transduced with adenovirus-expressed shLpcat3 or shCtrl. Gene expression in livers was analyzed by Affymetrix arrays after 8 d. Select inflammatory genes are presented by heatmap. N=5 per group.

(C) Gene expression of livers from *ob/ob* mice transduced with shLpcat3 or shCtrl for 7 d. Results were normalized to 36B4 and are presented as fold change over shCtrl. N=6 per group. Values are means ± SEM.

(D) Gene expression of livers from C57BL/6 mice transduced with adenoviral-expressed Lpcat3 (Ad-Lpcat3) or control EGFP (Ad-GFP) for 9 d. N=6 per group. Results were normalized to 36B4 and are presented as fold change over Ad-GFP. Values are means ± SEM.

(E) Gene expression of livers from *ob/ob* mice transduced with Ad-Lpcat3 or Ad-GFP for 7 days. N=6 per group. Results were normalized to 36B4 and are presented as fold change over Ad-GFP. Values are means ± SEM. Statistical analysis was by student's t-test. *p < 0.05; **p < 0.01.

Figure 2-10. Lpcat3 activity regulates inflammatory gene expression in mouse liver

(A) Quantitation of F4/80 expression in livers of mice transduced with adenoviral-expressed shRNA targeting Lpcat3 (shLpcat3) or control (Ctrl) for 8 days by real-time PCR. N=5 per group. Values are means ± SEM.

(B) Pro-inflammatory cytokine expression in liver of mice in (A) was quantified by real-time PCR. N=5 per group. Values are means ± SEM.

(C) Serum ASL and ALT level of ob/ob mice transduced with adenoviral-expressed shRNA targeting Lpcat3 (shLpcat3) or control (Ctrl) for 7 days. N=5 per group. Values are means ± SEM.

(D) Gene expression of livers from C57BL/6 mice transduced with adenoviral vectors expressing control (Ad-Ctrl) or Lpcat3 (Ad-Lpcat3) for 9 days. N=6 per group. Values are means ± SEM.

(E) Serum ASL and ALT level of db/db mice transduced with adenoviral-expressed Lpcat3 or control EGFP (Ctrl) for 7 days. N≥4 per group. Values are means ± SEM.

(F) Inflammatory gene expression in livers of mice transduced with adenoviral vectors expressing GFP (Ad-Ctrl) or Lpcat3 (Ad-Lpcat3) for 7 days was quantified by real-time PCR. N ≥4 per group. Values are means ± SEM.

Statistical analysis was performed using student's t-test. *$p < 0.05$; **$p < 0.01$.

Figure 2-11. Lpcat3 activity controls lipid mediator availability and c-Src activation

(A) Primary hepatocytes were transduced with adenoviral-expressed shLpcat3 or shCtrl at MOI 10 for 60 h and treated with vehicle or GW3965 for 24 h, followed by PA stimulation. Gene expression was analyzed by real-time PCR, normalized to 36B4 and shown as fold change over veh+DMSO+shctrl. Values are means ± SD.

(B) ESI-MS/MS analysis of lysophosphatidylcholine species in the livers from C57BL/6 mice transduced with shLpcat3 or shCtrl for 8 d, and gavaged with GW3965 at 40 mg/kg body weight once per day on day 6, 7 and 8. N=5 per group. Values are means ± SEM.

(C) GC-MS analysis of free fatty acid species in the livers from C57BL/6 mice transduced with shLpcat3 or shCtrl for 8 d. Results are presented as % of total free fatty acid.

(D) GC-MS analysis of free fatty acid species in the livers from C57BL/6 mice transduced with aA-Lpcat3 or Ad-EGFP. N=6 per group. Results are presented as % of total free fatty acid.

(E) Primary mouse macrophages were treated with GW3965 (1 μM) and stimulated with 10 ng/ml LPS. Cellular membranes were isolated by ultracentrifugation and analyzed by immunoblotting.

(F) Immunoblot analysis of livers from *ob/ob* mice transduced with adenoviral shLpcat3 or shCtrl for 7 d.

(G) Hep3B cells were transfected with adenoviral shLpcat3 or shCtrl for 48 h, followed by stimulation with 500 μM BSA-conjugated palmitic acid (PA). Detergent-resistant membrane were isolated by gradient centrifugation and analyzed by immunoblotting.

Statistical analysis was by student's t-test (A, D and E) or two-way ANOVA with Bonferroni post hoc tests (B). For (C), student's t-test was performed between vehicle and GW treatment in each subgroup. *$p < 0.05$; **$p < 0.01$.

Figure 2-12. LXR activation of Lpcat3 suppresses inflammation in primary macrophages

(A) Primary macrophages were transfected with siRNA targeting Lpcat3 (siLpcat3) or control (siCtrl) and treated with GW3965 (1 μM). Inflammatory responses were induced by LPS at 10 ng/ml. Gene expression was analyzed by real-time PCR. Values are means ± SD.

(B) Primary mouse macrophages were treated with the LXR ligand GW3965 (1 μM) and stimulated with 10 ng/ml LPS. Prostaglandin E2 (PGE) secretion in the medium was measured by ELISA. *$p < 0.05$ by two-way ANOVA with Bonferroni post-hoc tests. Values are means ± SD.

Figure 2-1 LXRs regulate Lpcat3 expression and activity

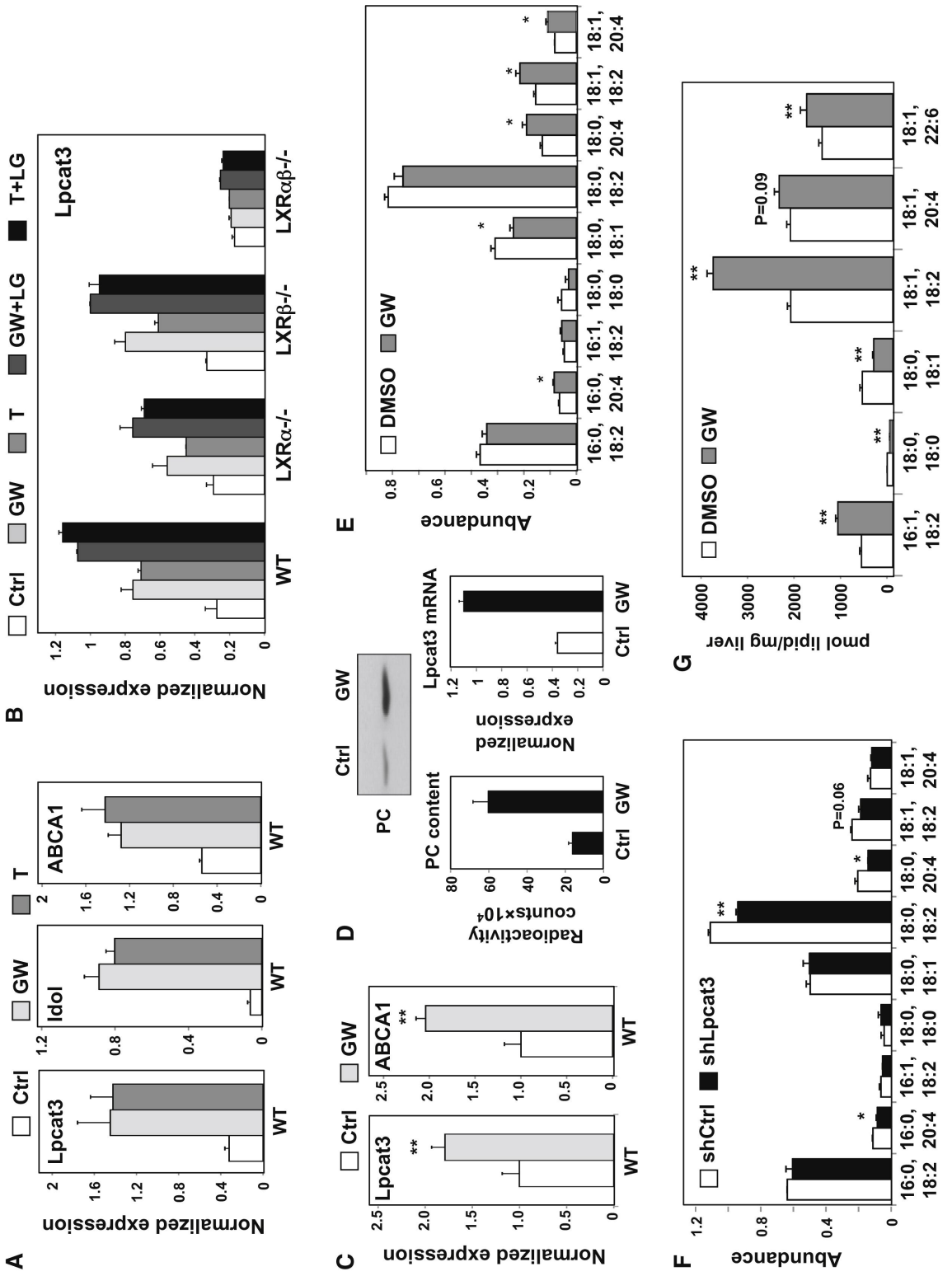

Figure 2-2. Transcription of Lpcat3 is directly activated by LXRs

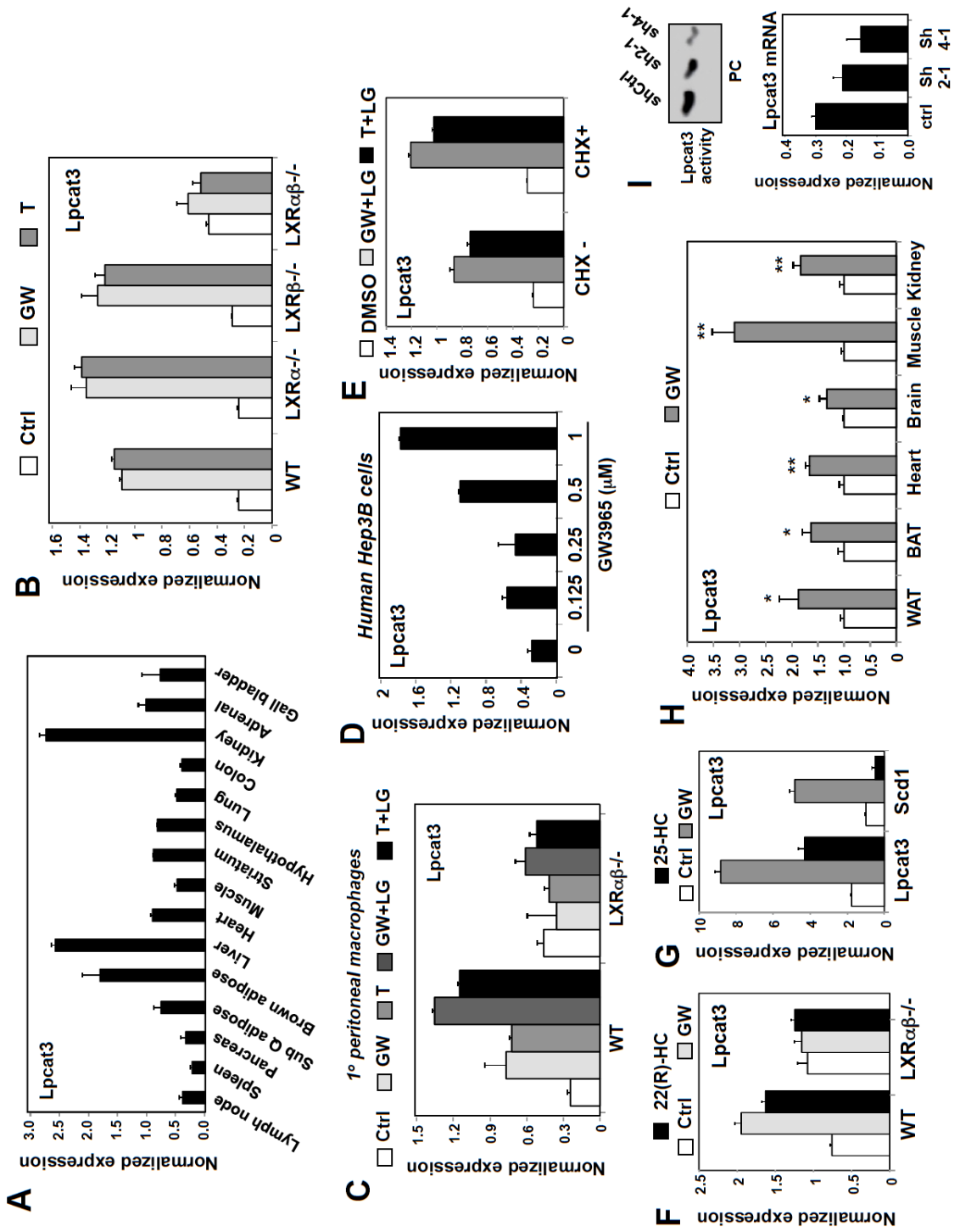

Figure 2-3. LXRs and Lpcat3 attenuate lipid-induced ER stress

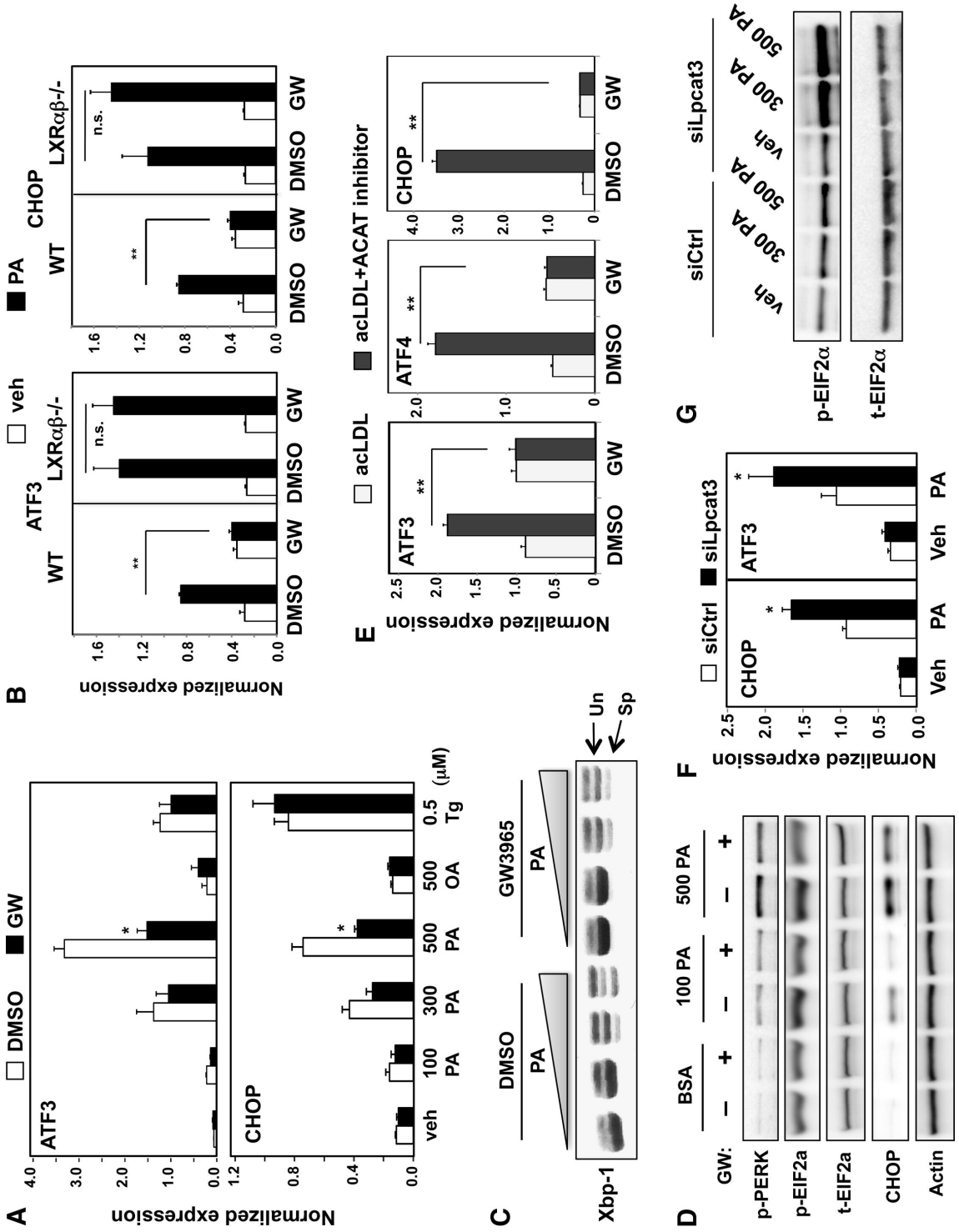

Figure 2-4. LXR agonist attenuates saturated fatty acid-induced ER stress and apoptosis

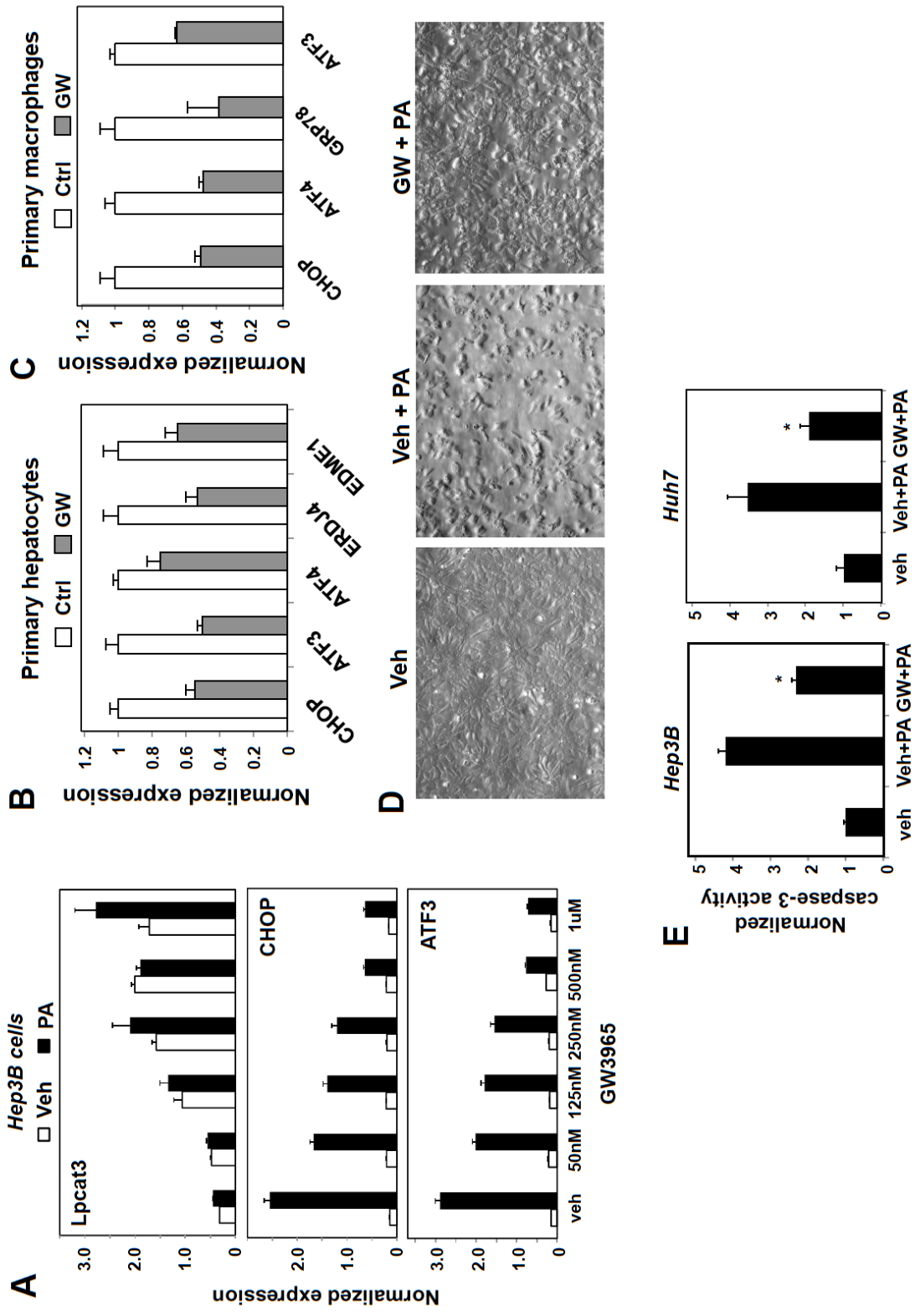

Figure 2-5. Lpcat3 contributes to LXR-dependent PL remodeling and ER stress reduction

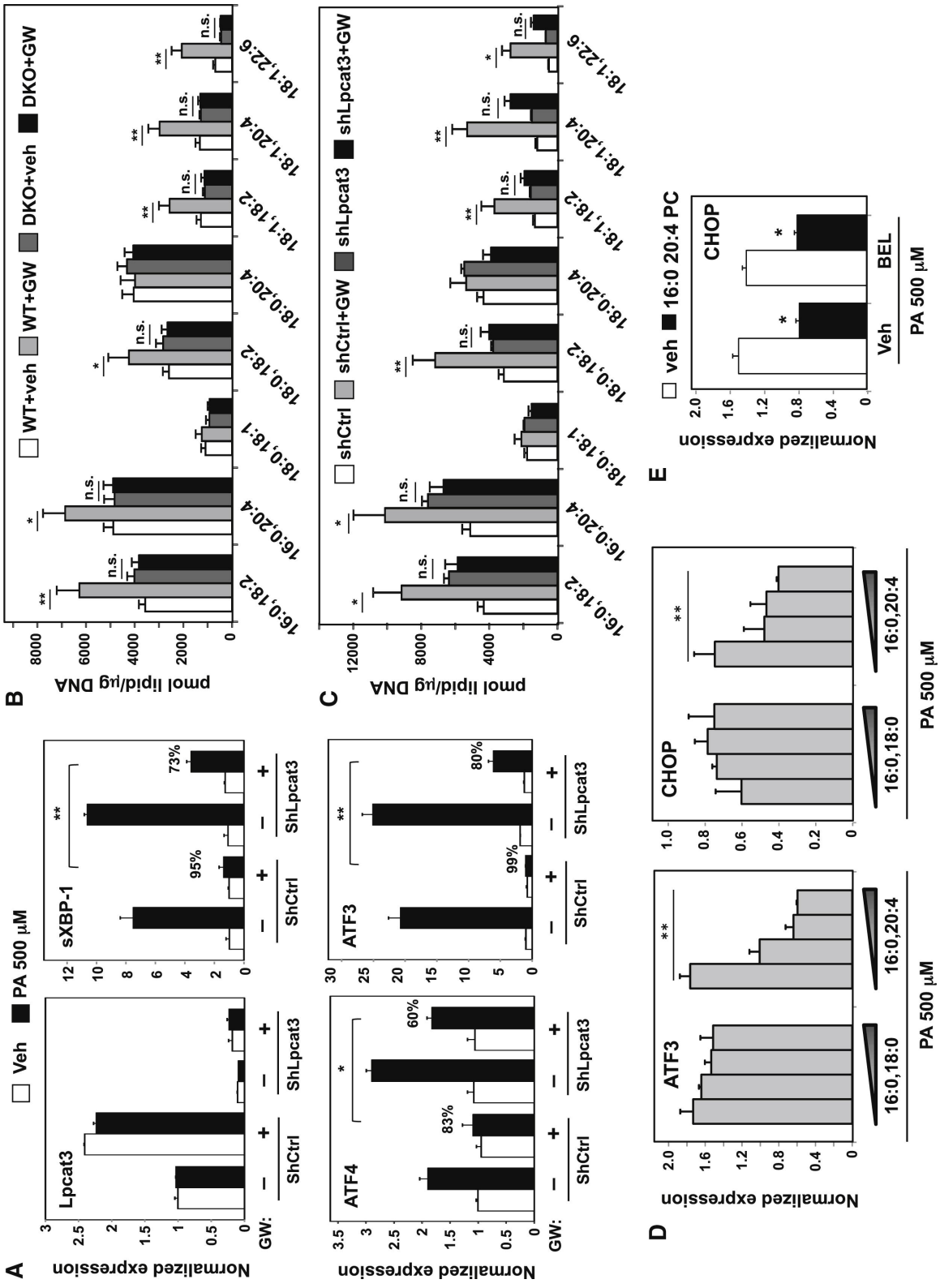

Figure 2-6 Inhibition of the LXR-Lpcat3 pathway increases ER stress *in vivo*

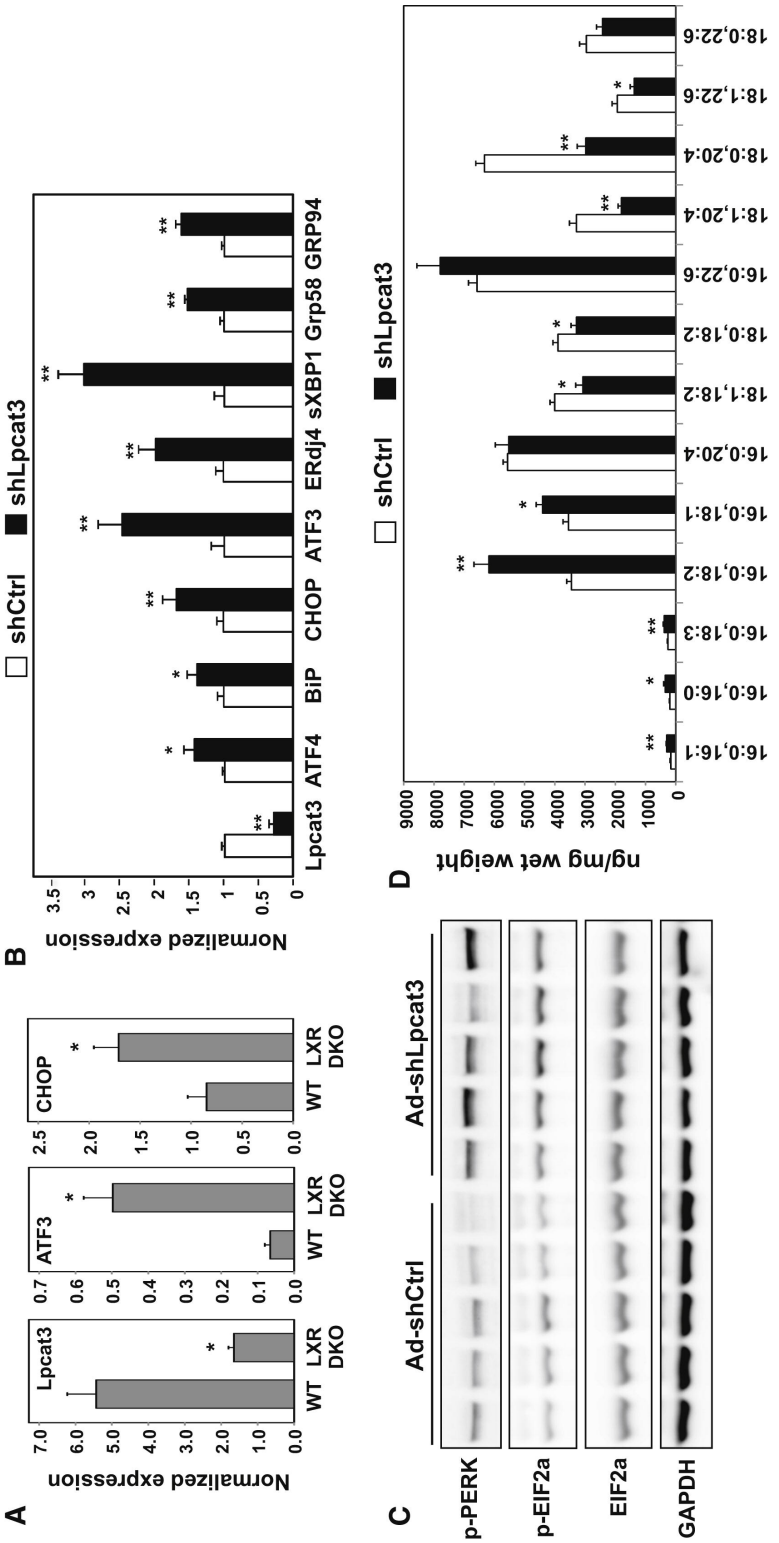

Figure 2-7. Lpcat3 activity modulates phosphatidylethanolamine (PE) profiles *in vivo*

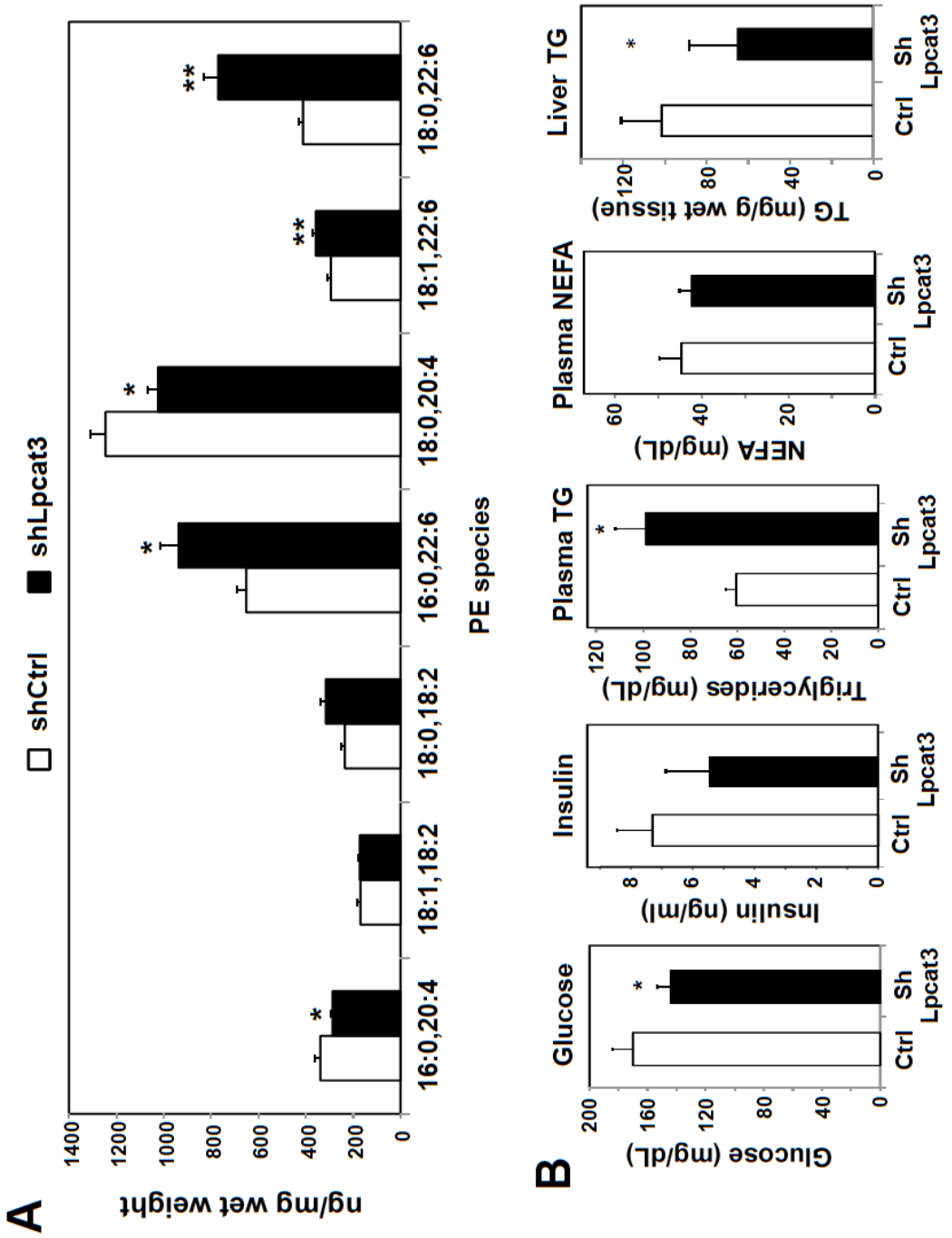

Figure 2-8. Expression of Lpcat3 in mouse liver affects metabolism and reduces ER stress

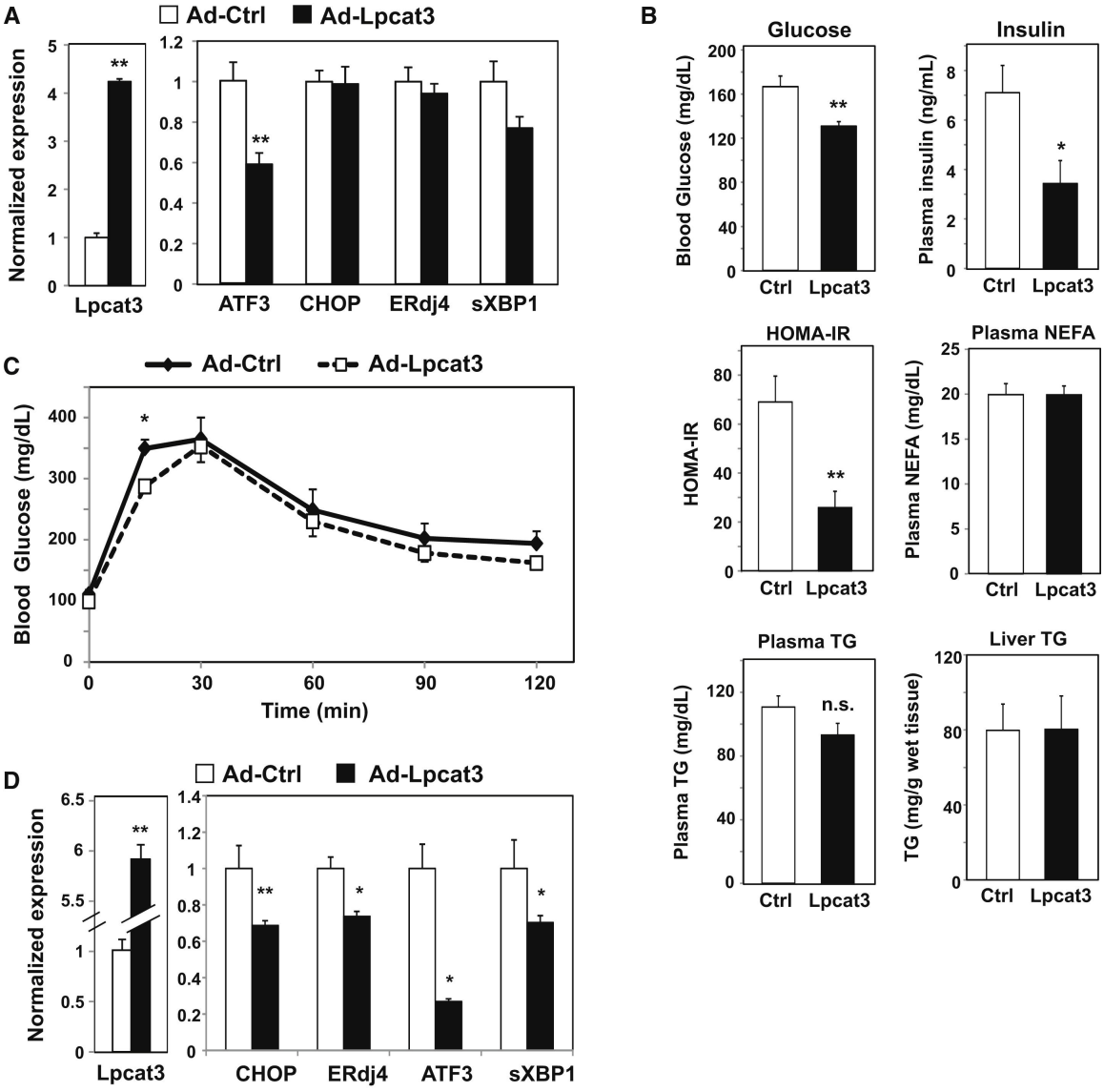

Figure 2-9. Lpcat3 activity modulates hepatic inflammation *in vivo*

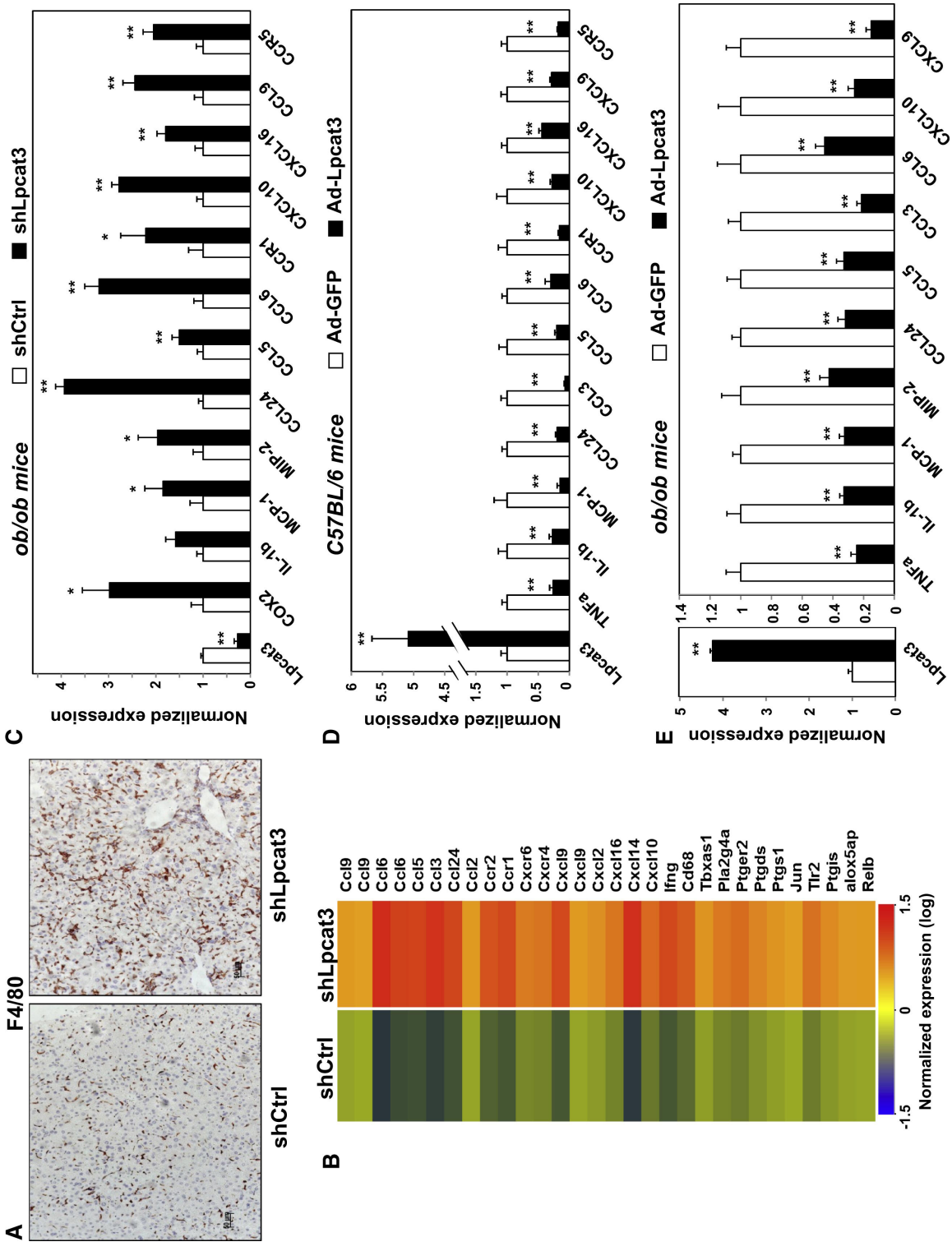

Figure 2-10. Lpcat3 activity regulates inflammatory gene expression in mouse liver

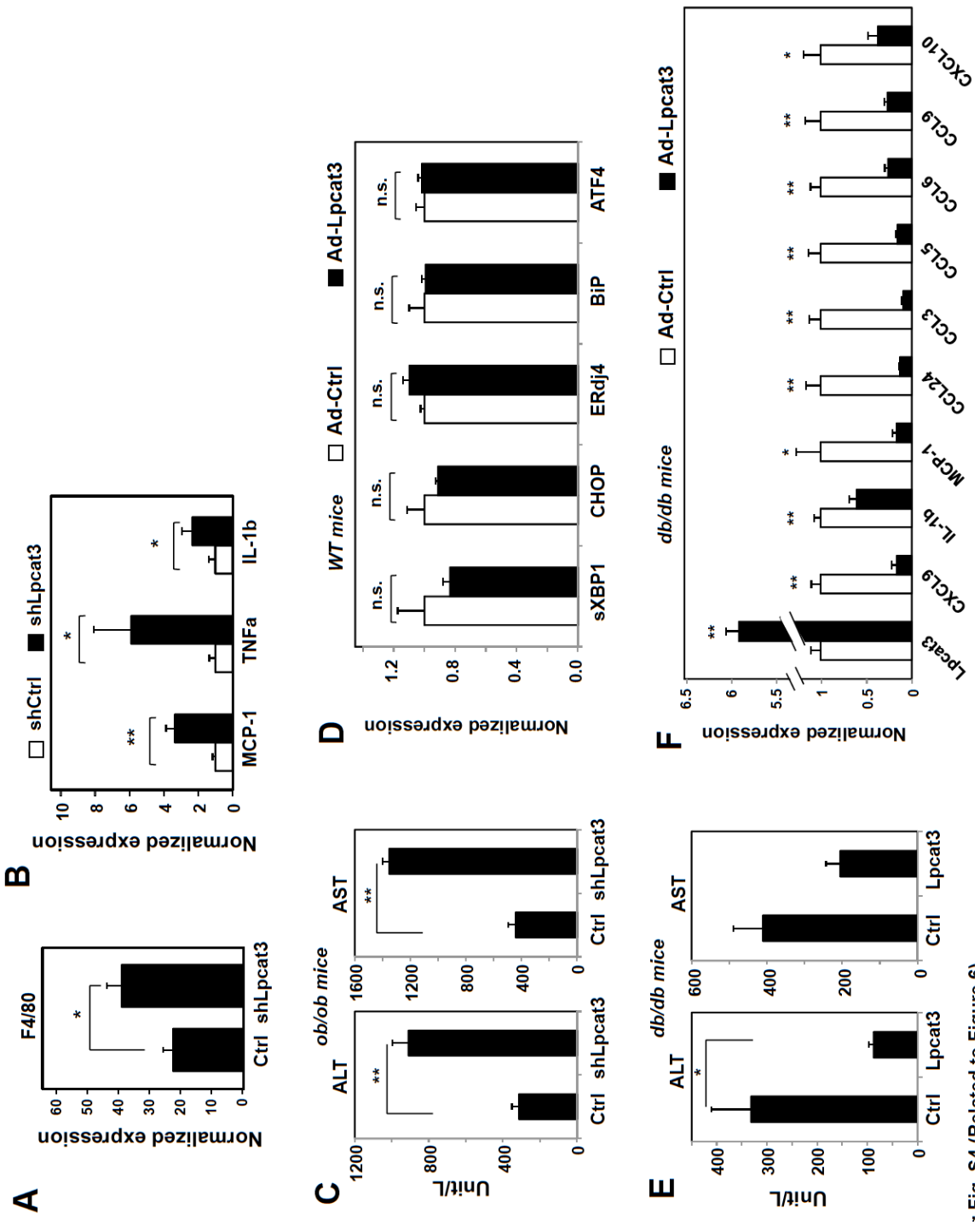

Figure 2-11. Lpcat3 activity controls lipid mediator availability and c-Src activation

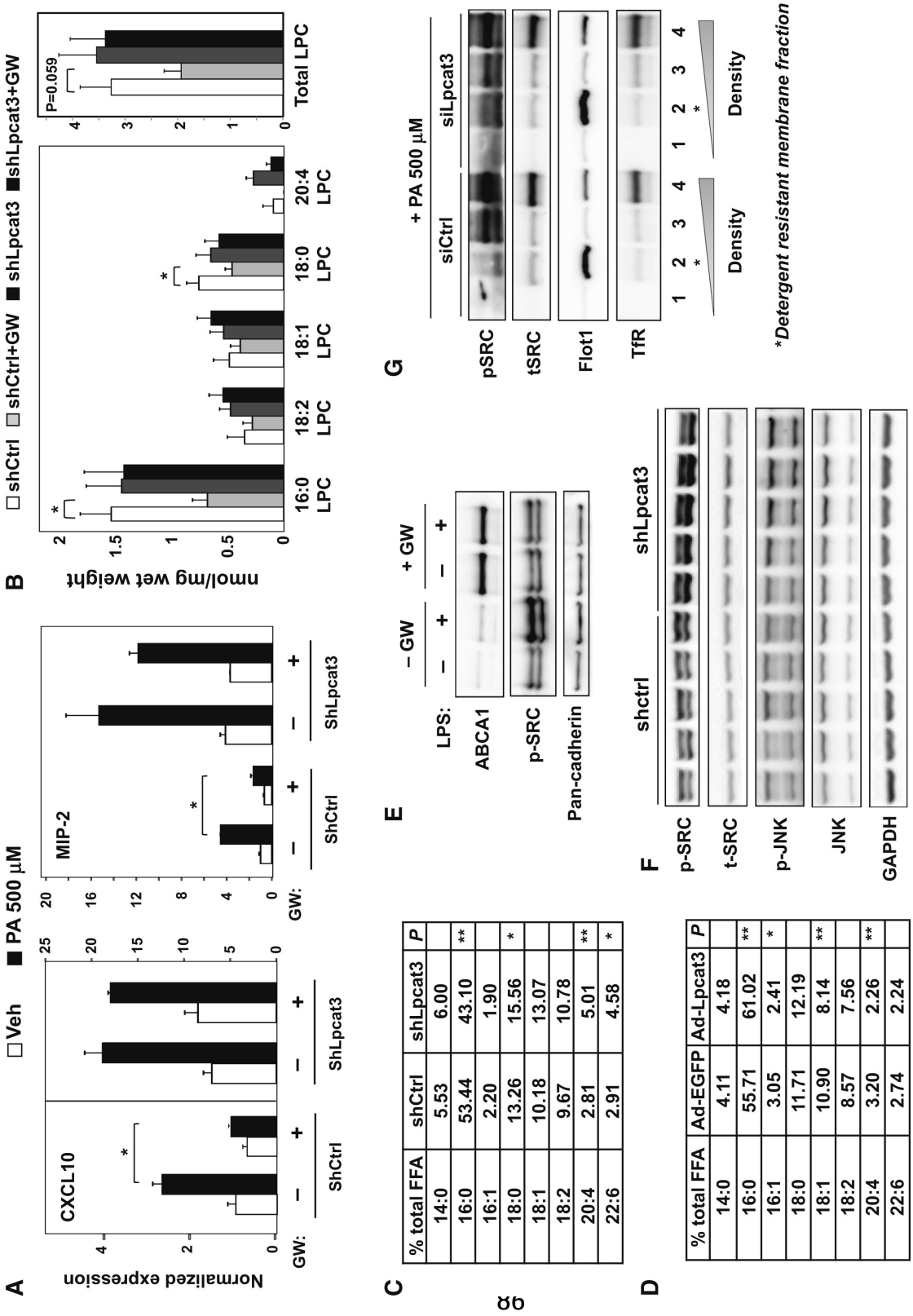

% total FFA	shCtrl	shLpcat3	*P*
14:0	5.53	6.00	
16:0	53.44	43.10	**
16:1	2.20	1.90	
18:0	13.26	15.56	*
18:1	10.18	13.07	
18:2	9.67	10.78	
20:4	2.81	5.01	**
22:6	2.91	4.58	*

% total FFA	Ad-EGFP	Ad-Lpcat3	*P*
14:0	4.11	4.18	
16:0	55.71	61.02	**
16:1	3.05	2.41	*
18:0	11.71	12.19	
18:1	10.90	8.14	**
18:2	8.57	7.56	
20:4	3.20	2.26	**
22:6	2.74	2.24	

Figure 2-12. LXR activation of Lpcat3 suppresses inflammation in primary macrophages

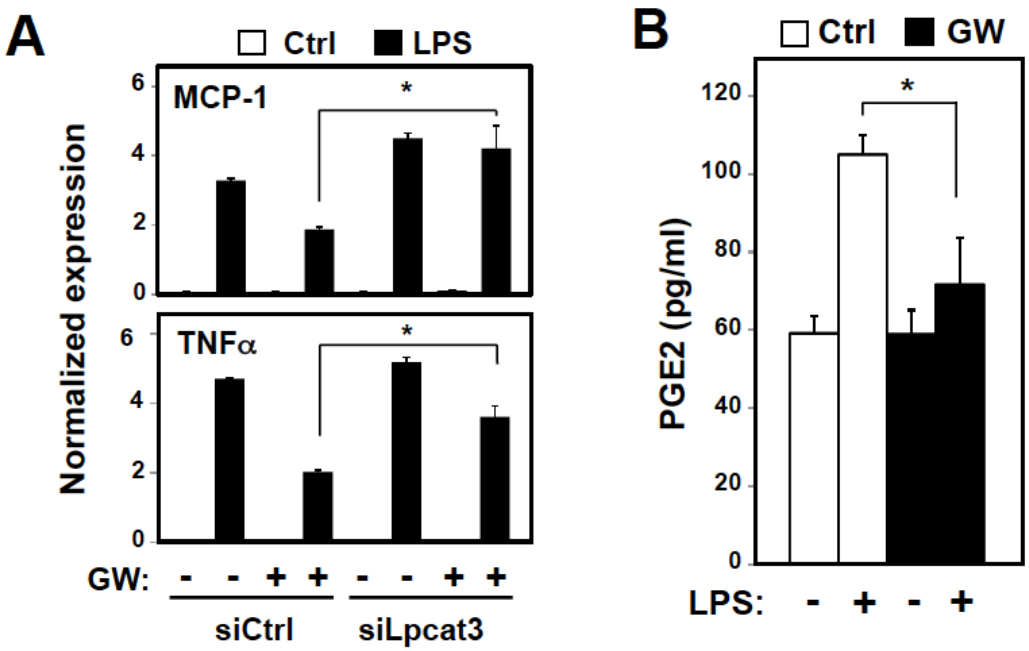

References:

Ariyama, H., Kono, N., Matsuda, S., Inoue, T., and Arai, H. (2010). Decrease in membrane phospholipid unsaturation induces unfolded protein response. The Journal of biological chemistry 285, 22027-22035.

Bligh, E.G., and Dyer, W.J. (1959). A rapid method of total lipid extraction and purification. Canadian journal of biochemistry and physiology 37, 911-917.

Borradaile, N.M., Han, X., Harp, J.D., Gale, S.E., Ory, D.S., and Schaffer, J.E. (2006). Disruption of endoplasmic reticulum structure and integrity in lipotoxic cell death. Journal of lipid research 47, 2726-2737.

Brown, M.S., and Goldstein, J.L. (1999). A proteolytic pathway that controls the cholesterol content of membranes, cells, and blood. Proceedings of the National Academy of Sciences of the United States of America 96, 11041-11048.

Calder, P.C. (2008). The relationship between the fatty acid composition of immune cells and their function. Prostaglandins, leukotrienes, and essential fatty acids 79, 101-108.

Calkin, A.C., and Tontonoz, P. (2012). Transcriptional integration of metabolism by the nuclear sterol-activated receptors LXR and FXR. Nature reviews. Molecular cell biology 13, 213-224.

Castrillo, A., Joseph, S.B., Vaidya, S.A., Haberland, M., Fogelman, A.M., Cheng, G., and Tontonoz, P. (2003). Crosstalk between LXR and toll-like receptor signaling mediates bacterial and viral antagonism of cholesterol metabolism. Molecular cell 12, 805-816.

Chen, M., Mason, R.P., and Tulenko, T.N. (1995). Atherosclerosis alters the composition, structure and function of arterial smooth muscle cell plasma membranes. Biochimica et biophysica acta 1272, 101-112.

Chu, K., Miyazaki, M., Man, W.C., and Ntambi, J.M. (2006). Stearoyl-coenzyme A desaturase 1 deficiency protects against hypertriglyceridemia and increases plasma high-density lipoprotein cholesterol induced by liver X receptor activation. Molecular and cellular biology 26, 6786-6798.

Collins, J.L., Fivush, A.M., Maloney, P.R., Stewart, E.L., and Willson, T.M. (2002a). Preparation of substituted phenylacetamides and benzamides as agonists for Liver X receptors (LXR). PCT Int. Appl. WO 2002/024632 A2 20020328.

Collins, J.L., Fivush, A.M., Watson, M.A., Galardi, C.M., Lewis, M.C., Moore, L.B., Parks, D.J., Wilson, J.G., Tippin, T.K., Binz, J.G., Plunket, K.D., Morgan, D.G., Beaudet, E.J., Whitney, K.D., Kliewer, S.A., and Willson, T.M. (2002b). Identification of a nonsteroidal liver X receptor agonist through parallel array synthesis of tertiary amines. Journal of medicinal chemistry 45, 1963-1966.

Cornelius, F. (2001). Modulation of Na,K-ATPase and Na-ATPase activity by phospholipids and cholesterol. I. Steady-state kinetics. Biochemistry 40, 8842-8851.

Cuschieri, J., and Maier, R.V. (2007). Oxidative stress, lipid rafts, and macrophage reprogramming. Antioxidants & redox signaling 9, 1485-1497.

Demarco, V.G., Ford, D.A., Henriksen, E.J., Aroor, A.R., Johnson, M.S., Habibi, J., Ma, L., Yang, M., Albert, C.J., Lally, J.W., Ford, C.A., Prasannarong, M., Hayden, M.R., Whaley-Connell, A.T., and Sowers, J.R. (2013). Obesity-related alterations in cardiac lipid profile and nondipping blood pressure pattern during transition to diastolic dysfunction in male db/db mice. Endocrinology 154, 159-171.

Demeure, O., Lecerf, F., Duby, C., Desert, C., Ducheix, S., Guillou, H., and Lagarrigue, S. (2011). Regulation of LPCAT3 by LXR. Gene 470, 7-11.

Erbay, E., Babaev, V.R., Mayers, J.R., Makowski, L., Charles, K.N., Snitow, M.E., Fazio, S., Wiest, M.M., Watkins, S.M., Linton, M.F., and Hotamisligil, G.S. (2009). Reducing endoplasmic reticulum stress through a macrophage lipid chaperone alleviates atherosclerosis. Nature medicine 15, 1383-1391.

Faloia, E., Garrapa, G.G., Martarelli, D., Camilloni, M.A., Lucarelli, G., Staffolani, R., Mantero, F., Curatola, G., and Mazzanti, L. (1999). Physicochemical and functional modifications induced

by obesity on human erythrocyte membranes. European journal of clinical investigation 29, 432-437.

Feng, B., Yao, P.M., Li, Y., Devlin, C.M., Zhang, D., Harding, H.P., Sweeney, M., Rong, J.X., Kuriakose, G., Fisher, E.A., Marks, A.R., Ron, D., and Tabas, I. (2003). The endoplasmic reticulum is the site of cholesterol-induced cytotoxicity in macrophages. Nature cell biology 5, 781-792.

Fessler, M.B., and Parks, J.S. (2011). Intracellular lipid flux and membrane microdomains as organizing principles in inflammatory cell signaling. J Immunol 187, 1529-1535.

Fu, S., Yang, L., Li, P., Hofmann, O., Dicker, L., Hide, W., Lin, X., Watkins, S.M., Ivanov, A.R., and Hotamisligil, G.S. (2011). Aberrant lipid metabolism disrupts calcium homeostasis causing liver endoplasmic reticulum stress in obesity. Nature 473, 528-531.

Funk, C.D. (2001). Prostaglandins and leukotrienes: advances in eicosanoid biology. Science 294, 1871-1875.

Gillies, P., and Robinson, C. (1988). Decreased plasma membrane fluidity in the development of atherosclerosis in cholesterol-fed rabbits. Atherosclerosis 70, 161-164.

Han, X., and Gross, R.W. (2005). Shotgun lipidomics: electrospray ionization mass spectrometric analysis and quantitation of cellular lipidomes directly from crude extracts of biological samples. Mass spectrometry reviews 24, 367-412.

Hishikawa, D., Shindou, H., Kobayashi, S., Nakanishi, H., Taguchi, R., and Shimizu, T. (2008). Discovery of a lysophospholipid acyltransferase family essential for membrane asymmetry and diversity. Proceedings of the National Academy of Sciences of the United States of America 105, 2830-2835.

Holzer, R.G., Park, E.J., Li, N., Tran, H., Chen, M., Choi, C., Solinas, G., and Karin, M. (2011). Saturated fatty acids induce c-Src clustering within membrane subdomains, leading to JNK activation. Cell 147, 173-184.

Hong, C., and Tontonoz, P. (2008). Coordination of inflammation and metabolism by PPAR and LXR nuclear receptors. Current opinion in genetics & development 18, 461-467.

Hotamisligil, G.S. (2010). Endoplasmic reticulum stress and the inflammatory basis of metabolic disease. Cell 140, 900-917.

Ishibashi, M., Varin, A., Filomenko, R., Lopez, T., Athias, A., Gambert, P., Blache, D., Thomas, C., Gautier, T., Lagrost, L., and Masson, D. (2013). Liver x receptor regulates arachidonic acid distribution and eicosanoid release in human macrophages: a key role for lysophosphatidylcholine acyltransferase 3. Arteriosclerosis, thrombosis, and vascular biology 33, 1171-1179.

Kabarowski, J.H. (2009). G2A and LPC: regulatory functions in immunity. Prostaglandins & other lipid mediators 89, 73-81.

Kennedy, E.P., and Weiss, S.B. (1956). The function of cytidine coenzymes in the biosynthesis of phospholipides. The Journal of biological chemistry 222, 193-214.

Klein, I., Moore, L., and Pastan, I. (1978). Effect of liposomes containing cholesterol on adenylate cyclase activity of cultured mammalian fibroblasts. Biochimica et Biophysica Acta (BBA) - Biomembranes 506, 42-53.

Kume, N., Cybulsky, M.I., and Gimbrone, M.A., Jr. (1992). Lysophosphatidylcholine, a component of atherogenic lipoproteins, induces mononuclear leukocyte adhesion molecules in cultured human and rabbit arterial endothelial cells. J Clin Invest 90, 1138-1144.

Lands, W.E. (1958). Metabolism of glycerolipides; a comparison of lecithin and triglyceride synthesis. The Journal of biological chemistry 231, 883-888.

Li, L., Medina, J.C., Hasegawa, H., Cutler, S.T., Liu, J., Zhu, L., Shan, B., and Lustig, K. (2000). Preparation of bis(trifluoromethyl)hydroxymethylbenzenesulfonamides, -ureas, and -carbamates as liver X receptor modulators. PCT Int. Appl. WO 2000/054759 A2 20000921.

Li, Y., Ge, M., Ciani, L., Kuriakose, G., Westover, E.J., Dura, M., Covey, D.F., Freed, J.H., Maxfield, F.R., Lytton, J., and Tabas, I. (2004). Enrichment of endoplasmic reticulum with cholesterol inhibits sarcoplasmic-endoplasmic reticulum calcium ATPase-2b activity in parallel with increased order of membrane lipids: implications for depletion of endoplasmic reticulum calcium stores and apoptosis in cholesterol-loaded macrophages. The Journal of biological chemistry 279, 37030-37039.

Li, Z., Ding, T., Pan, X., Li, Y., Li, R., Sanders, P.E., Kuo, M.S., Hussain, M.M., Cao, G., and Jiang, X.C. (2012). Lysophosphatidylcholine acyltransferase 3 knockdown-mediated liver lysophosphatidylcholine accumulation promotes very low density lipoprotein production by enhancing microsomal triglyceride transfer protein expression. The Journal of biological chemistry 287, 20122-20131.

Miyazaki, M., Kim, Y.C., Gray-Keller, M.P., Attie, A.D., and Ntambi, J.M. (2000). The biosynthesis of hepatic cholesterol esters and triglycerides is impaired in mice with a disruption of the gene for stearoyl-CoA desaturase 1. The Journal of biological chemistry 275, 30132-30138.

Ozcan, U., Cao, Q., Yilmaz, E., Lee, A.H., Iwakoshi, N.N., Ozdelen, E., Tuncman, G., Gorgun, C., Glimcher, L.H., and Hotamisligil, G.S. (2004). Endoplasmic reticulum stress links obesity, insulin action, and type 2 diabetes. Science 306, 457-461.

Quehenberger, O., Armando, A., Dumlao, D., Stephens, D.L., and Dennis, E.A. (2008). Lipidomics analysis of essential fatty acids in macrophages. Prostaglandins, leukotrienes, and essential fatty acids 79, 123-129.

Quinn, M.T., Parthasarathy, S., and Steinberg, D. (1988). Lysophosphatidylcholine: a chemotactic factor for human monocytes and its potential role in atherogenesis. Proceedings of the National Academy of Sciences of the United States of America 85, 2805-2809.

Repa, J.J., Liang, G., Ou, J., Bashmakov, Y., Lobaccaro, J.M., Shimomura, I., Shan, B., Brown, M.S., Goldstein, J.L., and Mangelsdorf, D.J. (2000). Regulation of mouse sterol regulatory element-binding protein-1c gene (SREBP-1c) by oxysterol receptors, LXRalpha and LXRbeta. Genes & development 14, 2819-2830.

Schroeder, F., and Goh, E.H. (1980). Effect of fatty acids on physical properties of microsomes from isolated perfused rat liver. Chemistry and physics of lipids 26, 207-224.

Solinas, G., Vilcu, C., Neels, J.G., Bandyopadhyay, G.K., Luo, J.L., Naugler, W., Grivennikov, S., Wynshaw-Boris, A., Scadeng, M., Olefsky, J.M., and Karin, M. (2007). JNK1 in hematopoietically derived cells contributes to diet-induced inflammation and insulin resistance without affecting obesity. Cell metabolism 6, 386-397.

Spector, A.A., and Yorek, M.A. (1985). Membrane lipid composition and cellular function. Journal of lipid research 26, 1015-1035.

Takahara, N., Kashiwagi, A., Maegawa, H., and Shigeta, Y. (1996). Lysophosphatidylcholine stimulates the expression and production of MCP-1 by human vascular endothelial cells. Metabolism: clinical and experimental 45, 559-564.

Tuncman, G., Hirosumi, J., Solinas, G., Chang, L., Karin, M., and Hotamisligil, G.S. (2006). Functional in vivo interactions between JNK1 and JNK2 isoforms in obesity and insulin resistance. Proceedings of the National Academy of Sciences 103, 10741-10746.

Venkateswaran, A., Laffitte, B.A., Joseph, S.B., Mak, P.A., Wilpitz, D.C., Edwards, P.A., and Tontonoz, P. (2000). Control of cellular cholesterol efflux by the nuclear oxysterol receptor LXR alpha. Proceedings of the National Academy of Sciences of the United States of America 97, 12097-12102.

Volmer, R., van der Ploeg, K., and Ron, D. (2013). Membrane lipid saturation activates endoplasmic reticulum unfolded protein response transducers through their transmembrane domains. Proceedings of the National Academy of Sciences of the United States of America 110, 4628-4633.

Walker, A.K., Jacobs, R.L., Watts, J.L., Rottiers, V., Jiang, K., Finnegan, D.M., Shioda, T., Hansen, M., Yang, F., Niebergall, L.J., Vance, D.E., Tzoneva, M., Hart, A.C., and Naar, A.M. (2011). A conserved SREBP-1/phosphatidylcholine feedback circuit regulates lipogenesis in metazoans. Cell 147, 840-852.

Wang, S., Chen, Z., Lam, V., Han, J., Hassler, J., Finck, B.N., Davidson, N.O., and Kaufman, R.J. (2012). IRE1alpha-XBP1s induces PDI expression to increase MTP activity for hepatic VLDL assembly and lipid homeostasis. Cell metabolism 16, 473-486.

Wellen, K.E., and Hotamisligil, G.S. (2005). Inflammation, stress, and diabetes. The Journal of clinical investigation 115, 1111-1119.

Zelcer, N., Khanlou, N., Clare, R., Jiang, Q., Reed-Geaghan, E.G., Landreth, G.E., Vinters, H.V., and Tontonoz, P. (2007). Attenuation of neuroinflammation and Alzheimer's disease pathology by liver x receptors. Proceedings of the National Academy of Sciences of the United States of America 104, 10601-10606.

Zhao, Y., Chen, Y.Q., Bonacci, T.M., Bredt, D.S., Li, S., Bensch, W.R., Moller, D.E., Kowala, M., Konrad, R.J., and Cao, G. (2008). Identification and characterization of a major liver lysophosphatidylcholine acyltransferase. The Journal of biological chemistry 283, 8258-8265.

Chapter 3: Lpcat3-dependent production of arachidonoyl phospholipids is a key determinant of triglyceride-rich lipoprotein secretion

Abstract

The role of specific phospholipids in lipid transport has been difficult to assess due to an inability to selectively manipulate membrane composition *in vivo*. Here we show that the phospholipid remodeling enzyme lysophosphatidylcholine acyltransferase 3 (Lpcat3) is a critical determinant of triglyceride secretion due to its unique ability to catalyze the incorporation of arachidonate into membranes. Mice lacking *Lpcat3* in the intestine fail to thrive during weaning and exhibit enterocyte lipid accumulation and reduced plasma triglycerides. Mice lacking *Lpcat3* in the liver show reduced plasma triglycerides, hepatosteatosis, and secrete lipid-poor VLDL lacking arachidonoyl phospholipids. Mechanistic studies indicate that Lpcat3 activity impacts membrane lipid mobility in living cells, suggesting a biophysical basis for the requirement of arachidonoyl phospholipids in lipidating lipoprotein particles. These data identify Lpcat3 as a key factor in lipoprotein production and illustrate how manipulation of membrane composition can be used as a regulatory mechanism to control metabolic pathways.

Introduction

Phospholipids (PLs) are important components of biological membranes and also serve as precursors for the generation of diverse signaling molecules (Spector and Yorek, 1985). In mammalian cells PLs synthesized *de novo* undergo further remodeling through deacylation by phospholipases and the subsequent and reacylation by lysophospholipid acyltransferases (Lpcats). Membrane PLs ultimately reach an equilibrium in which the majority of PL species contain a saturated acyl chain at the *sn*-1 position and an unsaturated chain at the *sn*-2 position. The Lpcat-dependent remodeling process is essential for the diversity and asymmetric distribution of acyl chains because the *de novo* PL synthesis pathway has little substrate specificity (Yamashita et al., 2014).

We previously identified the sterol-activated nuclear receptor LXR as an integrator of cellular lipid levels and membrane PL composition. LXR controls the expression of Lpcat3, which is the most abundant Lpcat family member in liver and intestine. Cell-based assays suggest that Lpcat3 preferentially catalyzes the synthesis of phosphatidylcholine (PC) species containing an unsaturated fatty acyl chain at the sn-2 position (Hishikawa et al., 2008; Zhao et al., 2008), but the importance of Lpcat3 activity for membrane PL composition *in vivo* remains to be established. We found that acute overexpression or knockdown of Lpcat3 in cultured cells or mouse liver altered the distribution of PL species, particularly those containing unsaturated fatty acyl chains (Rong et al., 2013). Moreover, we showed that the ability of the LXR-Lpcat3 pathway to promote unsaturation of membrane lipids was protective against ER stress and inflammation in the setting of cellular lipid excess. However, the *in vivo* relevance of LXR-dependent modulation of endogenous PL composition for systemic lipid homeostasis was unclear.

Moreover, the larger topic of the regulatory potential of dynamic phospholipid remodeling has been largely unexplored. It has been reported that modifications of PL composition influence a range of cellular processes (Holzer et al., 2011; Pinot et al., 2014). However, most analyses of the consequences of altered PL fatty acyl composition have been performed in purified membrane systems or have involved treating cells with high levels of exogenous lipids. Such experimental manipulations are unlikely to accurately model physiologic perturbations in membrane composition. The recognition that Lpcat3 activity can be regulated by cellular lipid status through LXRs raises the possibility that Lpcat3 activity could contribute to some of the well-documented effects of LXR on systemic lipid homeostasis.

The rate of lipoprotein production has been linked with the availability of phosphatidylcholine (PC), but the mechanisms underlying this link are not clear (Abumrad and Davidson, 2012; Vance, 2008). PC is the major PL component of lipoproteins (Ågren et al., 2005). It has been reported that active PC *de novo* synthesis is necessary for the biogenesis and/or secretion of very low-density lipoprotein (VLDL) from hepatocytes (Vance, 2008). However, impaired *de novo* PC synthesis impacts all the PC species and reduces the total PC content of cellular membranes. Whether a specific PC species is selectively required for hepatocyte lipoprotein production is unclear. In the intestine, it has been proposed that PC may enhance lipid uptake by enterocytes and/or promote chylomicron assembly and secretion (Tso et al., 1977; Tso et al., 1978; Voshol et al., 2000). Luminal PC is not absorbed intact, but is hydrolyzed into lysophosphatidylcholine (Lyso-PC) in the lumen and subsequently re-acylated within enterocytes by Lpcat enzymes (Nilsson, 1968; Parthasarathy et al., 1974). The mechanistic role of specific PL species in lipid transport and lipoprotein production has been difficult to address due to an inability to selectively manipulate membrane PL composition *in*

vivo. Interestingly, the LXR pathway has been reported to promote hepatic triglyceride secretion by the liver (Okazaki et al., 2010). The possibility that PL remodeling contributes to this effect has not been tested.

We demonstrate here that Lpcat3 is uniquely required for the incorporation of arachidonic acid into membranes *in vivo*, and that an absence of arachidonoyl phospholipids profoundly affects lipid transport and lipoprotein production. Biophysical, electron microscopy and and biochemical studies indicate that Lpcat3-dependent production of arachidonoyl phospholipids is important for lipid movement within membranes and for the efficient lipidation of apoB–containing lipoproteins. We also show that induction of Lpcat3 activity is required for the ability of LXRs to promote hepatic VLDL production. These data identify Lpcat3-dependent phospholipid remodeling as a critical, LXR-regulated step in triglyceride secretion, and suggest that this step might be further explored as a strategy to treat hyperlipidemias.

Results

To examine the consequence of Lpcat3 deficiency *in vivo,* we generated Lpcat3-deficient mice from targeted ES cells (**Fig. 3-1A**). The targeted allele was "conditional-ready," making it possible to create both global and tissue-specific knockout mice. The global knockout mice (*i.e.,* homozygous for the targeted allele) showed markedly reduced levels of *Lpcat3* transcripts in liver and intestine (**Fig. 3-1B,C**). Global *Lpcat3*–/– mice on a C57BL/6 background were born at the expected Mendelian frequency, and their weights were indistinguishable from WT mice at birth (**Fig. 3-1D, Table 3-1**). However, the blood glucose levels of *Lpcat3*–/– mice were very low at birth, and none survived beyond day 2 (**Fig. 3-1D, E**). *Lpcat3*–/– pups survived for up to six days when given subcutaneous glucose injections, but the pups did not thrive and invariably died (**Fig. 3-1E,F**). Analysis of gene expression in liver and small intestines of the pups revealed changes in a number of genes linked to lipid metabolism, some of which were common in both tissues (**Fig. 3-1G,H**). Although these changes appeared consistent with a role for Lpcat3 in lipid metabolism, it was impossible to exclude the possibility that these gene-expression alterations were simply due to the extremely poor health of the mice. We therefore turned our attention to tissue-selective knockout mice, with the hope that we could obtain viable mice and decipher the function of Lpcat3.

We generated a conditional knockout allele (*Lpcat3*^{fl}) by breeding the global heterozygous knockout mice with mice expressing FLPe recombinase (Rodriguez et al., 2000). Mice harboring the "floxed" *Lpcat3* allele were then crossed with albumin-Cre transgenic mice to create liver-specific Lpcat3 knockout mice (here designated "L-Lpcat3 KO"; **Fig. 3-2A**). In contrast to the global *Lpcat3* knockout mice, L-Lpcat3 mice were born at the expected Mendelian frequency, survived to adulthood, and appeared (at least by external inspection) to be

indistinguishable from control (homozygous floxed, Cre-negative) mice (**Table 3-2** and data not shown). Expression of *Lpcat3* transcripts in whole liver from L-Lpcat3 KO mice was markedly reduced (**Fig. 3-2B**). The residual expression of *Lpcat3* mRNA in the liver of Lpcat3 KO mice was likely due to persistent expression of Lpcat3 in cell types that do not express the albumin-Cre transgene (Kupffer cells, endothelial cells). Consistent with that idea, *Lpcat3* expression was reduced by >90% in primary hepatocytes from L-Lpcat3 KO mice (Fig. 3-2B). Unfortunately, we were unable to measure levels of Lpcat3 protein because specific antibodies are not currently available. We observed no compensatory upregulation of *Lpcat1* or *Lpcat2* in livers of L-Lpcat3 KO mice (**Fig. 3-2B**). *Lpcat4* expression was undetectable in the liver.

Analysis of plasma lipid levels revealed lower plasma triglyceride levels following an overnight fast in L-Lpcat3 KO mice compared to controls (**Fig. 3-2C**). Levels of plasma total cholesterol and non-esterified free fatty acids (NEFA) were not different between groups. Body weight and fasting blood glucose levels were also not different between groups (Fig. 3-2, Supplement 1). Although total levels of plasma apolipoprotein B (apoB) were similar between groups (**Fig. 3-2D**), fractionation of plasma lipoproteins revealed lower levels of apoB in the VLDL fraction in L-Lpcat3 KO mice (**Fig. 3-2E, Fig. 3-3A**). Moreover, triglyceride (TG) levels in the VLDL fraction were markedly reduced. We also observed a trend towards TG stores in the liver of L-Lpcat3 KO mice, along with histological evidence of increased lipid accumulation (**Fig. 3-2F,G**).

As a complement to our analysis of L-Lpcat3 KO mice, which lack Lpcat3 expression in their livers from birth, we acutely deleted Lpcat3 in the liver of adult *Lpcat3*$^{fl/fl}$ mice with a Cre-expressing adenoviral vector. Interestingly, acute inactivation of Lpcat3 resulted in a more prominent decrease in fasting plasma TG levels compared to developmental deletion (**Fig. 3-**

2H). Furthermore, acute deletion uncovered a decrease in ad-lib plasma TG levels that was not observed with developmental deletion (**Fig. 3-2C,H**). This finding suggests that there may be partial compensation for the chronic loss of Lpcat3 in the L-Lpcat3 KO mice. Collectively, the data of Figure 2 are consistent with a potential role for Lpcat3 in hepatic triglyceride metabolism.

To further explore a role for Lpcat3 in triglyceride secretion, we challenged control and L-Lpcat3 KO mice with western diet (40% high fat and 0.2% cholesterol) for 9 weeks. Mice lacking hepatic Lpcat3 again showed lower total plasma TG levels (**Fig. 3-4A**) and a striking loss of TG in the VLDL plasma lipoprotein fraction (**Fig. 3-4B**). In addition, these mice had increased levels of plasma apoB-100 compared to controls (**Fig. 3-4C**). Analysis of tissue lipids revealed prominent accumulation of hepatic TG and cholesterol in the liver of L-Lpcat3 KO mice (**Fig. 3-4D,E**). We also challenged mice with a high-sucrose diet, which strongly stimulates hepatic lipid synthesis and secretion. On the high-sucrose diet, L-Lpcat3 KO mice exhibited hepatic triglyceride accumulation (**Fig. 3-4F,G**). The accumulation of hepatic TG in L-Lpcat3 KO mice in the setting of reduced plasma VLDL TG implied that Lpcat3 activity might be crucial for the assembly and secretion of triglyceride-rich lipoproteins from the liver.

Lpcat3 is expressed at high levels in intestine as well as in the liver. We showed previously that hepatic *Lpcat3* expression is regulated by the sterol-activated nuclear receptor LXR (Rong et al., 2013). Here, we showed that intestinal Lpcat3 expression is strongly responsive to the administration of a synthetic LXR-agonist, GW3965 (**Fig. 3-5A**). To address whether Lpcat3 activity may also be important for TG metabolism in intestinal enterocytes, we generated intestine-specific Lpcat3 KO mice (I-Lpcat3 KO) by crossing the floxed mice to villin-*Cre* transgenics. I-Lpcat3 KO mice were born at the predicted Mendelian frequency, and their body weights at birth were comparable to controls (**Table 3-3, Fig. 3-5B**). However, even though

the pups suckled, they failed to thrive and showed severe growth retardation by 1 week of age (**Fig. 3-5C**). Expression of *Lpcat3* was reduced more than 90% in duodenum of I-Lpcat3 KO mice as expected, and there was no compensatory increase in expression of *Lpcat1*, *Lpcat2* or *Lpcat4* (**Fig. 3-5D**). Blood glucose levels in 1-week-old I-Lpcat3 pups were very low (**Fig. 3-5E**), consistent with results obtained with global knockouts (**Fig. 3-1**). Plasma insulin levels were also correspondingly reduced. Plasma TG levels were lower and total cholesterol and NEFA levels were unchanged in I-Lpcat3 KO pups (**Fig. 3-5E**). Histological analysis of intestines from I-Lpcat3 KO pups revealed a dramatic accumulation of cytosolic lipid droplets in intestinal enterocytes (**Fig. 3-5F**), a phenotype reminiscent of intestinal apoB-deficient mice. Analysis of intestinal gene expression in I-Lpcat3 KO mice revealed reduced expression of several genes linked to intestinal TG metabolism, including *Apob*, *Cd36*, *Dgat2*, and *Mogat2* (**Fig. 3-5G**). Given the massive enterocyte lipid accumulation in enterocytes, it is conceivable that some of those gene-expression changes were due, at least in part, to poor nutrition or cell toxicity. Nevertheless, these data were consistent with a role for Lpcat3 in TG mobilization and secretion–in the intestine as well as in the liver.

To gain insight into how the enzymatic activity of Lpcat3 was linked to these phenotypes, we performed lipidomic analyses. Previous studies using *in vitro* systems have profiled the substrate specificities of the 4 mammalian Lpcat family members (Hishikawa et al., 2008; Zhao et al., 2008). These studies suggested that Lpcat3 exhibited a preference for LysoPC and polyunsaturated fatty acyl-CoAs as substrates. Consistent with those results, we previously observed subtle changes in the levels of PC species containing polyunsaturated acyl in response to acute Lpcat3 knockdown in hepatocytes and macrophages (Rong et al., 2013). However, the consequences of a genetic inactivation of *Lpcat3* for membrane composition *in vivo* have never

been addressed. Unexpectedly, analysis of phospholipid species in whole liver extracts from L-Lpcat3 KO mice by ESI-MS/MS revealed that Lpcat3 activity is uniquely required for the incorporation of arachidonate chains into phospholipids. Thus, despite the fact that Lpcat3 can catalyze the esterification of multiple unsaturated acyl chains into PC *in vitro*, and despite the fact that Lpcat3 is by far the most abundant Lpcat family member in the liver, the consequences of loss of Lpcat3 for PL composition were remarkably selective. The total level of PC was not different between L-Lpcat3 KO and control livers (**Fig. 3-6A**). However, there were striking reductions (~70%) in the abundance of 16:0, 20:4 PC and 18:0, 20:4 PC (nomenclature: a:b, c:d; where a and c are the number of carbons and b and d are the number of double bonds of the sn-1 and sn-2 aliphatic groups, respectively), two of the most abundant arachidonoyl PC species in liver membranes (**Fig. 3-6A**). However, the actual reduction of 16:0, 20:4 PC and 18:0, 20:4 PCs in *hepatocyte* membranes was almost certainly much greater, given that a significant fraction of membranes in total liver extracts originate from other cell types (where Lpcat3 activity is preserved). Furthermore, we observed compensatory increases in the abundance of other PC species in L-Lpcat3 KO livers, notably those containing monounsaturated chains (e.g., 16:0, 18:1 PC and 18:0, 18:1 PC; **Fig. 3-6A**).

We also analyzed the effect of western diet on hepatic phospholipid composition in the presence and absence of Lpcat3. The diet increased the abundance of certain PC species, such as 16:0, 18:1 PC, presumably reflecting the abundance of oleate in the western diet. However, we observed the same prominent deficits in 16:0, 20:4 PC and 18:0, 20:4 PC on western diet as we observed on chow diet, with no change in total levels of PC (**Fig. 3-6B**). In addition, there were reductions in 16:1, 18:2 PC and 18:1, 20:4 PC in western diet-fed Lpcat3 KO livers compared to controls. Severe reductions of phosphatidlyethanolamine (PE) species containing arachidonate

chains were also observed in L-Lpcat3 KO mice on both chow and western diets (**Fig. 3-7**). Interestingly, 16:0, 20:4 PE and 18:0, 20:4 PE are particularly abundant PE species in liver on western diet, and reductions in their levels was sufficient to reduce total PE levels.

Since unsaturated PC species are abundant in plasma lipoproteins, and since mice lacking Lpcat3 in liver or intestine show reduced plasma TG levels, we tested whether loss of Lpcat3 expression in liver would alter the phospholipid composition of VLDL secreted from the liver. After fasting L-Lpcat3 KO and control mice overnight, the VLDL was isolated from pooled plasma (n = 5 mice/group). Analysis of PC species in the pooled VLDL fractions by ESI-MS/MS revealed highly selective reductions in 16:0, 20:4 PC and 18:0, 20:4 PC (**Fig. 3-6C**). Thus, the phospholipid deficits of L-Lpcat3 KO hepatic membranes are passed on to the VLDL particles that they generate, strongly suggesting that loss of these PC species is mechanistically related to the altered TG content of the particles.

Interestingly, the severe loss of arachidonate in livers of Lpcat3 KO mice on chow diet was observed in phospholipids, but not in TG (**Fig. 3-6D**) nor in cholesterol esters (**Fig. 3-8A**). There was an increase in total cholesterol ester and a number of cholesterol ester species in L-Lpcat3 KO mice, consistent with the histologic evidence of increased neutral lipid content in the liver (**Fig. 3-2**). There was no accumulation of the major lipid substrates of Lpcat3 (16:0 lysoPC and 18:0 lysoPC) in L-Lpcat3 KO mice (**Fig. 3-8B**), suggesting these precursors are efficiently shuttled into alternative pathways in the absence of Lpcat3. Broadly similar results were obtained from mice fed western diet, although we did observe modestly lower levels of 20:4 lysoPC (**Fig. 3-8 C,D**).

To determine the consequence of loss of Lpcat3 activity for hepatic gene expression we performed transcriptional profiling. Despite the marked changes in membrane composition in L-

Lpcat3 KO livers, the effect on gene expression was surprisingly limited (**Fig. 3-9A**). On chow diet, only a handful of genes were altered more than 2-fold. Among the highest changes were increased expression of the lipoprotein remodeling enzyme *Pltp* and the lipid transport protein *Cd36*. A number of additional genes involved in lipid metabolism were induced to a more modest degree, including *Txnip* and *Fabp2*. Interestingly, many of the genes that were induced are known targets for the lipid-activated nuclear receptor PPARα, suggesting a compensatory gene expression response to increased cellular lipid levels in the absence of Lpcat3 (**Figs. 3-2 and 3-4**).

More prominent changes in gene expression in L-Lpcat3 KO mice were observed in the setting of western diet feeding (**Fig. 3-9B**). Multiple genes involved in lipid metabolism and transport and in lipid droplet formation were upregulated, again likely reflecting a response to increased hepatic TG and cholesterol content. Interestingly, the putative transporter Mfsd2a (Nguyen et al., 2014) was induced in Lpcat3-deficient livers on both chow and western diet, perhaps as compensation for the loss of arachidonoyl phospholipids. In addition, there was increased expression of a number of genes linked to inflammation and inflammatory cell recruitment (**Fig. 3-9C**). These data are consistent with our earlier study showing that adenoviral expression of Lpcat3 is protective against hepatic inflammation in the setting of lipid excess (Rong et al., 2013). We validated the microarray results for a number of genes by real-time PCR and also assessed the expression of other genes relevant to lipoprotein production (**Fig. 3-9D,E**). Importantly, there was no change in the expression of mRNAs encoding apoB or of the critical lipid transfer protein MTTP in livers of Lpcat3 KO mice, indicating that altered plasma TG levels cannot be attributed to changes in expression of these factors.

We previously reported that acute knockdown of Lpcat3 expression in livers of genetically obese mice exacerbated lipid-induced ER stress (Rong et al., 2013). Genetic deletion of Lpcat3 from liver did not lead to increased mRNA expression of ER stress markers in mice fed chow or western diet (**Fig. 3-10**). These observations suggest that there may be compensatory responses in membrane composition that prevent induction of the ER stress response in the setting of chronic Lpcat3 deletion. In support of this idea, we observed a prominent increase in the abundance of oleoyl-PC species in L-Lpcat3 mice (**Fig. 3-6**). We cannot exclude the possibility that ER stress may be increased in L-Lpcat3 mice in the setting of genetic obesity or other causes of severe lipotoxicity.

We next investigated the etiology of reduced VLDL TG levels in mice lacking Lpcat3. Protein levels of apoB in liver were not different between control and L-Lpcat3 KO mice (**Fig. 3-11A**). Together with the preserved levels of apoB in plasma (**Figs. 3-2 and 3-4**), these data suggest that a defect in production or secretion of apoB alone cannot explain the change in plasma VLDL. We directly assessed hepatic TG secretion by treating mice with the lipase inhibitor Tyloxapol and measuring TG accumulation in fasted mice. L-Lpact3 KO mice showed a markedly reduced rate of TG secretion **(Fig. 3-11B**), suggesting that reduced incorporation of triglycerides into lipoproteins was the likely cause of the reduced VLDL TG levels. Consistent with this hypothesis, negative staining of plasma VLDL fractions by electron microscopy revealed markedly smaller VLDL particles in L-Lpcat3 KO mice compared to controls (**Fig. 3-11C**).

To obtain further insight into the nature of the lipoprotein production defect in L-Lpcat3 KO mice, we examined liver samples by electron microscopy. Nascent lipoproteins, ranging between 0.05 and 0.11 microns in diameter, were easily visualized in the Golgi apparatus and

secretory vesicles of control mice (**Fig. 3-12**). Lipoprotein particles were also present in Golgi and secretory vesicles of L-Lpcat3 KO mice, however they were markedly smaller, ranging between 0.03 to 0.08 microns in diameter (**Fig. 3-12**). We also observed small lipoprotein particles in the ER in mice of both genotypes (**Fig. 3-13**). We did not find differences in the morphology of Golgi, ER or mitochondria between control and L-Lpcat3 KO livers, suggesting that loss of arachidonoyl phospholipids does not dramatically alter membrane structure in these organelles (**Fig. 3-13**).

To further investigate the hypothesis that defective apoB lipidation was responsible for the phenotype of L-Lpcat3 KO mice, we isolated the Golgi apparatus from livers, fractionated the luminal contents by density gradient centrifugation, and analyzed the distribution of ApoB in the different fractions. There was reduced apoB in the most buoyant lipoprotein fractions, consistent with reduced lipidation of apoB particles in the absence of Lpcat3 (**Fig. 3-14A**). In line with this finding, we found reduced TG levels in Golgi membrane fractions isolated by density gradient centrifugation from L-Lpcat3 KO mice compared to controls in two independent purifications (**Fig. 3-14B**).

To understand how changes in membrane phospholipid composition in Lpcat3-deficient mice might lead to reduced mobilization and secretion of triglycerides, we performed biophysical studies on the impact of Lpcat3 deficiency on lipid movement in living cells. Prior studies have employed the lipophilic dye laurdan to interrogate lipid dynamics in membranes (Golfetto et al., 2013; Parasassi and Gratton, 1995; Vest et al., 2006). Laurdan is a fluorescent lipophilic molecule that can be used to detect changes in membrane dynamics due to its sensitivity to the polarity of the membrane environment. Changes in membrane dynamics shift the laurdan emission spectrum, which can be quantified by the generalized polarization (GP)

calculated from the spectrum shifts (Parasassi et al., 1990). We isolated primary hepatocytes from L-Lpcat3 KO mice and controls, stained with laurdan, and monitored fluorescence in live cells by microscopy. A visual representation of the calculated GP intensity is presented in F**ig. 3-14C**, and the data are quantitated in **Fig. 3-14D**. The prominent increase in GP (as shown by the yellow/orange pseudocolor signal) in cells lacking Lpcat3 is indicative of areas of cellular membrane with reduced dynamics. These data show that membranes are less dynamic, and their component lipids move less readily, in the absence of Lpcat3, an observation that is consistent with the reduced amount of arachidonate groups in membrane phospholipids. We propose that efficient transfer of bulk TG to nascent VLDL particles is enabled by the presence of arachidonoyl phospholipids in the ER/Golgi membrane due to its unique ability to facilitate optimal lipid movement and membrane dynamics.

Finally, as LXR agonists have previously been reported to promote hepatic TG secretion (Schultz et al., 2000), we tested the requirement for Lpcat3 induction in this effect. Control and L-Lpcat3 KO mice were treated for 2 days with the LXR agonist GW3965 (20 mpk/day) by oral gavage. The triglyceride levels in fractionated plasma were then determined after 6 h fast. In line with prior studies, treatment of control mice with LXR agonist led to a prominent (95%) increase in plasma VLDL triglyceride levels (**Fig. 3-15**). By contrast, treatment of L-Lpcat3 KO mice with LXR agonist had a much more modest effect (45% increase). These data suggest that induction of Lpcat3 expression plays an important role in the control of hepatic VLDL production by LXRs.

Discussion

It has long been appreciated that phospholipid availability can influence the production of lipoproteins (Abumrad and Davidson, 2012; Vance, 2008), but the molecular basis of these connections, beyond the obvious need for sufficient phospholipids to coat the surface of lipoprotein particles, has been unclear. We have shown here that Lpcat3 is uniquely required for the incorporation of arachidonic acid into membranes, and that selective reduction in the abundance of these lipids impairs TG mobilization and lipoprotein production. These studies highlight a previously unrecognized requirement for a specific membrane lipid class in lipoprotein metabolism.

Earlier studies using *in vitro* systems have demonstrated that changes in polyunsaturated PL can affect membrane-associated biological processes, including the assembly of signalsomes on membranes and endocytosis (Koeberle et al., 2013; Pinot et al., 2014). However, assessing the physiological impact of changing the abundance of individual PL species in animals has been a difficult experimental problem. Our study identifies Lpcat3 as a critical determinant of the abundance of arachidonoyl phospholipids in mice. The largely preserved levels of other PL species containing polyunsaturated chains in Lpcat3-deficient livers suggests that other Lpcats may be able to catalyze the incorporation of certain polyunsaturated fatty acids into membranes in the absence of Lpcat3. However, Lpcat3 is apparently unique in its ability to catalyze arachidonoyl PL synthesis. Lpcat3-deficient mouse models therefore provide an unprecedented opportunity to study the physiological and pathophysiological consequences of manipulation of membrane phospholipid composition *in vivo*.

Previous research has elucidated a requirement for *de novo* PC biogenesis in the production and secretion of VLDL from liver. Feeding mice a choline-deficient diet or deleting

genes involved in *de novo* PC synthesis (e.g, *Pemt*, *CT*-α) impairs VLDL secretion and induces hepatosteatosis (Jacobs et al., 2004; Noga and Vance, 2003). These models exhibit reduced total apoB protein in plasma as well as lower plasma triglycerides, suggesting that adequate PC biosynthesis is important for both apoB secretion and VLDL lipidation. In our study, mice lacking Lpcat3 retain the ability to secrete apoB and are capable of producing small poorly-lipidated VLDL particles. However, they are unable to transfer TG to lipoproteins at an appropriate rate in the setting of increased metabolic demand. Our results suggest that the reduced availability of arachidonoyl phospholipids becomes especially problematic when there is a need to mobilize a large bolus of TG into lipoproteins. For example, when L-Lpcat3 KO mice are challenged with the lipogenic sucrose diet, they are unable to efficiently mobilize the newly synthesized TG into plasma lipoproteins and it instead accumulates in cytosolic lipid droplets in the liver.

Similarly, mice lacking Lpcat3 in the intestine are unable to handle the high TG load of milk during suckling and accumulate large amounts of lipid in enterocytes. Given that Lpcat3 is the major Lpcat enzyme in enterocytes (**Fig. 3-5D**), loss of Lpcat3 would be expected to impair the re-esterification of LysoPC to PC in enterocytes, which has been demonstrated to be important for lipid absorption. Unfortunately, the early lethality of the I-Lpcat3 KO pups presents a challenge to the analysis of lipid absorption. An inducible knockout system may prove a better model for studying the impact of Lpcat3 on intestinal lipid transport in adult mice.

Lpcat3 is a integral membrane protein of the ER and is therefore ideally positioned to produce arachidonoyl PC at the site of lipoprotein biogenesis (Fisher and Ginsberg, 2002; Zhao et al., 2008). Our observations suggest that Lpcat3 and its lipid products are likely not essential for the cotranslational lipidation of apoB and the generation of primordial VLDL particles

(Fisher and Ginsberg, 2002). However, the small size of plasma VLDL particles, together with the reduced TG-rich apoB-containing particles in the Golgi fraction of L-Lpcat3 KO livers, strongly suggest that Lpcat3 impacts the second step of VLDL assembly–bulk TG addition to lipid-poor apoB particles and the generation of mature VLDL. TG-rich VLDL assembly is highly dependent on the efficient trafficking of stored cytosolic lipid from lipid droplets or newly synthesized lipid to primordial VLDL particles. One factor that could affect this transfer is the membrane environment where the bulk lipidation occurs. Although the precise mechanism that links membrane PL composition and VLDL lipidation is not clear, biophysical studies suggested that greater lipid transport is generally observed with more fluid and highly curved membrane surfaces (Lev, 2012).

Results from our laurdan staining experiments support the notion that the presence of arachidonoyl phospholipids in intracellular membranes promotes the dynamics of the membranes. However, detailing these biophysical changes and elucidating how they influence lipid movement will require further study with specialized tools and systems. Nevertheless, our data suggest that membrane dynamics may play an important role in VLDL lipidation *in vivo*. Interestingly, a recent proteomic study identified Lpcat3 as a component of the VLDL transport vesicle, indicating that Lpcat3 travels with primordial VLDL particles as they bud from the ER and move to the Golgi (Rahim et al., 2012). Together with prior work, our data favor a model in which Lpcat3 modifies the arachidonoyl-PC composition of both membranes and lipoprotein particles during VLDL assembly, thereby generating a local membrane environment that facilitates lipid transport and bulk lipidation.

Our prior studies showed that acute shRNA-mediated knockdown of Lpcat3 expression in liver exacerbated ER in the setting of obesity and hepatic steatosis. However, genetic deletion

of Lpcat3 expression in liver did not lead to overt ER stress pathway activation, suggesting that increased abundance of monounsaturated PC species (e.g. 16:0, 18:1 PC, Fig. 3-6) may partially compensate to maintain ER membrane homeostasis. It remains to be determined whether stronger lipotoxic stimuli, such as the hepatosteatosis observed in *ob/ob* mice, may yet provoke increased ER stress responses in the genetic absence of Lpcat3.

This work illustrates how manipulation of membrane composition can be used as regulatory mechanism to control metabolic pathways. A model for Lpcat3 action is presented in **Fig. 3-16**. Lpcat3 is not only a required component of lipoprotein production; it is also a regulated one. The fact that Lpcat3 expression is dynamically regulated by LXRs in liver and intestine strongly suggests that the level of Lpcat3 enzymatic activity has evolved to respond to dietary and metabolic demands. LXR is transcriptionally activated as cellular cholesterol levels rise. Thus, the LXR-Lpcat3 pathway provides a mechanism to integrate sterol metabolism and membrane PL composition. We speculate that Lpcat3 expression is induced in response to lipid loading in order to increase ER/Golgi membrane flexibility and to facilitate efficient TG secretion (thereby unloading cells of excess lipids). In support of this idea, we found that the ability of pharmacologic LXR agonist to stimulate hepatic VLDL production was impaired in the genetic absence of Lpcat3.

Finally, these studies open the door to new strategies for pharmacologic intervention in systemic lipid metabolism. Abnormal phospholipid metabolism has been associated with several metabolic diseases. For example, lower amounts of polyunsaturated phospholipids have been observed in liver biopsies from nonalcoholic steatohepatitis patients (Puri et al., 2007), and cell membranes from patients with atherosclerotic disease tend to show decreased membrane fluidity (Chen et al., 1995). However, it has heretofore been difficult to draw a causal link between

aberrant PL composition and the pathogenesis of metabolic diseases. Our studies provide direct evidence that alterations in arachidonoyl PC abundance impair lipoprotein metabolism in liver and intestine *in vivo*. Recently, a human GWAS reported a highly significant association between *LPCAT3* and the phospholipid composition of red blood cell membranes, indicating that Lpcat3 is also a key regulator of phospholipid composition in humans (Tintle et al., 2014). Therefore, an improved understanding of the mechanisms by which Lpcat3 and arachidonoyl PCs regulate lipid homeostasis could lead to new approaches to metabolic diseases. We speculate that small molecule inhibitors of Lpcat3 could be of potential utility for lowering plasma lipid levels in hyperlipidemic individuals. In pursuing such a strategy, one would need to monitor the impact of Lpcat3 inhibition on liver triglyceride stores, hepatic inflammation and lipid malabsorption, in addition to the plasma lipids. However, modest increases in liver triglyceride stores, even if they occurred in humans, might not doom such a strategy. Inhibiting apoB synthesis with antisense compounds has found a place in the management of some cases of hyperlipidemia, despite modest increases in liver triglyceride stores.

Acknowledgments

We thank Jinkuk Choi and Ito Ayaka for technical support. This work was supported by grants HL090553, DK063491, HL030568, HL074214, GM103540, GM076516 and AHA Fellowship 13PRE17150049. P.T. is an Investigator of the Howard Hughes Medical Institute.

Methods

Gene Expression—Total RNA was isolated from cells and tissues with Trizol (Invitrogen). cDNA was synthesized, and gene expression was quantified by real-time PCR with SYBR Green (Diagenode, Denville, NJ) and an ABI 7900. Gene expression levels were normalized to 36B4 or GAPDH. Primer sequences are listed in Table 3-4. For microarray experiments, RNA was pooled from $n = 5$ biological replicates and processed in the UCLA Microarray Core Facility with Gene-Chip Mouse Gene 430.2 Arrays (Affymetrix, Santa Clara, CA). Data analysis was performed with GenespringGX (Agilent, Santa Clara, CA). The GEO accession number is GSE65352 and GSE65353.

Protein Analysis—Cells and tissue lysates were prepared by homogenization in RIPA buffer (50 mM Tris-HCl, pH 7.4; 150 mM NaCl, 1% NP-40, 0.5% Sodium deoxycholate, 0.1% SDS) supplemented with protease and phosphatase inhibitors (Roche Molecular Biochemicals). Lysates were cleared by centrifugation. Plasma samples were diluted with RIPA buffer. Protein lysate were then mixed with NuPAGE® LDS Sample Buffer, size-fractionated on 4–12% Bis-Tris Gels (Invitrogen), transferred to hybond ECL membrane (GE Healthcare, Piscataway, NJ), and incubated with an apoB antibody (Abcam, Cambridge, MA). Primary antibody binding was detected with a goat anti-rabbit secondary antibody and visualized with chemiluminescence (ECL, Amersham Pharmacia Biotech).

Generation of Lpcat3 Knockout Mice—A conditional knockout allele for *Lpcat3* was generated with a sequence replacement "knock-out first/conditional-ready" gene-targeting vector. The vector was electroporated into JM8A1.N3 ES cell line from C57BL/6N mice.

Positive clones were identified by genotyping and long-range PCR at both the 5′ and 3′ ends. Two targeted ES cell clones were injected into C57BL/6 blastocysts to generate chimeric mice. High-percentage male chimeras were obtained, and resulting chimeras bred with female C57BL/6 mice to obtain heterozygous knockout mice (*Lpcat3*$^{+/-}$). *Lpcat3*$^{+/-}$ mice were intercrossed to produce homozygous knockout mice (*Lpcat3*$^{-/-}$). To create a conditional knockout allele, *Lpcat3*$^{+/-}$ mice were mated with mice expressing a Flpe recombinase deleter transgene (Jackson Laboratory, Bar Harbor, Maine). That transgene excises the gene-trapping cassette in intron 2 of *Lpcat3*, producing a conditional knockout allele containing loxP sites in intron 2 and intron 3. *Lpcat3*$^{Fl/Fl}$ mice were crossed with albumin-*Cre* or villin-*Cre* transgenic mice from The Jackson Laboratory (Bar Harbor, ME).

Triglyceride Secretion Assay in Mice—Mice were fasted for 4 h and then injected intravenously with 500 mg/kg body weight of tyloxapol (Fisher, Pittsbugh, PA). Blood was subsequently collected, and the plasma separated by centrifugation for the measurement of triglycerides.

Animal Studies—*Lpcat3*$^{-/-}$*; Lpcat3*$^{fl/fl}$; *Lpcat3*$^{fl/fl}$, *Albumin-Cre*; and *Lpcat3*$^{fl/fl}$*, Villin-Cre* mice were generated as described above. All the mice were housed under pathogen-free conditions in a temperature-controlled room with a 12-h light/dark cycle. Mice were fed a chow diet, a western diet (Research Diets #D12079B), or a high-sucrose diet (Research Diets #D07042201). Liver tissues were collected and frozen in liquid nitrogen and stored at –80°C or fixed in 10% formalin. Blood was collected by retro-orbital bleeding, and the plasma was separated by centrifugation. Small intestines were excised and cut into three segments with length ratios of

1:3:2 (corresponding to duodenum, jejunum and ileum). For adenoviral infections, VQAd-CMV Cre/eGFP and VQAd-Empty eGFP were purchased from Viraquest. 8- to 10-week-old male *Lpcat3*$^{fl/fl}$ mice were injected (*via* the tail vein) with 2×10^9 plaque-forming units (pfu). Mice were sacrificed or used for triglyceride secretion studies 3–4 weeks after the adenovirus injection. Plasma lipids were measured with the Wako L-Type TG M kit, the Wako Cholesterol E kit; and the Wako HR series NEFA-HR(2) kit. Tissue lipids were extracted with Bligh-Dyer lipid extraction (Bligh and Dyer, 1959) and measured with the same enzymatic kits. Plasma fast protein liquid chromatography (FPLC) lipoprotein profiles were performed in the Lipoprotein Analysis Laboratory of Wake Forest University School of Medicine. Tissue histology was performed in the UCLA Translational Pathology Core Laboratory. Animal experiments were conducted in accordance with the UCLA Animal Research Committee.

Lipid Analyses–Liver tissue and plasma were snap frozen at the temperature of liquid nitrogen. Liver was homogenized on ice in phosphate buffered saline. Plasma or liver homogenates were subsequently subjected to a modified Bligh-Dyer lipid extraction (Bligh and Dyer, 1959) in the presence of lipid class internal standards including eicosanoic acid, 1-0-heptadecanoyl-sn-glycero-3-phosphocholine, 1,2-dieicosanoyl-sn-glycero-3-phosphocholine, cholesteryl heptadecanoate, and 1,2-ditetradecanoyl-sn-glycero-3-phosphoethanolamine (Demarco et al., 2013). Lipid extracts were diluted in methanol/chloroform (4/1, v/v) and molecular species were quantified using electrospray ionization mass spectrometry on a triple quadrupole instrument (Themo Fisher Quantum Ultra) employing shotgun lipidomics methodologies (Han and Gross, 2005). Lysophosphatidylcholine molecular species were quantified as sodiated adducts in the positive ion mode using neutral loss scanning for 59.1 amu (collision energy = -28eV).

Phosphatidylcholine molecular species were quantified as chlorinated adducts in the negative ion mode using neutral loss scanning for 50 amu (collision energy = 24eV). Phosphatidylethanolamine molecular species were first converted to fMOC derivatives and then quantified in the negative ion mode using neutral loss scanning for 222.2 amu (collision energy = 30eV) (Han et al., 2005b). Cholesteryl ester molecular species were quantified as sodiated adducts in the positive ion mode using neutral loss scanning of 368.5 amu as previously described (Bligh and Dyer, 1959; Bowden et al., 2011). Individual molecular species were quantified by comparing the ion intensities of the individual molecular species to that of the lipid class internal standard with additional corrections for type I and type II ^{13}C isotope effects (Han and Gross, 2005). Triacylglycerol fatty acid composition was determined as follows. Samples were subjected to Bligh-Dyer extraction in the presence of the internal standard, triheptadecenoin, followed by thin layer chromatographic purification of triacylglycerol using silica gel G plates with petroleum ether/ethyl ether/acetic acid; 80/20/1 as mobile phase. Purified triacylglycerol was then subjected to fatty acid methanolysis, and fatty acid methyl esters were then determined using gas chromatography with flame ionization detection as previously described (Ford and Gross, 1988, 1989).

Membrane dynamics—Membrane dynamics was analyzed as described (Golfetto et al., 2013). Briefly, primary hepatocytes from *Lpcat3*$^{fl/fl}$ and *Lpcat3*$^{fl/fl}$; *Albumin-Cre* mice were isolated as described (Rong et al., 2013). Cells were incubated with 1.8 mM Laurdan (6-dodecanoyl-2-dimethylaminonaphthalene; Invitrogen) at 37°C for 30 min. Cells were rinsed with PBS, and fresh culture medium was added. Spectral data were acquired with a Zeiss LSM710 META laser scanning microscope coupled to a 2-photon Ti:Sapphire laser (Mai Tai, Spectra Physics,

Newport Beach, CA) producing 80-fs pulses at a repetition of 80 MHz with two different filters: 460/80 nm for the blue channel and 540/50 nm for the green channel. Spectral data were processed by the SimFCS software (Laboratory for Fluorescence Dynamics). The GP value was calculated for each pixel using the two Laurdan intensity images (460/80nm and 540/50 nm). The GP value of each pixel was used to generate the pseudocolored GP image. GP distributions were obtained from the histograms of the GP images.

Organelle isolation—The Golgi fraction was isolated as described (Vance and Vance, 1988). Briefly, fresh liver tissue was homogenized with a motor driven Potter-Elvehjem homogenizer in homogenization buffer (37.5 mM TRIS-maleate, pH 7.4; 0.5 M sucrose; 1% dextran; and 5 mM $MgCl_2$). After an initial centrifugation at 5,000 × *g* for 15 min, most of the supernatant was removed and the yellow-brown portion (approximately the upper one-third) of the pellet was suspended in homogenization buffer, layered over 2.7 ml of 1.2 M sucrose and spin for 30 min at 100,000 × *g* in a swinging bucket rotor (SW50.1). The Golgi fraction was collected at the buffer/1.2 M sucrose interface. The Golgi was suspended in distilled water and pelleted by centrifugation at 5,500 × *g* for 20 min. Aliquots of the Golgi fraction were used to measure triglyceride and protein concentration. Golgi apoB was analyzed as described (Gusarova et al., 2003; Li et al., 2012). Briefly, the luminal contents were released from Golgi fraction by treatment with 0.1 M sodium carbonate (pH 11) and deoxycholic acid (0.025%) for 30 min at room temperature. Bovine serum albumin (BSA) was added to a final concentration of 5 mg/ml, followed by centrifugation (50,000 rpm in a Beckman SW60 rotor for 1 h at 4°C) to remove membranes. The luminal contents (supernatant) were adjusted to pH 7.4 with acetic acid, adjusted to a sucrose concentration of 12.5% (w/v), and placed on the top of a step gradient

consisting of 1.9 ml of 49% sucrose and 1.9 ml of 20% sucrose. Next, 2.8 ml of phosphate-buffered saline (PBS) was layered on the top of the supernatants. All solutions contained protease inhibitors. After centrifugation at 35,000 rpm for 65 h at 10°C in a Beckman SW41 rotor, 12 fractions with densities ranging from 1.0 to 1.125 g/ml were collected from the top of the tube. ApoB protein from each fraction was analyzed by western blotting.

Electron Microscopy—For VLDL isolation, 400 µl plasma from fasted mice was put into the bottom of a 1-ml thick-walled polycarbonate tube, overlaid with 600 µl of 1.006 g/mL KBr solution, and centrifuged at 100,000 rpm at 16°C for 2 h in a TLA 120.2 rotor. 300 µl from the top of the tube was collected as the VLDL fraction. For electron microscopy (EM), 5 µl of the VLDL preparation was applied to carbon-coated copper grids and stained with 2.0% uranyl acetate for 15 min. Grids were visualized with a JEOL 100CX transmission electron microscope.

For electron microscopy of liver samples, animals were perfused through the left ventricle of the heart with a fixative of 1.5% glutaraldehyde, 4% polyvinylpyrrolidone, and 0.05% calcium chloride in 0.1M sodium cacodylate buffer pH 7.4, after an initial flush with 0.1M sodium cacodylate buffer, pH 7.4. The imidazole-buffered osmium tetroxide procedure described by Angermuller and Fahimi (Angermuller and Fahimi, 1982) was used to stain for lipids. Tissue was en block stained in aqueous uranyl acetate, dehydrated, infiltrated and embedded in LX-112 resin (Ladd Research Industries, Burlington, VT). Samples were ultrathin sectioned on the Reichert Ultracut S ultramicrotome and counter stained with 0.8% lead citrate. Grids were examined on a JEOL JEM-1230 electron microscope (JEOL USA, Inc., Peabody, MA) and photographed using the Gatan Ultrascan 1000 digital camera (Gatan Inc., Warrendale, PA.

Figure Legends

Figure 3-1. Generation and analysis of global *Lpcat3* knockout mice

(A) Strategy for generating global *Lpcat3* knockout mice. A "knock-out first/conditional-ready" gene-targeting vector was used to generate targeted cells. A gene-trap cassette is located between the two FRT sites. *LacZ*, β-galactosidase; *neo*, neomycin phosphotransferase II.

(B) Genotyping of $Lpcat3^{+/+}$ (WT), $Lpcat3^{+/-}$ (Het), and $Lpcat3^{-/-}$ (KO) mice. Genomic DNA was prepared from tail biopsies, and PCR products were separated on a 1% agarose gel.

(C) Expression of Lpcat3 in liver and small intestine of newborn $Lpcat3^{-/-}$ and $Lpcat3^{+/+}$ pups. Gene expression was quantified by real-time PCR ($n \geq 5$/group). Values are means ± SEM.

(D) The body weight and blood glucose of $Lpcat3^{+/+}$ (WT), $Lpcat3^{-/+}$ (Het), and $Lpcat3^{-/-}$ (KO) newborn pups ($n \geq 8$/group). Values are means ± SEM.

(E) Kaplan-Meier survival curve of $Lpcat3^{+/+}$ (WT), $Lpcat3^{-/+}$ (Het) and $Lpcat3^{-/-}$ (KO) pups after birth ($n \geq 20$ mice/group). The neonatal lethality can be delayed by injection of 50 μl 10% glucose solution once per day after born. 5 $Lpcat3^{+/+}$ (WT), 9 $Lpcat3^{-/+}$ (Het) and 6 $Lpcat3^{-/-}$ (KO) mice were used in the rescue experiment.

(F) Representative photograph of $Lpcat3^{+/+}$ (WT) and $Lpcat3^{-/-}$ (KO) pups after 5 days of glucose injections.

(G-H) Gene expression in livers (G) and small intestines (H) of $Lpcat3^{+/+}$ (WT) and $Lpcat3^{-/-}$ (Lpcat3 KO) newborn pups. Gene expression was quantified by real-time PCR (n ≥ 5/group). Values are means ± SEM.

Statistical analysis was performed using student's *t*-test (C, G and H) and one-way ANOVA with Bonferroni post-hoc tests (D). $*p < 0.05$; $**p < 0.01$.

Figure 3-2. Altered triglyceride metabolism in liver-specific *Lpcat3* knockout mice

(A) Strategy for generating tissue-specific *Lpcat* knockout mice. *Lpcat3*$^{-/+}$ mice carrying the conditional-ready knockout allele were mated with *Flpe* transgenic mice to generate the *Lpcat3*$^{fl/fl}$ mice. *Lpcat3*$^{fl/fl}$ mice were bred with tissue-specific *Cre* transgenic mice to generate tissue-specific *Lpcat3* knockout mice.

(B) Expression of Lpcat family members in liver of *Lpcat3*$^{fl/fl}$ (F/F) and *Lpcat3*$^{fl/fl}$ *Albumin-Cre* (L-KO) mice fed a chow diet. Gene expression was quantified by real-time PCR ($n \geq 6$/group) (left panel). Primary hepatocytes from *Lpcat3*$^{fl/fl}$ (F/F) and *Lpcat3*$^{fl/fl}$ *Albumin-Cre* (L-KO) mice were treated overnight with 1 mM LXR agonist GW3965 (GW). Lpcat3 expression was quantified by real-time PCR (right panel). Ct values in *Lpcat3*$^{fl/fl}$ liver samples were shown. Ct value of 36B4 is about 20. Values are means ± SEM.

(C) Plasma lipid levels in chow diet-fed *Lpcat3*$^{fl/fl}$ (F/F) and *Lpcat3*$^{fl/fl}$ *Albumin-Cre* (L-KO) mice under fed (*ad libitum*) or overnight (o/n) fasting ($n \geq 8$/group). Plasma levels of cholesterol and non-esterified fatty acids (NEFA) were measured after an overnight fast. Values are means ± SEM.

(D) Plasma was harvested from chow diet-fed *Lpcat3*$^{fl/fl}$ (F/F) and *Lpcat3*$^{fl/fl}$ *Albumin-Cre* (L-KO) mice after an overnight fast. ApoB protein was analyzed by western blotting and quantified (Fig. 3-2 Supplemental 2B).

(E) Plasma from *Lpcat3*$^{fl/fl}$ (F/F) and *Lpcat3*$^{fl/fl}$ *Albumin-Cre* (L-Lpcat3-KO) mice fasted overnight was pooled ($n = 5$). Lipoprotein profiles were analyzed by fast protein liquid chromatography (FPLC) (upper panel). ApoB protein in each corresponding fraction was analyzed by western blot (lower panel) and quantified (Fig. 3-2 Supplemental 2A).

(F) Lipid contents in livers of chow diet-fed *Lpcat3*$^{fl/fl}$ (F/F) and *Lpcat3*$^{fl/fl}$ *Albumin-Cre* (L-KO) mice fasted overnight ($n \geq 8$/group). Values are means ± SEM.

(G) Hematoxylin and eosin staining of liver sections from chow-fed *Lpcat3*$^{fl/fl}$ (F/F) and *Lpcat3*$^{fl/fl}$ *Albumin-Cre* (L-KO) mice after an overnight fast.

(H) Liver expression of Lpcat3 (left panel) and plasma triglyceride levels (right panel) in *Lpcat3*$^{fl/fl}$ mice 3 weeks after being injected with an adenovirus encoding GFP or *Cre*. Mice were sacrificed under fed conditions (*ad libitum*) or after overnight fasting (o/n) ($n \geq 6$/group). Gene expression was measured by real-time. Values are means ± SEM.

Statistical analysis was performed with a student's *t*-test (B, C, F, H). *$p < 0.05$; **$p < 0.01$

Figure 3-3. Loss of Lpcat3 in liver does not alter body weight or fasting blood glucose level in mice

(A) Blood glucose and (B) body weight of Lpcat3 flox/flox (F/F) and L-Lpcat3 KO mice were measured after a 6 h fasting.

Figure 3-4. Dietary challenge accentuates metabolic phenotypes in liver-specific *Lpcat3* knockout mice

(A) Plasma lipids of *Lpcat3*$^{fl/fl}$ (F/F) and *Lpcat3*$^{fl/fl}$ *Albumin-Cre* (L-KO) mice fed on a western diet for 9 weeks. Plasma was collected from mice fasted for 6 hr ($n \geq 8$/group). Values are means ± SEM.

(B) Plasma samples same as in (A) were pooled ($n = 5$). Lipoprotein profile was analyzed by fast protein liquid chromatography (FPLC) (upper panel). ApoB protein in each fraction was analyzed by western blot (lower panel) and quantified (Fig. 3 Supplemental 1A).

(C) ApoB protein in plasma samples same as in (A) was analyzed by western blot and quantified (Fig. 3 Supplemental 1B).

(D-E) Hematoxylin and eosin staining (D) and lipid contents (E) of livers from western diet-fed *Lpcat3*$^{fl/fl}$ (F/F) and *Lpcat3*$^{fl/fl}$ *Albumin-Cre* (L-KO) mice. Values are means ± SEM.

(F-G) Hematoxylin and eosin staining (F) and lipid contents (G) of livers from high sucrose diet-fed *Lpcat3*$^{fl/fl}$ (F/F) and *Lpcat3*$^{fl/fl}$ *Albumin-Cre* (L-KO) mice. Mice were fed on diet for 3 weeks and sacrificed after 6 h fasting. Values are means ± SEM.

Statistical analysis was performed using student's t-test (A, E and G). *$p < 0.05$; **$p < 0.01$

Figure 3-5. Altered triglyceride metabolism in intestine-specific Lpcat3 knockout mice

(A) Induction of Lpcat3 mRNA expression in duodenum of mice treated with 40 mg/kg/day GW3956 by oral gavage for 3 days (n = 5/group). Gene expression was measured by real-time PCR. Values are means ± SEM.

(B) Representative photograph and body weight of newborn *Lpcat3*$^{fl/fl}$ *Villin-cre* (IKO) and control *Lpcat3*$^{fl/fl}$ (F/F) pups (n = 5/group for body weight measurement). Values are means ± SEM.

(C) Representative photograph and body weight of 1 week-old *Lpcat3*$^{fl/fl}$ *Villin-cre* (IKO) and control *Lpcat3*$^{fl/fl}$ (F/F) pups ($n \geq 6$/group for body weight measurement). Values are means ± SEM.

(D) Expression of Lpcat family members in 1 week-old *Lpcat3*$^{fl/fl}$ (F/F) and *Lpcat3*$^{fl/fl}$ *Villin-cre* (IKO) duodenum measured by real-time PCR ($n \geq 6$/group). Ct values of F/F samples were shown. Values are means ± SEM.

(E) Blood glucose, plasma lipids and insulin levels in 1 week-old *Lpcat3*$^{fl/fl}$ (F/F) and *Lpcat3*$^{fl/fl}$ *Villin-cre* (IKO) pups ($n \geq 6$/group). Values are means ± SEM.

(F) Hematoxylin and eosin staining of intestines from 1 week-old *Lpcat3*$^{fl/fl}$ (WT) and *Lpcat3*$^{fl/fl}$ *Villin-cre* (IKO) pups.

(G) Expression of genes in duodenum of 1 week-old *Lpcat3*$^{fl/fl}$ (WT) and *Lpcat3*$^{fl/fl}$ *Villin-cre* (IKO) pups. Gene expression was measured by real-time PCR ($n \geq 6$/group). Values are means ± SEM.

Statistical analysis was performed using student's *t*-test (A, B, D, E and F). *p < 0.05; **p < 0.01

Figure 3-6. Lpcat3 is required for the incorporation of arachidonate into phosphatidylcholine in mouse liver and VLDL

(A-B) ESI-MS/MS analysis of the abundance of PC species in livers from *Lpcat3*$^{fl/fl}$ (Flox/Flox) and *Lpcat3*$^{fl/fl}$ *Albumin-Cre* (L-Lpcat3 KO) mice fed on a chow diet (A) and a western diet (B) ($n \geq 5$/group).

(C) ESI-MS/MS analysis of the abundance of PC species in plasma VLDL fraction from *Lpcat3*$^{fl/fl}$ (fl/fl) and *Lpcat3*$^{fl/fl}$ *Albumin-Cre* (L-Lpcat3 KO) mice fed on a chow diet. Plasma was harvested from mice after overnight fasting. VLDL fractions were pooled from 5 mice/group.

(D) GC-FID analysis of the abundance of arachidonoyl acyl chain in triglyceride (TAG) in livers from *Lpcat3*$^{fl/fl}$ (F/F) and *Lpcat3*$^{fl/fl}$ *Albumin-Cre* (L-KO) mice fed on a chow diet.

Statistical analysis was performed using student's t-test. Values are means ± SEM. *p < 0.05; **p < 0.01

Figure 3-7. Lpcat3 is required for the incorporation of arachidonate into phosphatidylethanolamine in mouse liver

(A-B) ESI-MS/MS analysis of the abundance of PE species in livers from *Lpcat3*$^{fl/fl}$ (Flox/Flox) and *Lpcat3*$^{fl/fl}$ *Albumin-Cre* (L-Lpcat3 KO) mice fed on a chow diet (A) and a western diet (B).

Figure 3-8. Analysis of cholesteryl ester and lysoPC species in L-Lpcat3 KO mice

(A-B) ESI-MS/MS analysis of the abundance of cholesteryl ester (A) and lysophosphatidylcholine (LysoPC) (B) species in livers of *Lpcat3*$^{fl/fl}$ (Flox/Flox) and *Lpcat3*$^{fl/fl}$ *Albumin-Cre* (L-Lpcat3 KO) mice fed on a chow diet ($n \geq 5$/group).

(C-D) ESI-MS/MS analysis of the abundance of cholesteryl ester (C) and lysophosphatidylcholine (LysoPC) (D) species in livers of *Lpcat3*$^{fl/fl}$ (Flox/Flox) and *Lpcat3*$^{fl/fl}$ *Albumin-Cre* (L-Lpcat3 KO) mice fed on a western diet ($n \geq 5$/group).

Statistical analysis was performed using student's t-test. Values are means ± SEM. *$p < 0.05$; **$p < 0.01$

Figure 3-9. Altered gene expression linked to lipid metabolism and inflammation in liver-specific Lpcat3 knockout mice

(A) Gene expression in livers of *Lpcat3*$^{fl/fl}$ (F/F) and *Lpcat3*$^{fl/fl}$ *Albumin-Cre* (L-KO) mice fed on a chow diet was analyzed by Affymetrix arrays. Select genes under the gene ontology (GO) term "lipid metabolism" are presented by heatmap. Samples from 5 mice/group were pool for analysis.

(B-C) Gene expression in livers of *Lpcat3*$^{fl/fl}$ (F/F) and *Lpcat3*$^{fl/fl}$ *Albumin-Cre* (L-KO) mice fed on a western diet for 9 weeks was analyzed by Affymetrix arrays. Select genes under the gene

ontology (GO) term "lipid metabolism" (B) and "immune system process" (C) are presented by heatmap. Samples from 5 mice/group were pool for analysis.

(D) Expression of selective lipid metabolism genes in livers of *Lpcat3*$^{fl/fl}$ (Fl/Fl) and *Lpcat3*$^{fl/fl}$ *Albumin-Cre* (L-Lpcat3 KO) mice fed on a chow diet was analyzed by real-time PCR ($n \geq$ 5/group). Values are means ± SEM.

(E-F) Expression of selective lipid metabolism (E) and inflammation (F) genes in livers of *Lpcat3*$^{fl/fl}$ (Fl/Fl) and *Lpcat3*$^{fl/fl}$ *Albumin-Cre* (L-Lpcat3 KO) mice fed on a western diet was analyzed by real-time PCR ($n \geq 5$/group). Values are means ± SEM.

Statistical analysis was performed using student's t-test (D, E and F). **p < 0.01.

Figure 3-10. Chronic deletion of Lpcat3 does not induce unfolded protein response downstream gene expression

(A) Gene expression in livers of *Lpcat3*$^{fl/fl}$ (F/F) and *Lpcat3*$^{fl/fl}$ *Albumin-Cre* (L-KO) mice fed on a chow diet was analyzed by Affymetrix arrays. Select ER stress marker genes are presented by heatmap. Samples from 5 mice/group were pool for analysis.

(B) Gene expression in livers of *Lpcat3*$^{fl/fl}$ (F/F) and *Lpcat3*$^{fl/fl}$ *Albumin-Cre* (L-KO) mice fed on a western diet was analyzed by Affymetrix arrays. Select ER stress marker genes are presented by heatmap. Samples from 5 mice/group were pool for analysis.

Figure 3-11. Loss of Lpcat3 from liver impairs hepatic TG secretion

(A) ApoB protein in livers from *Lpcat3*$^{fl/fl}$ (Flox/Flox) and *Lpcat3*$^{fl/fl}$ *Albumin-Cre* (L-Lpcat3 KO) mice fed on a chow diet was analyzed by western blot (n = 3).

(B) VLDL-TG secretion in *Lpcat3*$^{fl/fl}$ mice transduced with adenoviral expressed Cre (Ad-Cre), compared to control GPF (Ad-GFP) for 4 weeks. Mice were fasted for 6 hr followed by intravenous injection of tyloxapol. Plasma triglyceride was measured at indicated durations after tyloxapol injection. Values are means ± SEM.

(C) Plasma VLDL particle size in *Lpcat3*$^{fl/fl}$ *Albumin-Cre* mice. Isolated VLDL particles from *Lpcat3*$^{fl/fl}$ (Fl/Fl) and *Lpcat3*$^{fl/fl}$ *Albumin-Cre* (L-Lpcat3 KO) mice fed on a western diet were stained with 2.0% uranyl acetate and visualized by electron microscopy (left) and their size quantified (right).

Statistical analysis was performed using two-way ANOVA with Bonferroni post hoc tests (B).

**$p < 0.01$

Figure 3-12. Reduced nascent lipoprotein particle size in the lumen of Golgi and secretory vesicles in Lpcat3-deficient liver

Electron microscopy of imidazole-stained liver sections. *Lpcat3*$^{fl/fl}$ (Fl/Fl) and *Lpcat3*$^{fl/fl}$ *Albumin-Cre* (L-Lpcat3 KO) mice were fasted for 6 h. Samples were fixed and processed as described in the methods. Arrowheads indicate nascent lipoprotein particles.

Figure 3-13. Loss of Lpcat3 in liver does not alter membrane structure in ER and mitochondria

A. Electron microscopy of imidazole-stained liver sections. Arrowheads indicate nascent lipoprotein particles in smooth ER lumen.

B. Electron microscopy of imidazole-stained liver sections. Mitochondria are shown.

C. Electron microscopy of imidazole-stained liver sections. Rough ER is shown.

Figure 3-14. Lpcat3 activity regulates membrane lipid mobility and apoB lipidation in hepatocytes

(A) The distribution of apoB-containing lipoproteins in the Golgi fractions isolated from livers of *Lpcat3*$^{fl/fl}$ (F/F) and *Lpcat3*$^{fl/fl}$ *Albumin-Cre* (LKO) mice. Golgi luminal contents were subject to a density gradient ultracentrifugation. 12 fractions from the gradient were harvested from top to bottom and analyzed by western blot.

(B) Triglyceride contents of the Golgi fractions isolated from livers of *Lpcat3*$^{fl/fl}$ (F/F) and *Lpcat3*$^{fl/fl}$ *Albumin-Cre* (LKO) mice. Results from two representative experiments were shown.

(C) Live primary hepatocytes from *Lpcat3*$^{fl/fl}$ (Flox/Flox) and *Lpcat3*$^{fl/fl}$ *Albumin-Cre* (L-Lpcat3 KO) mice were stained with laurdan. The laurdan emission spectrum was captured by a 2-photon laser-scan microscope. Generalized polarization (GP) was calculated from the emission intensities obtained from images. Higher GP value indicates that membranes are more ordered and less dynamic. The GP value of each pixel was used to generate a pseudocolor GP image.

(D) The binary histograms of the GP distribution of the GP images (n = 4). The size of the GP binary is 0.05.

Figure 3-15. Lpcat3 is required for LXR-dependent VLDL triglyceride secretion from liver

Plasma lipoprotein profile from flox/flox and L-Lpcat3 mice gavaged with LXR agonist GW 3965 (20mg/kg) for 2 days. Pooled plasma (5 mice/group) was analyzed by FPLC. Increases in VLDL triglyceride were calculated based on the area under the curve.

Figure 3-16. Schematic illustration of the role of the LXR-Lpcat3 pathway in VLDL lipidation

Activation of LXRs promotes the incorporation of arachidonate into intracellular membranes through the induction of Lpcat3 expression. This change in membrane composition creates a dynamic membrane environment that facilitates the transfer of TG synthesized on ER and/or in cytosolic LD to nascent apoB–containing lipoproteins particles, leading to the efficient lipidation of apoB–containing lipoproteins.

Table 3-1. Breeding data for global Lpcat3-deficient mice

Genotypic ratio of newborns and weanlings obtained from Lpcat3 heterozygote intercrosses.

Table 3-2. Breeding data for liver-specific Lpcat3-deficient mice

Genotypic ratio of adult mice obtained from *Lpcat3*$^{fl/fl}$ and Lpca*t3*$^{fl/fl}$ *Albumin-Cre* intercrosses.

Table 3-3. Breeding data for intestine-specific Lpcat3-deficient mice

Genotypic ratio of newborns and 1 week-old pups obtained from *Lpcat3*$^{fl/fl}$ and *Lpcat3*$^{+/F}$ *Villin-Cre* intercrosses.

Table 3-4. Quantitative real-time PCR primer sequences

Figure 3-1. Generation and analysis of global *Lpcat3* knockout mice

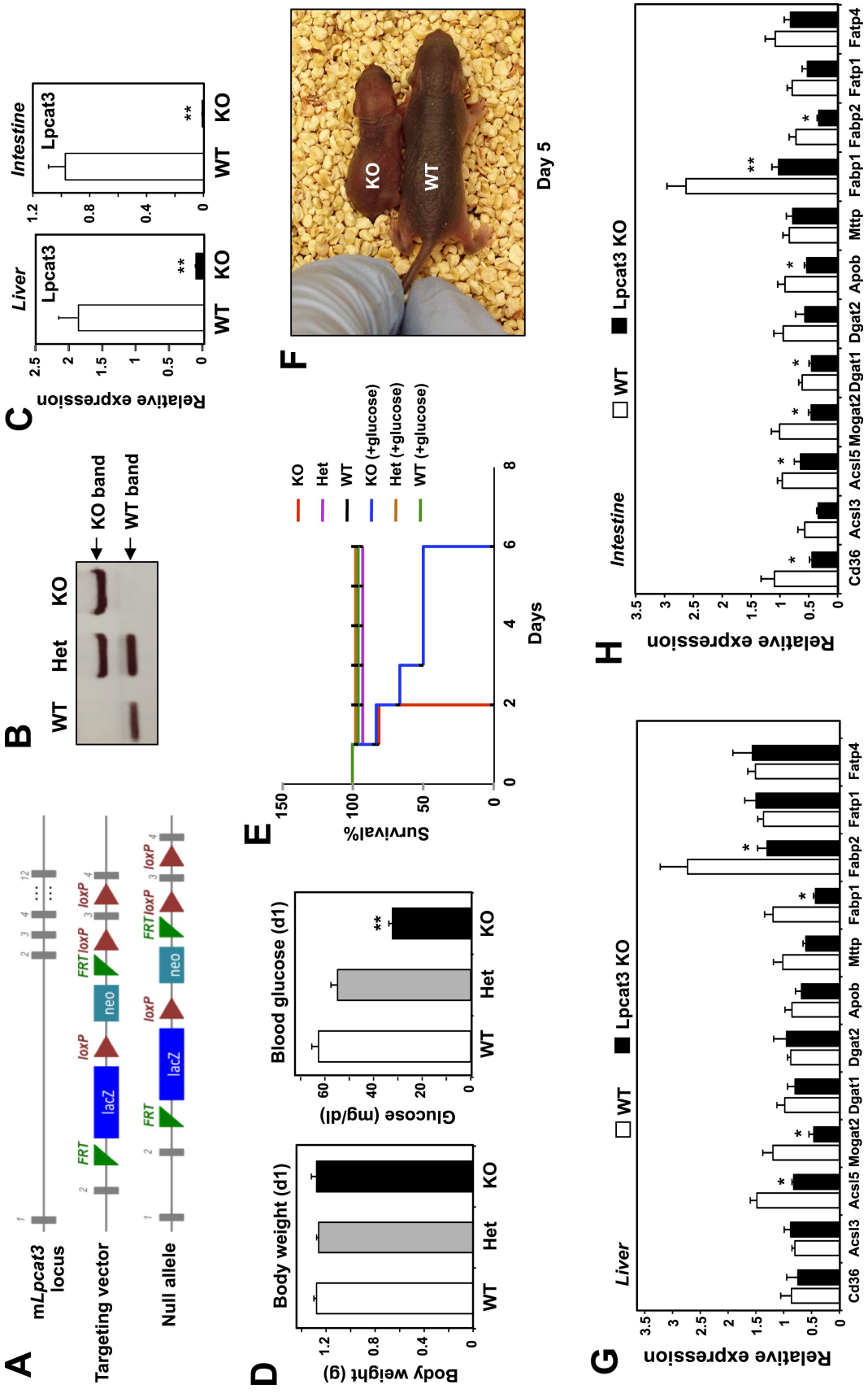

Figure 3-2. Altered triglyceride metabolism in liver-specific *Lpcat3* knockout mice

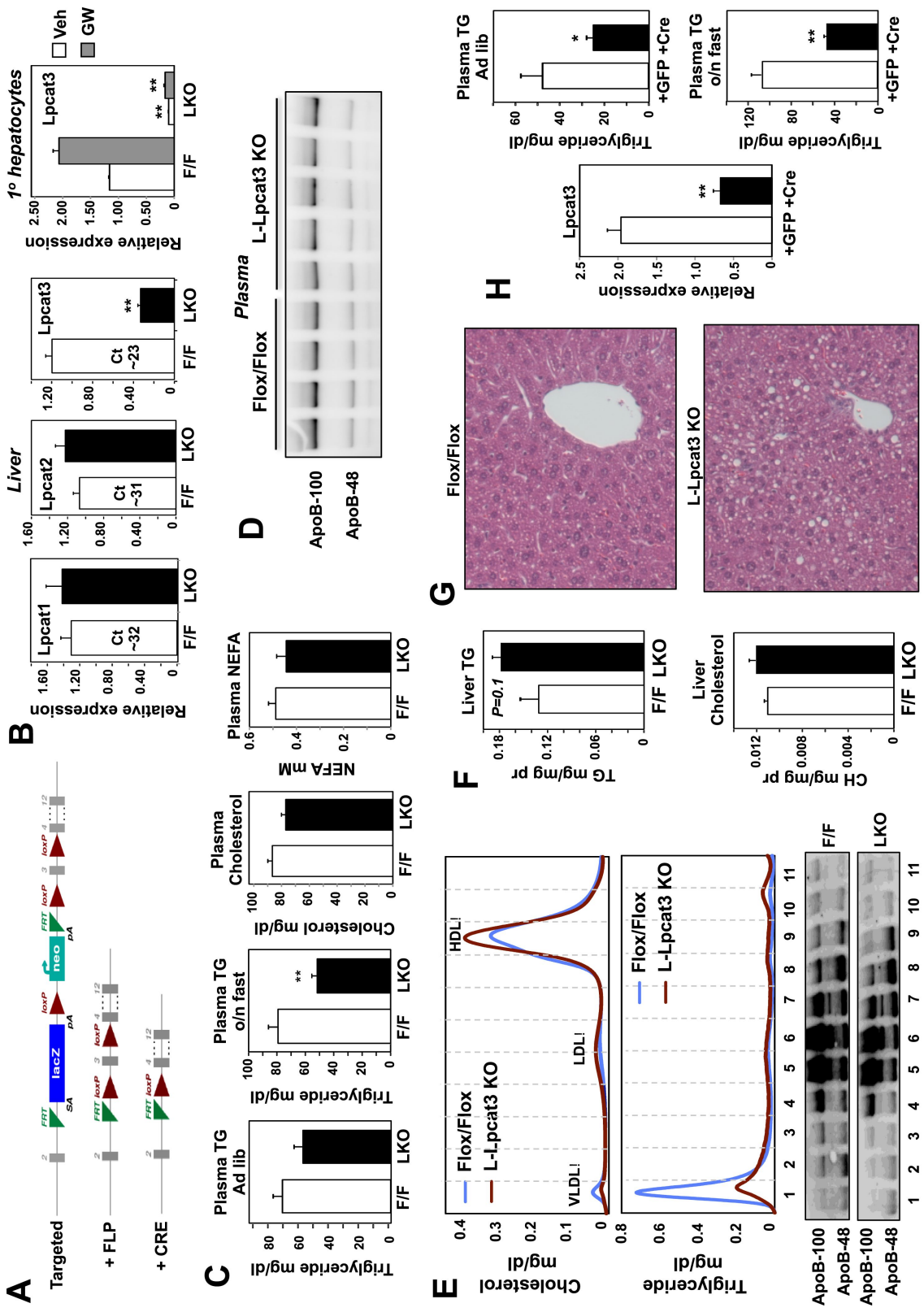

Figure 3-3. Loss of Lpcat3 in liver does not alter body weight or fasting blood glucose level in mice

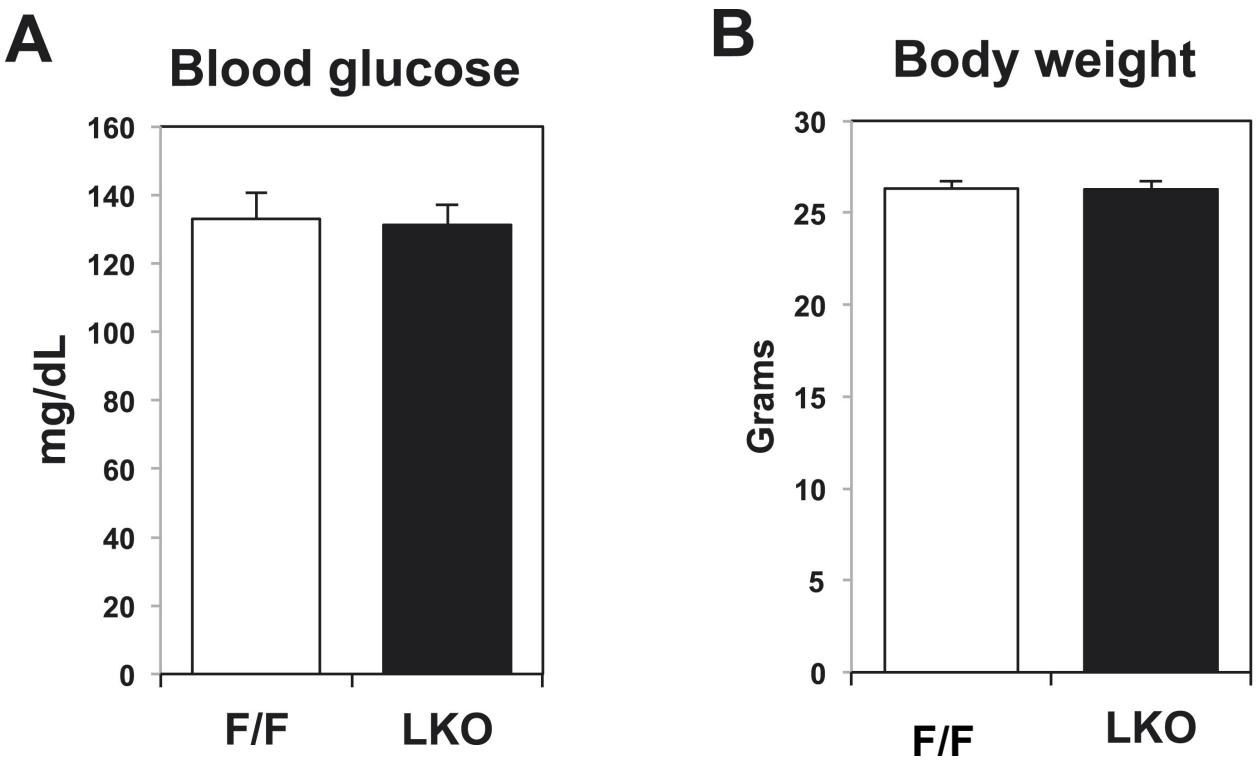

Figure 3-4. Dietary challenge accentuates metabolic phenotypes in liver-specific *Lpcat3* knockout mice

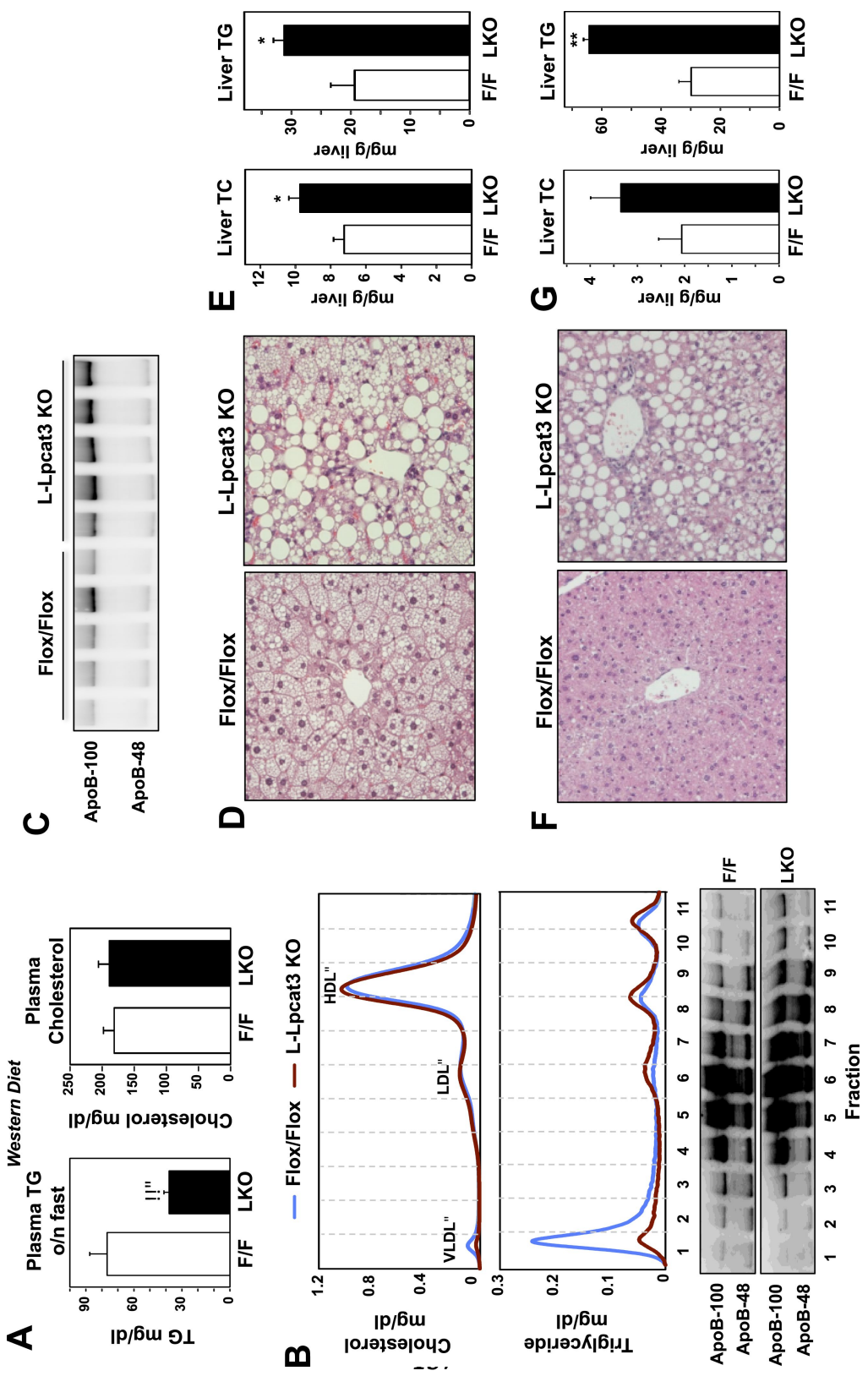

Figure 3-5. Altered triglyceride metabolism in intestine-specific Lpcat3 knockout mice

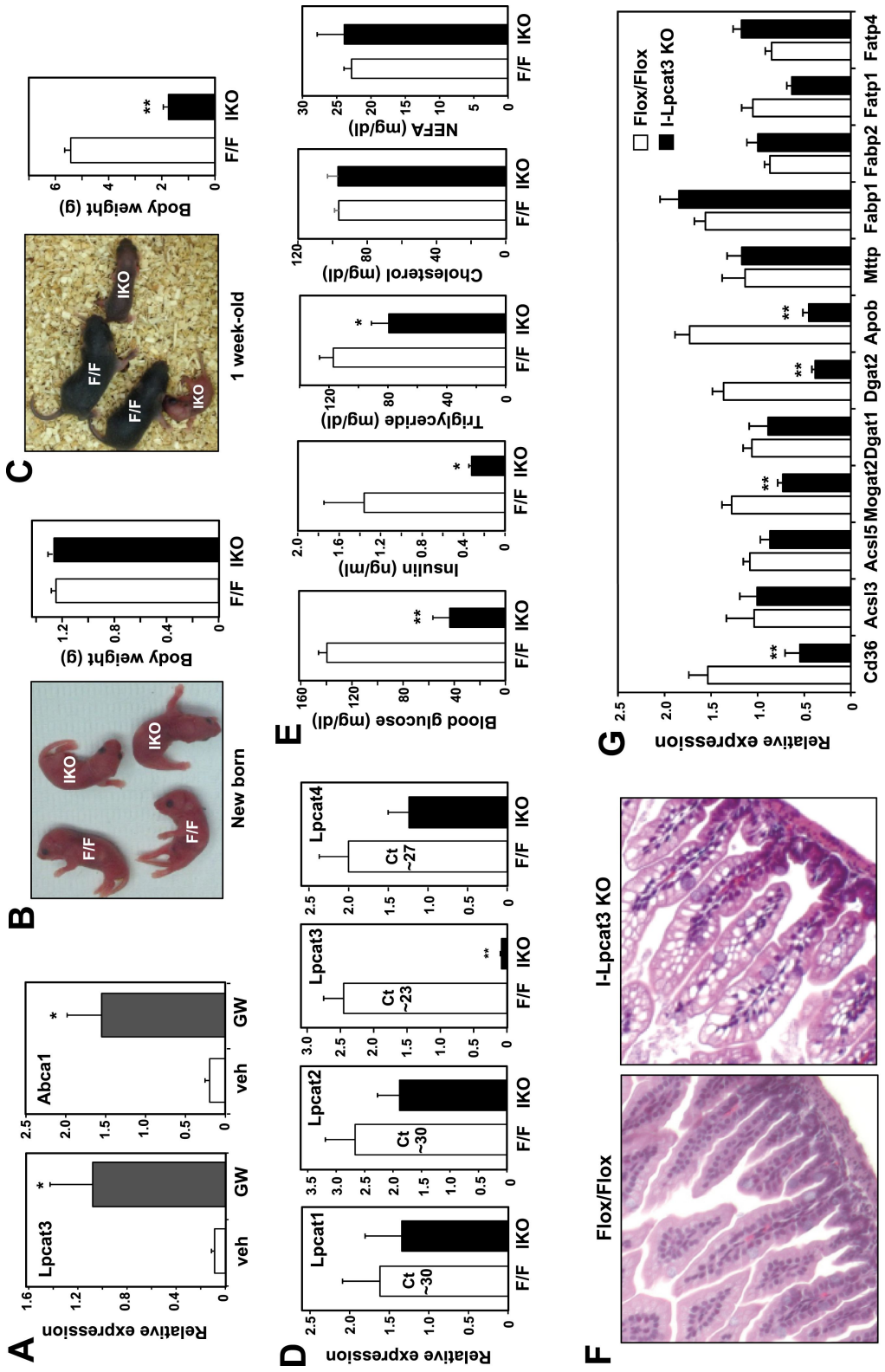

Figure 3-6. Lpcat3 is required for the incorporation of arachidonate into phosphatidylcholine in mouse liver and VLDL

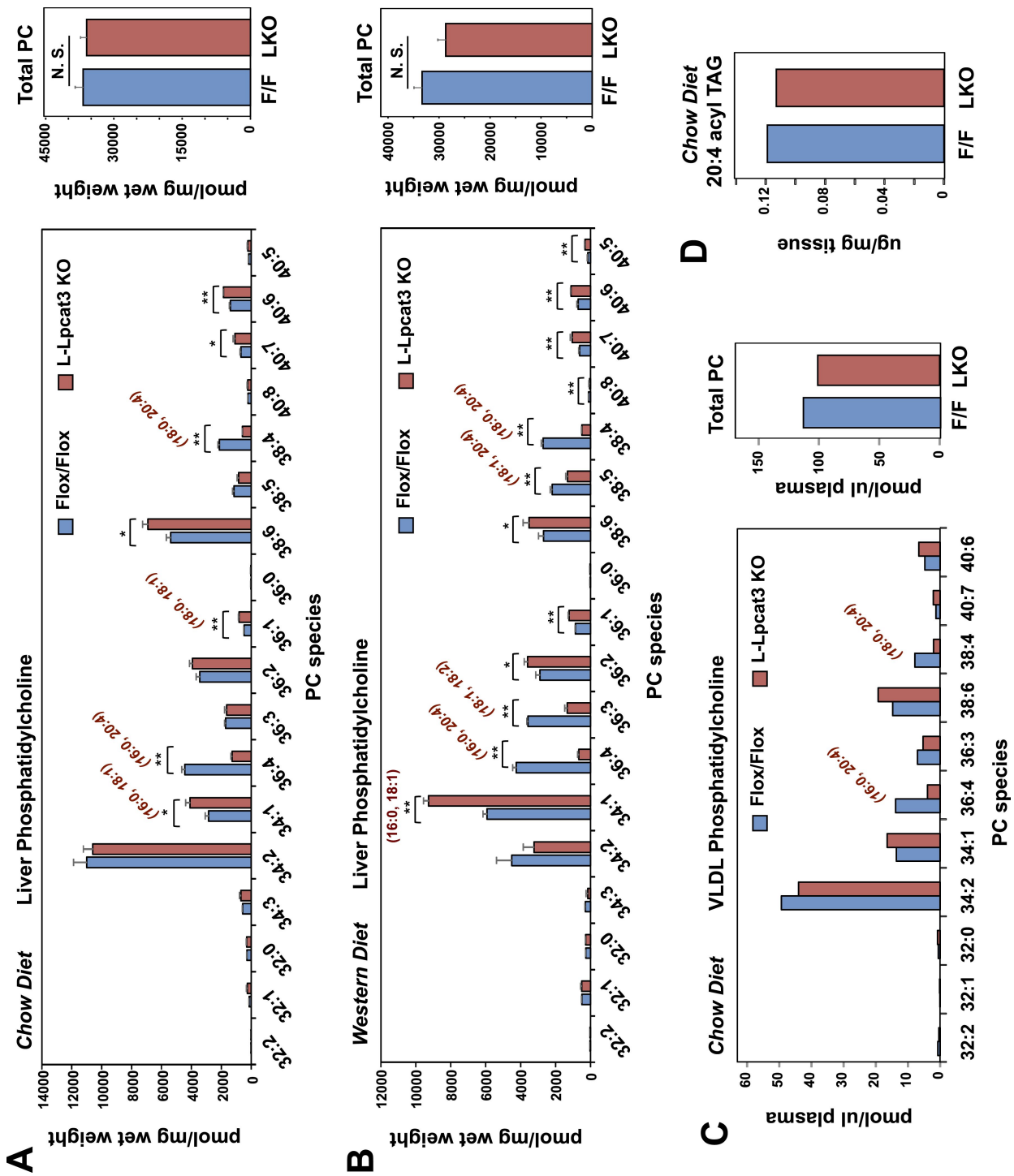

Figure 3-7. Lpcat3 is required for the incorporation of arachidonate into phosphatidylethanolamine in mouse liver

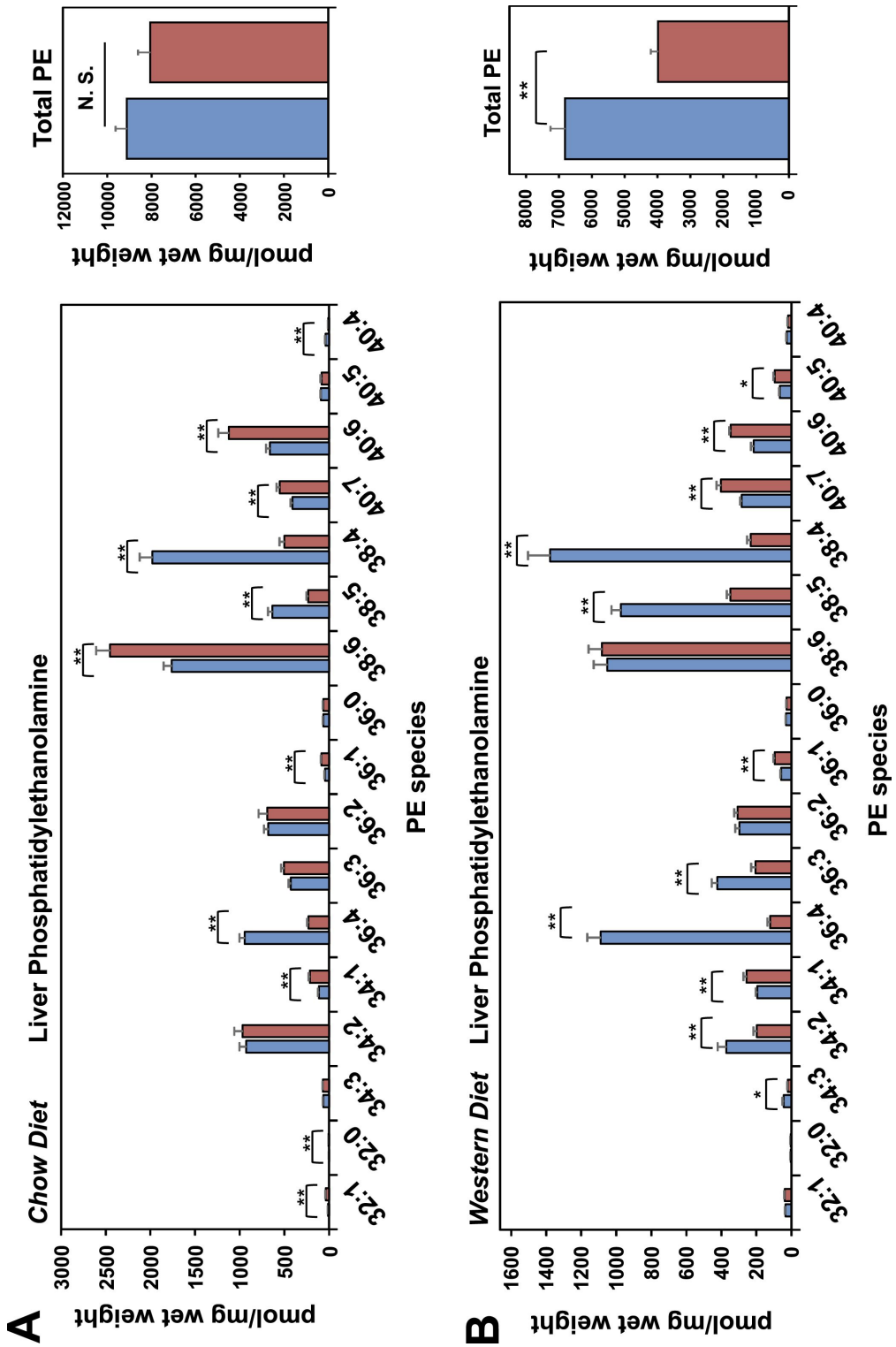

Figure 3-8. Analysis of cholesteryl ester and lysoPC species in L-Lpcat3 KO mice

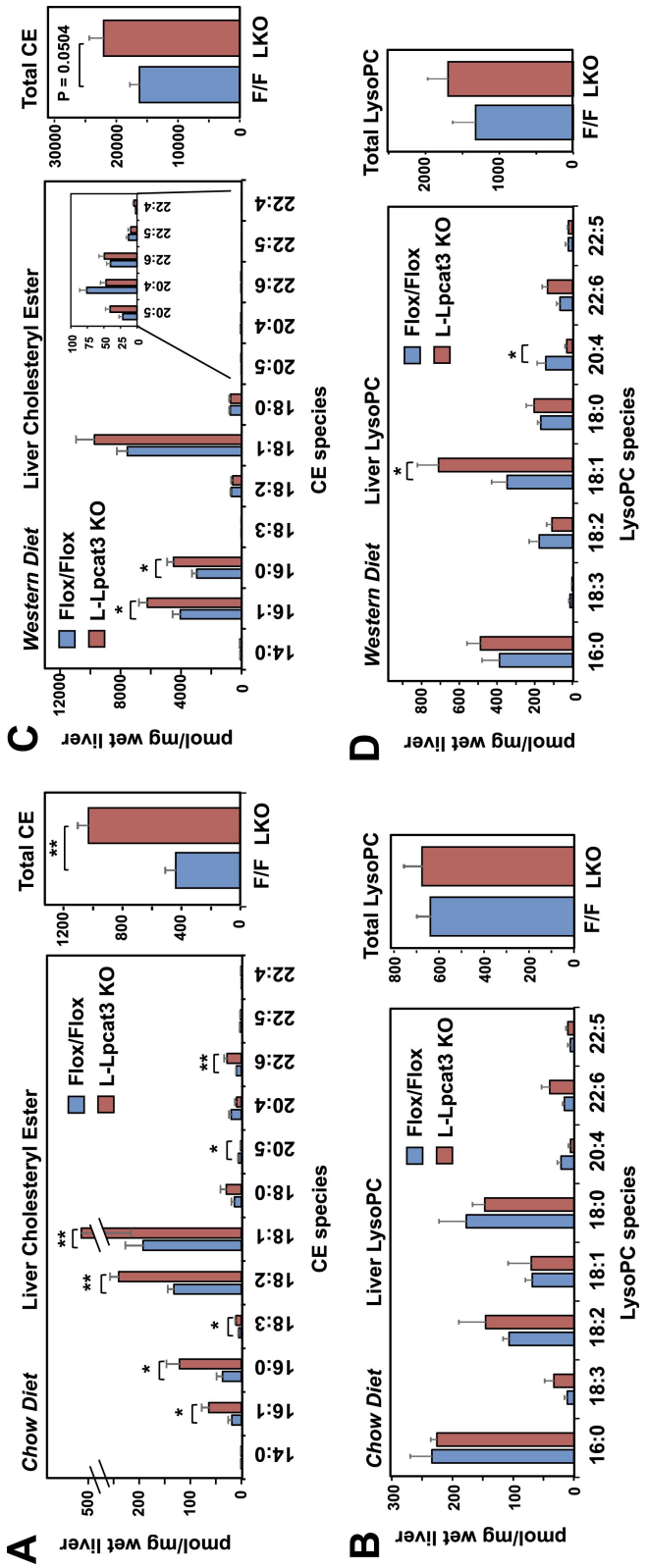

Figure 3-9. Altered gene expression linked to lipid metabolism and inflammation in liver-specific Lpcat3 knockout mice

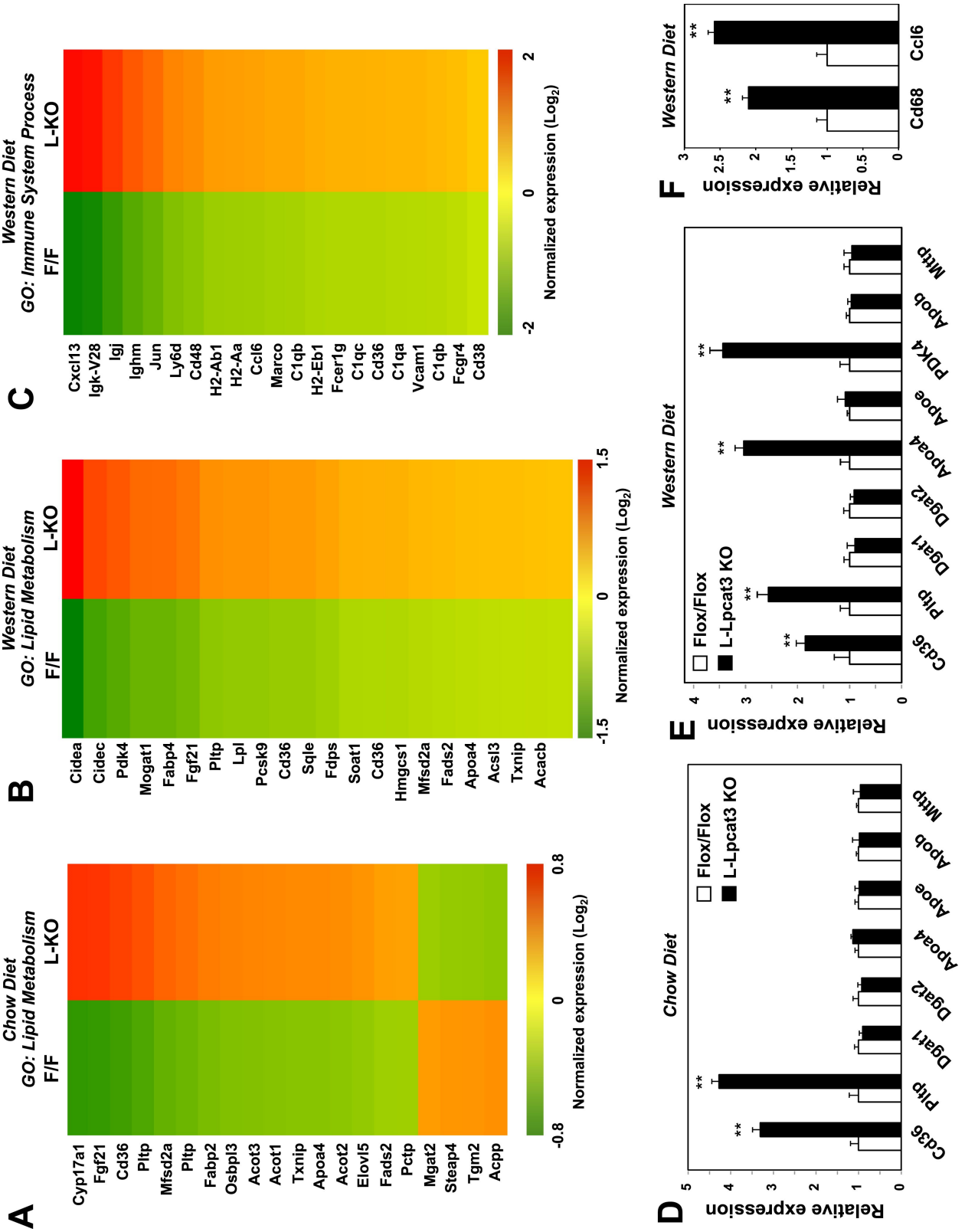

Figure 3-10. Chronic deletion of Lpcat3 does not induce unfolded protein response downstream gene expression

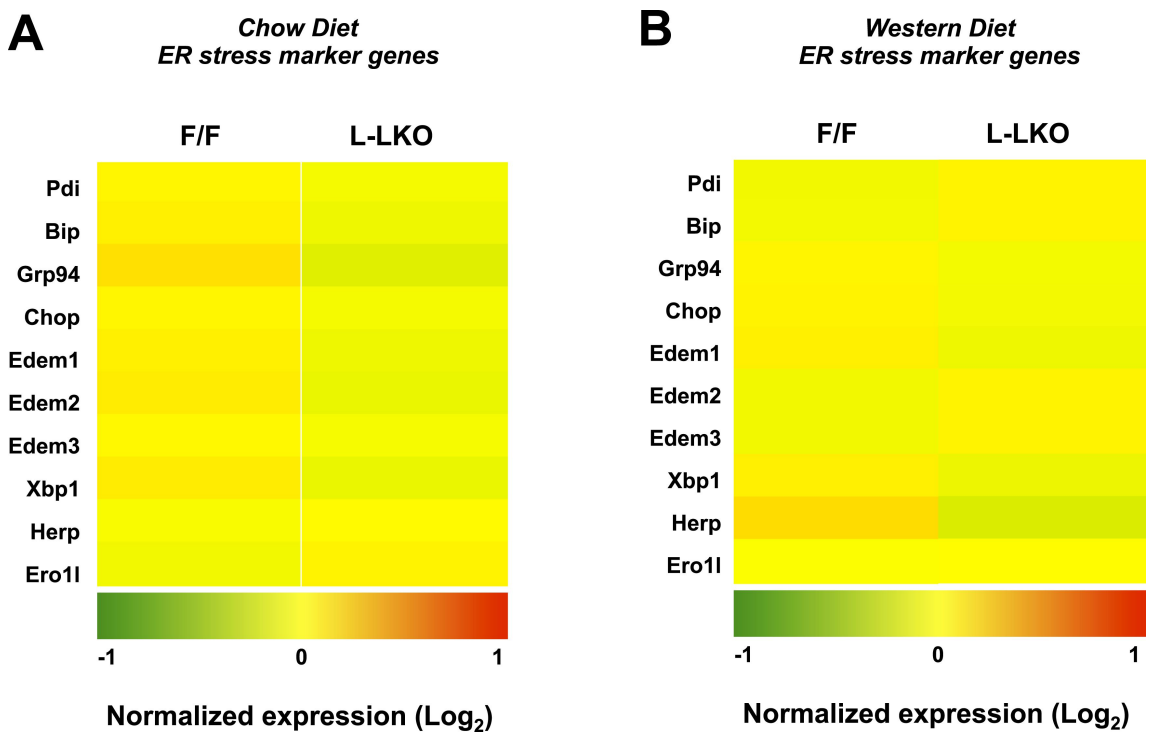

Figure 3-11. Loss of Lpcat3 from liver impairs hepatic TG secretion

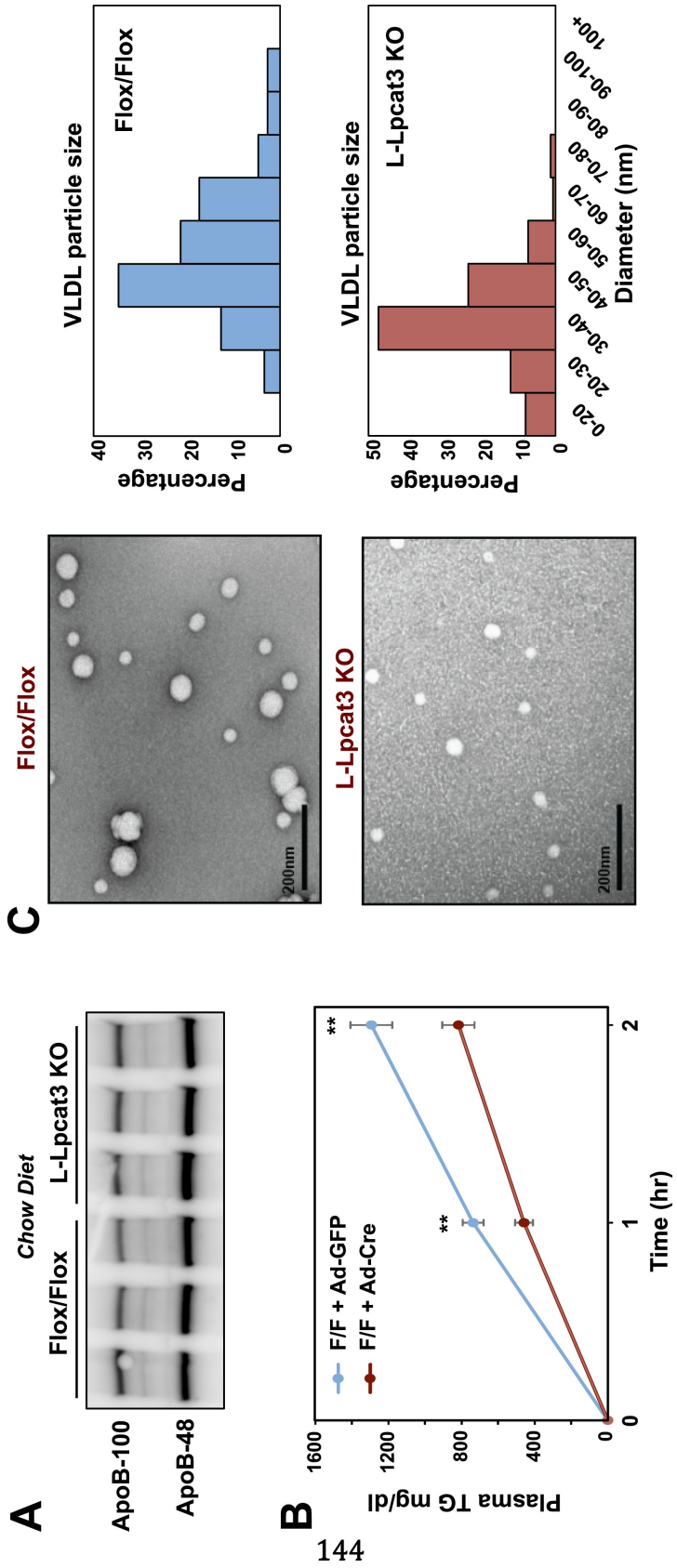

Figure 3-12. Reduced nascent lipoprotein particle size in the lumen of Golgi and secretory vesicles in Lpcat3-deficient liver

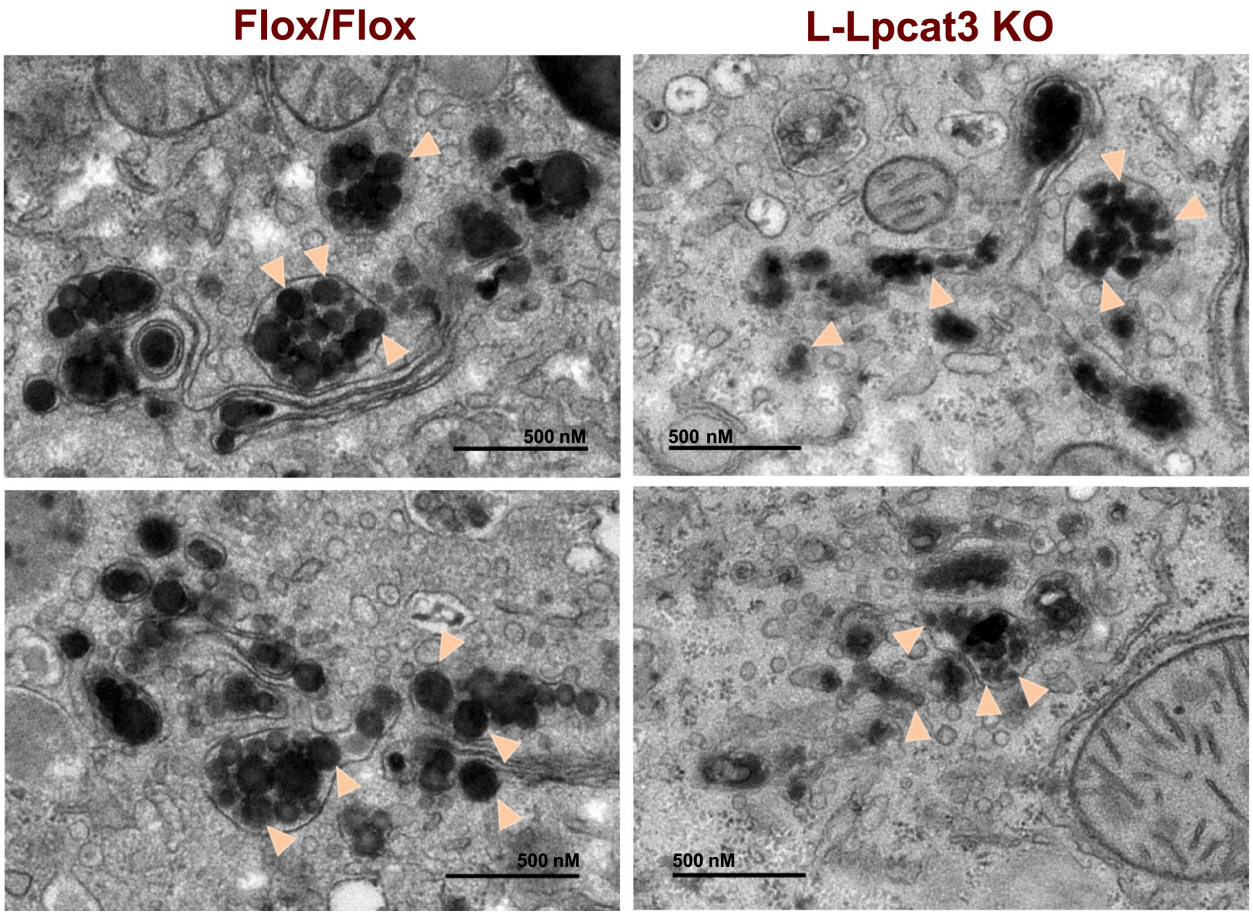

Figure 3-13. Loss of Lpcat3 in liver does not alter membrane structure in ER and mitochondria

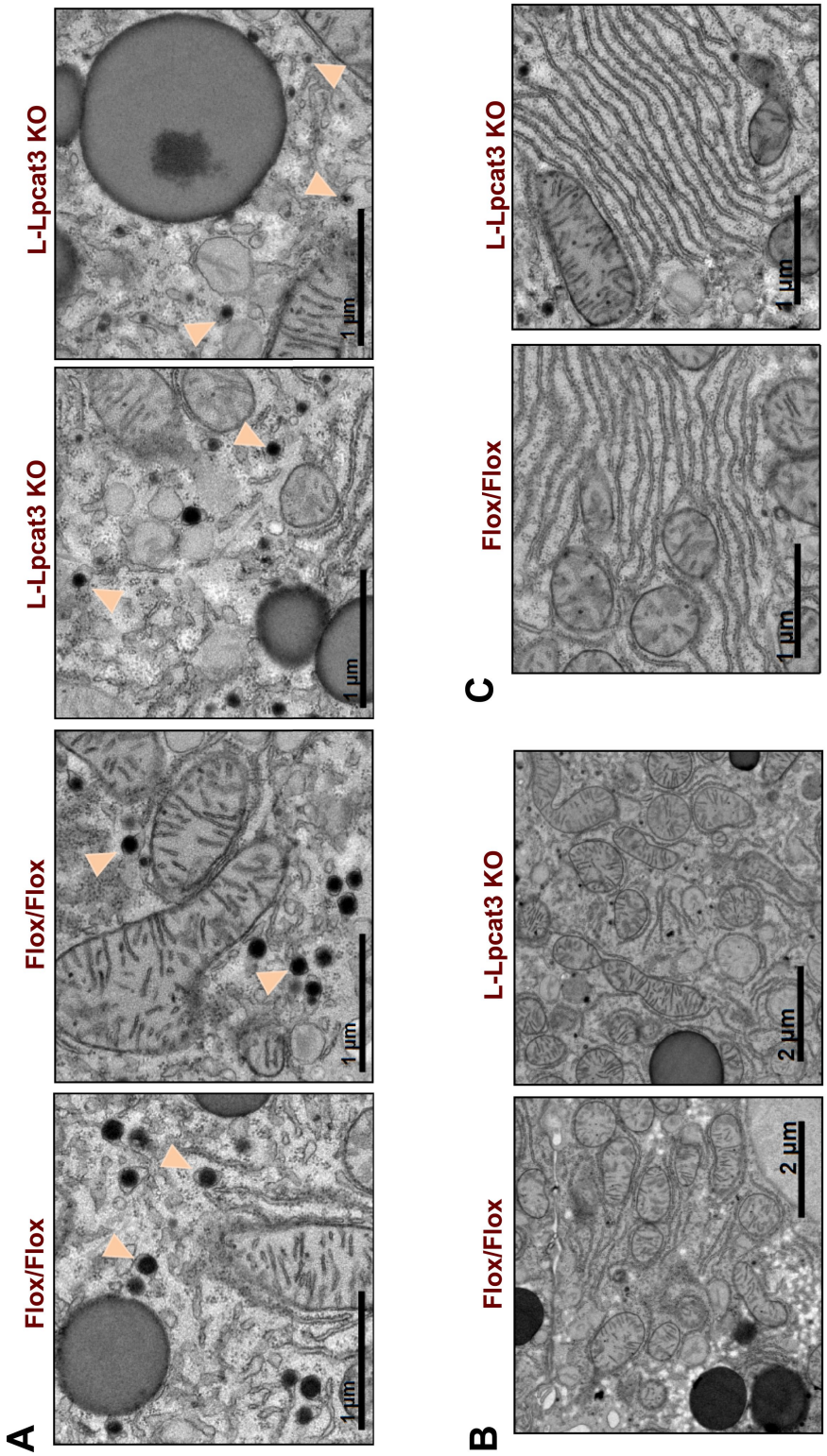

Figure 3-14. Lpcat3 activity regulates membrane lipid mobility and apoB lipidation in hepatocytes

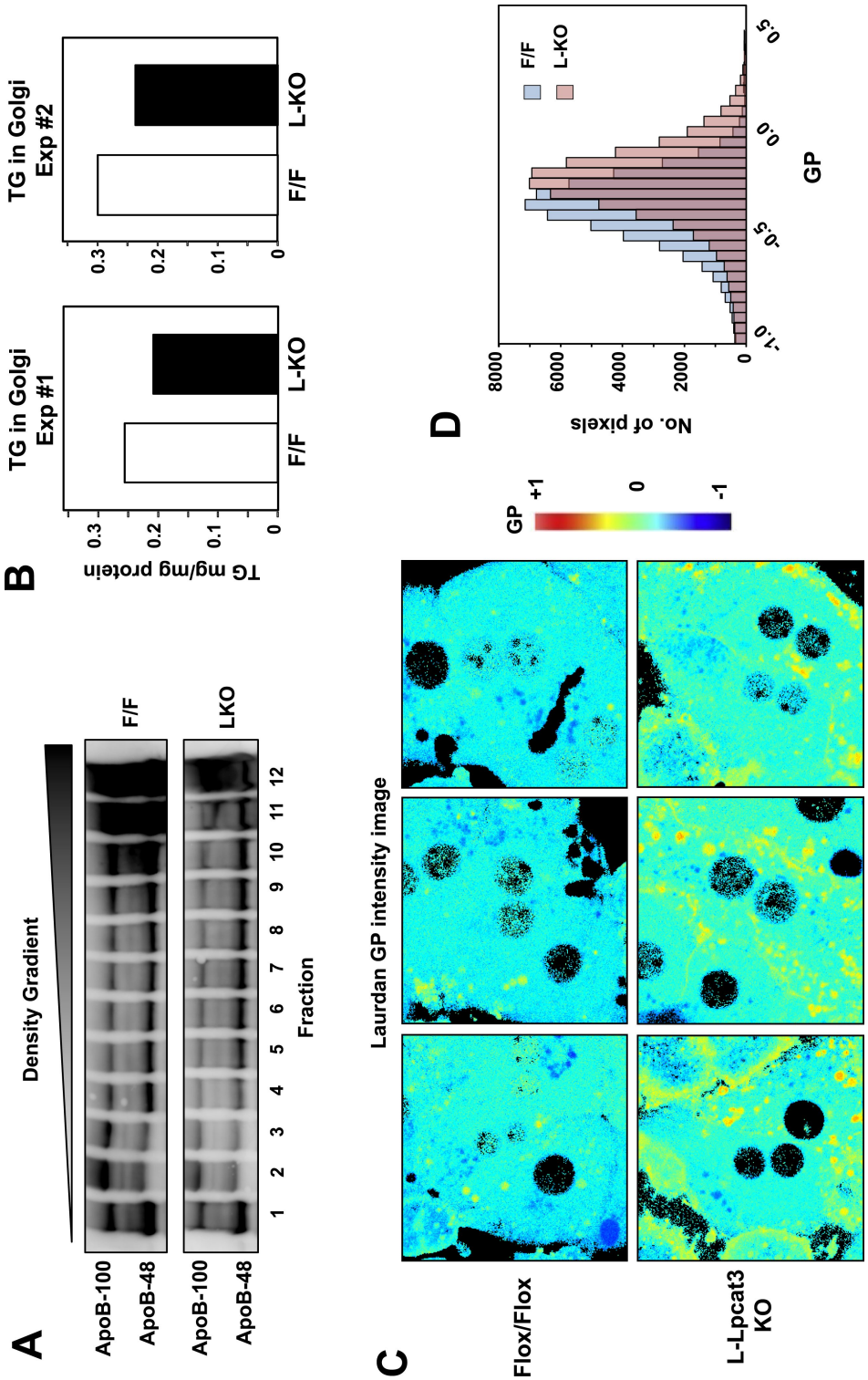

Figure 3-15. Lpcat3 is required for LXR-dependent VLDL triglyceride secretion from liver

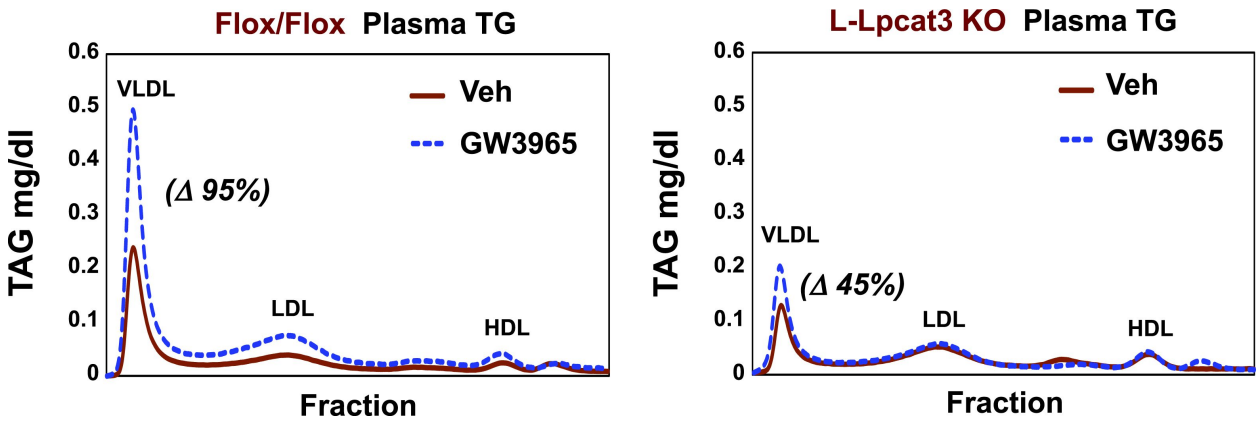

Figure 3-16. Schematic illustration of the role of the LXR-Lpcat3 pathway in VLDL lipidation

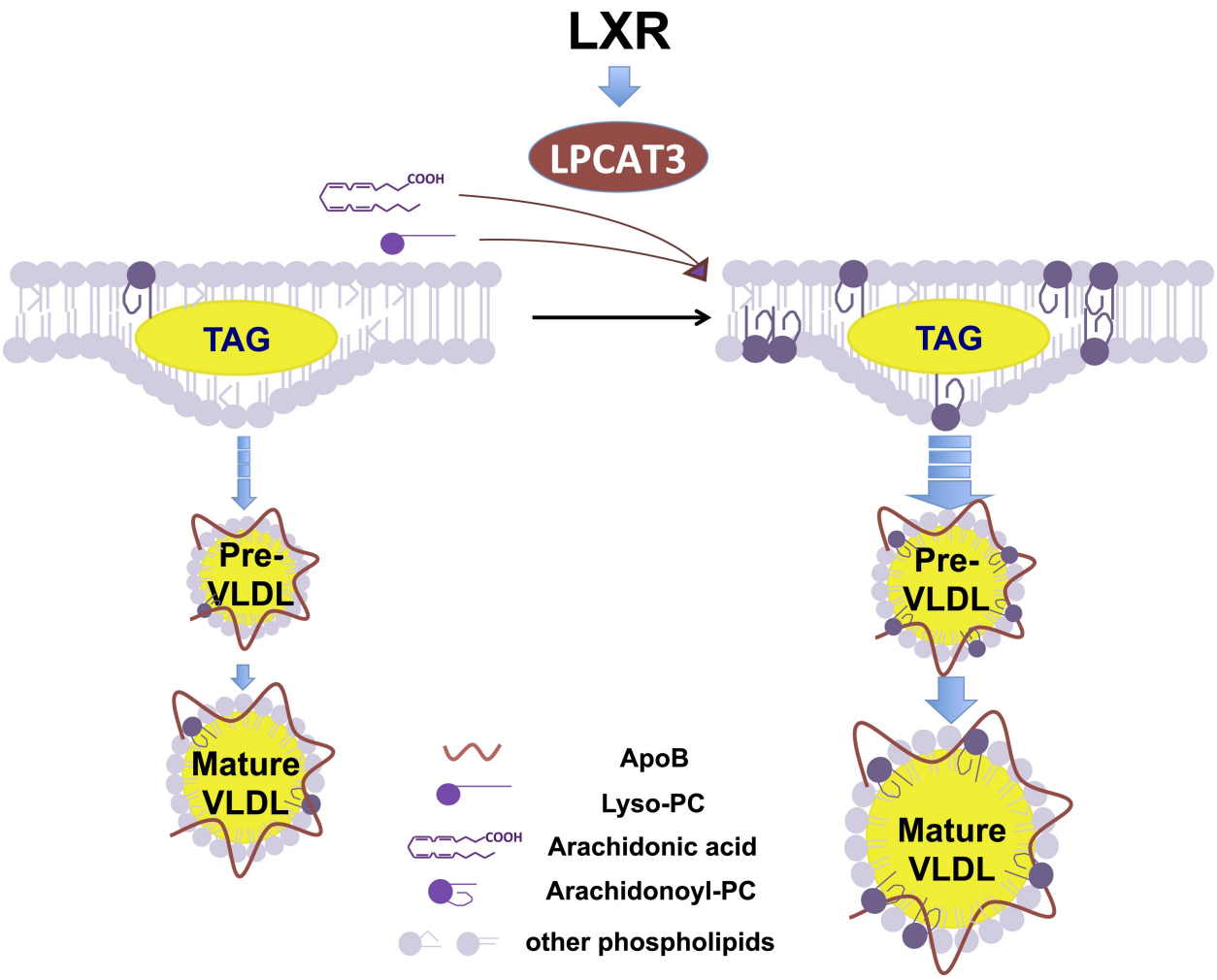

Table 3-1. Breeding data for global Lpcat3-deficient mice

Table 1. Breeding data for global Lpcat3-deficient mice

Genotype	Number of pups/mice	Observed %	Expected %	Time
WT	25	28	25	
Het	43	48	50	At birth
KO	21	23	25	
WT	50	35	25	
Het	91	64	50	At weaning
KO	0	0	25	

Table 3-2. Breeding data for liver-specific Lpcat3-deficient mice

Table 2. Breeding data for liver-specific Lpcat3-deficient mice

Genotype	Number of mice	Observed %	Expected %
Flox/Flox	26	53	50
Flox/Flox$^{albumin\text{-}cre}$	23	46	50

Table 3-3. Breeding data for intestine-specific Lpcat3-deficient mice

Table 3. Breeding data for intestine-specific Lpcat3-deficient mice

Genotype	Number of pups/mice	Observed %	Expected %	Time
WT	25	28	25	At birth
Het	43	48	50	
KO	21	23	25	
Genotype	**Number of pups**	**Observed %**	**Expected %**	**Time**
F/F, Cre+	20	24	25	At birth
F/F, Cre−	24	28	25	
F/+, Cre+	19	22	25	
F/+, Cre−	20	24	25	
F/F, Cre+	12	16	25	1 week old
F/F, Cre−	24	32	25	
F/+, Cre+	19	25	25	
F/+, Cre−	20	26	25	

Table 3-4. Quantitative real-time PCR primer sequences

Table 4. Quantitative real-time PCR primer sequences

Murine qPCR primers	Forward	Reverse
CD36	TTGAAAAGTCTCGGACATTGAG	TCAGATCCGAACACAGCGTA
PLPT	GTCTAAAATGAATATGGCCTTCG	CCAGAAGTGATGAACGTGGA
DGAT1	TTCCGCCTCTGGGCATT	GCCCACAATCCAGGCCA
DGAT2	GGCGCTACTTCCGAGACTAC	TGGTCAGCAGGTTGTGTGTC
APOA4	ACCCAGCTAAGCAACAATGC	TGTCCTGGAAGAGGGTACTGA
APOE	GACTTGTTTCGGAAGGAGCTG	CCACTCGAGCTGATCTGTCA
AOPB	CTGAACATCAAGAGGGGCATC	GGTAACCTGAGTTGAGCAGTTT
MTTP	GGCAGTGCTTTTTCTCTGCT	TGAGAGGCCAGTTGTGTGAC
PDK4	ACCGAAGAACCTGGCGAAG	TGATCCCGTAAAATGTCAGGC
CD68	GACCTACATCAGAGCCCGAGT	CGCCATGAATGTCCACTG
CCL6	TCTTTATCCTTGTGGCTGTCC	TGGAGGGTTATAGCGACGAT
ACSL3	TCTAGGAGTGAAGGCCAACG	GCAATATCTGAGGGCAGTGG
ACSL5	AACCAGTCTGTGGGGATTGAG	CGTCTTGGCGTCTGAGAAGTA
MOGAT2	TCTTCCAGTACAGCTTTGGCCTCA	TGATATAGCGCTGATGAAGCCGGT
FABP1	AGTACCAATTGCAGAGCCAGGAGA	GACAATGTCGCCCAATGTCATGGT
FABP2	AGAGGAAGCTTGGAGCTCATGACA	TCGCTTGGCCTCAACTCCTTCATA
FATP1	CGCTTTCTGCGTATCGTCTG	GATGCACGGGATCGTGTCT
LPCAT3	GGCCTCTCAATTGCTTATTTCA	AGCACGACACATAGCAAGGA
LPCAT1	GTGCACGAGCTGCGACT	GCTGCTCTGGCTCCTTATCA
LPCAT2	TGTACTAATCGCTCCTGTTTGATT	CACTGGAACTCCTGGGATG
LPCAT4	TTCGGTTTCAGAGGATACGACAA	AATGTCTGGATTGTCGGACTGAA
36B4	AGATGCAGCAGATCCGCAT	GTTCTTGCCCATCAGCACC
GAPDH	TGTGTCCGTCGTGGATCTGA	CCTGCTTCACCACCTTCTTGAT

References:

Abumrad, N.A., and Davidson, N.O. (2012). Role of the gut in lipid homeostasis. Physiological reviews *92*, 1061-1085.

Ågren, J.J., Kurvinen, J.-P., and Kuksis, A. (2005). Isolation of very low density lipoprotein phospholipids enriched in ethanolamine phospholipids from rats injected with Triton WR 1339. Biochimica et Biophysica Acta (BBA) - Molecular and Cell Biology of Lipids *1734*, 34-43.

Angermuller, S., and Fahimi, H.D. (1982). Imidazole-buffered osmium tetroxide: an excellent stain for visualization of lipids in transmission electron microscopy. The Histochemical journal *14*, 823-835.

Bligh, E.G., and Dyer, W.J. (1959). A rapid method of total lipid extraction and purification. Canadian journal of biochemistry and physiology *37*, 911-917.

Bowden, J.A., Shao, F., Albert, C.J., Lally, J.W., Brown, R.J., Procknow, J.D., Stephenson, A.H., and Ford, D.A. (2011). Electrospray ionization tandem mass spectrometry of sodiated adducts of cholesteryl esters. Lipids *46*, 1169-1179.

Chen, M., Preston Mason, R., and Tulenko, T.N. (1995). Atherosclerosis alters the composition, structure and function of arterial smooth muscle cell plasma membranes. Biochimica et Biophysica Acta (BBA) - Molecular Basis of Disease *1272*, 101-112.

Demarco, V.G., Ford, D.A., Henriksen, E.J., Aroor, A.R., Johnson, M.S., Habibi, J., Ma, L., Yang, M., Albert, C.J., Lally, J.W., et al. (2013). Obesity-related alterations in cardiac lipid profile and nondipping blood pressure pattern during transition to diastolic dysfunction in male db/db mice. Endocrinology *154*, 159-171.

Fisher, E.A., and Ginsberg, H.N. (2002). Complexity in the Secretory Pathway: The Assembly and Secretion of Apolipoprotein B-containing Lipoproteins. Journal of Biological Chemistry *277*, 17377-17380.

Ford, D.A., and Gross, R.W. (1988). Identification of endogenous 1-O-alk-1'-enyl-2-acyl-sn-glycerol in myocardium and its effective utilization by choline phosphotransferase. Journal of Biological Chemistry *263*, 2644-2650.

Ford, D.A., and Gross, R.W. (1989). Differential accumulation of diacyl and plasmalogenic diglycerides during myocardial ischemia. Circulation Research *64*, 173-177.

Golfetto, O., Hinde, E., and Gratton, E. (2013). Laurdan fluorescence lifetime discriminates cholesterol content from changes in fluidity in living cell membranes. Biophysical journal *104*, 1238-1247.

Gusarova, V., Brodsky, J.L., and Fisher, E.A. (2003). Apolipoprotein B100 exit from the endoplasmic reticulum (ER) is COPII-dependent, and its lipidation to very low density lipoprotein occurs post-ER. The Journal of biological chemistry *278*, 48051-48058.

Han, X., and Gross, R.W. (2005). Shotgun lipidomics: electrospray ionization mass spectrometric analysis and quantitation of cellular lipidomes directly from crude extracts of biological samples. Mass spectrometry reviews *24*, 367-412.

Hishikawa, D., Shindou, H., Kobayashi, S., Nakanishi, H., Taguchi, R., and Shimizu, T. (2008). Discovery of a lysophospholipid acyltransferase family essential for membrane asymmetry and diversity. Proceedings of the National Academy of Sciences of the United States of America *105*, 2830-2835.

Holzer, R.G., Park, E.J., Li, N., Tran, H., Chen, M., Choi, C., Solinas, G., and Karin, M. (2011). Saturated fatty acids induce c-Src clustering within membrane subdomains, leading to JNK activation. Cell *147*, 173-184.

Jacobs, R.L., Devlin, C., Tabas, I., and Vance, D.E. (2004). Targeted deletion of hepatic CTP:phosphocholine cytidylyltransferase alpha in mice decreases plasma high density and very low density lipoproteins. The Journal of biological chemistry *279*, 47402-47410.

Koeberle, A., Shindou, H., Koeberle, S.C., Laufer, S.A., Shimizu, T., and Werz, O. (2013). Arachidonoyl-phosphatidylcholine oscillates during the cell cycle and counteracts proliferation by suppressing Akt membrane binding. Proceedings of the National Academy of Sciences of the United States of America *110*, 2546-2551.

Lev, S. (2012). Nonvesicular Lipid Transfer from the Endoplasmic Reticulum. Cold Spring Harbor Perspectives in Biology *4*.

Li, X., Ye, J., Zhou, L., Gu, W., Fisher, E.A., and Li, P. (2012). Opposing roles of cell death-inducing DFF45-like effector B and perilipin 2 in controlling hepatic VLDL lipidation. Journal of lipid research *53*, 1877-1889.

Nguyen, L.N., Ma, D., Shui, G., Wong, P., Cazenave-Gassiot, A., Zhang, X., Wenk, M.R., Goh, E.L., and Silver, D.L. (2014). Mfsd2a is a transporter for the essential omega-3 fatty acid docosahexaenoic acid. Nature *509*, 503-506.

Nilsson, A. (1968). Intestinal absorption of lecithin and lysolecithin by lymph fistula rats. Biochimica et biophysica acta *152*, 379-390.

Noga, A.A., and Vance, D.E. (2003). A gender-specific role for phosphatidylethanolamine N-methyltransferase-derived phosphatidylcholine in the regulation of plasma high density and very low density lipoproteins in mice. The Journal of biological chemistry *278*, 21851-21859.
Okazaki, H., Goldstein, J.L., Brown, M.S., and Liang, G. (2010). LXR-SREBP-1c-phospholipid transfer protein axis controls very low density lipoprotein (VLDL) particle size. The Journal of biological chemistry *285*, 6801-6810.

Parasassi, T., De Stasio, G., d'Ubaldo, A., and Gratton, E. (1990). Phase fluctuation in phospholipid membranes revealed by Laurdan fluorescence. Biophysical journal *57*, 1179-1186.

Parasassi, T., and Gratton, E. (1995). Membrane lipid domains and dynamics as detected by Laurdan fluorescence. Journal of fluorescence *5*, 59-69.

Parthasarathy, S., Subbaiah, P.V., and Ganguly, J. (1974). The mechanism of intestinal absorption of phosphatidylcholine in rats. The Biochemical journal *140*, 503-508.

Pinot, M., Vanni, S., Pagnotta, S., Lacas-Gervais, S., Payet, L.-A., Ferreira, T., Gautier, R., Goud, B., Antonny, B., and Barelli, H. (2014). Polyunsaturated phospholipids facilitate membrane deformation and fission by endocytic proteins. Science *345*, 693-697.

Puri, P., Baillie, R.A., Wiest, M.M., Mirshahi, F., Choudhury, J., Cheung, O., Sargeant, C., Contos, M.J., and Sanyal, A.J. (2007). A lipidomic analysis of nonalcoholic fatty liver disease. Hepatology *46*, 1081-1090.

Rahim, A., Nafi-valencia, E., Siddiqi, S., Basha, R., Runyon, C.C., and Siddiqi, S.A. (2012). Proteomic analysis of the very low density lipoprotein (VLDL) transport vesicles. Journal of proteomics *75*, 2225-2235.

Rodriguez, C.I., Buchholz, F., Galloway, J., Sequerra, R., Kasper, J., Ayala, R., Stewart, A.F., and Dymecki, S.M. (2000). High-efficiency deleter mice show that FLPe is an alternative to Cre-loxP. Nature genetics *25*, 139-140.

Rong, X., Albert, C.J., Hong, C., Duerr, M.A., Chamberlain, B.T., Tarling, E.J., Ito, A., Gao, J., Wang, B., Edwards, P.A., et al. (2013). LXRs regulate ER stress and inflammation through dynamic modulation of membrane phospholipid composition. Cell metabolism *18*, 685-697.

Schultz, J.R., Tu, H., Luk, A., Repa, J.J., Medina, J.C., Li, L., Schwendner, S., Wang, S., Thoolen, M., Mangelsdorf, D.J., et al. (2000). Role of LXRs in control of lipogenesis. Genes & development *14*, 2831-2838.

Spector, A.A., and Yorek, M.A. (1985). Membrane lipid composition and cellular function. Journal of lipid research *26*, 1015-1035.

Tintle, N.L., Pottala, J.V., Lacey, S., Ramachandran, V., Westra, J., Rogers, A., Clark, J., Olthoff, B., Larson, M., Harris, W., et al. (2014). A genome-wide association study of saturated, mono- and polyunsaturated red blood cell fatty acids in the Framingham Heart Offspring Study. Prostaglandins, leukotrienes, and essential fatty acids.

Tso, P., Balint, J.A., and Simmonds, W.J. (1977). Role of biliary lecithin in lymphatic transport of fat. Gastroenterology *73*, 1362-1367.

Tso, P., Lam, J., and Simmonds, W.J. (1978). The importance of the lysophosphatidylcholine and choline moiety of bile phosphatidylcholine in lymphatic transport of fat. Biochimica et biophysica acta *528*, 364-372.

Vance, D.E. (2008). Role of phosphatidylcholine biosynthesis in the regulation of lipoprotein homeostasis. Current opinion in lipidology *19*, 229-234.

Vance, J.E., and Vance, D.E. (1988). Does rat liver Golgi have the capacity to synthesize phospholipids for lipoprotein secretion? The Journal of biological chemistry *263*, 5898-5909.

Vest, R., Wallis, R., Jensen, L.B., Haws, A.C., Callister, J., Brimhall, B., Judd, A.M., and Bell, J.D. (2006). Use of steady-state laurdan fluorescence to detect changes in liquid ordered phases in human erythrocyte membranes. The Journal of membrane biology *211*, 15-25.

Voshol, P.J., Minich, D.M., Havinga, R., Elferink, R.P., Verkade, H.J., Groen, A.K., and Kuipers, F. (2000). Postprandial chylomicron formation and fat absorption in multidrug resistance gene 2 P-glycoprotein-deficient mice. Gastroenterology *118*, 173-182.

Yamashita, A., Hayashi, Y., Nemoto-Sasaki, Y., Ito, M., Oka, S., Tanikawa, T., Waku, K., and Sugiura, T. (2014). Acyltransferases and transacylases that determine the fatty acid composition of glycerolipids and the metabolism of bioactive lipid mediators in mammalian cells and model organisms. Progress in Lipid Research *53*, 18-81.

Zhao, Y., Chen, Y.Q., Bonacci, T.M., Bredt, D.S., Li, S., Bensch, W.R., Moller, D.E., Kowala, M., Konrad, R.J., and Cao, G. (2008). Identification and characterization of a major liver lysophosphatidylcholine acyltransferase. The Journal of biological chemistry *283*, 8258-8265.

Chapter 4: Conclusions and Future Directions

Ever since the discovery of the first phospholipid (PL) in the early nineteenth century, studies of PLs have been intimately tied to the research of biology. PLs are traditionally considered as inert structural components of cellular membranes to separate cells from the external environment and provide a platform for various biological processes. The fluid mosaic model proposed in 1972 (Singer and Nicolson, 1972) pointed out a possibility that the lipid bilayer might dynamically interact with membrane proteins and influence their functions. Thereafter, multiple biochemical studies have demonstrated that changes in membrane lipid composition could affect the properties of membrane proteins. While these studies acknowledged the influence of PL composition on membrane protein function, they provided no information about the physiological relevance of these effects. From the standpoint of physiology and metabolic regulation, two critical questions need to be answered: 1) is endogenous PL composition dynamically modulated by metabolic regulation? 2) If so, does the dynamic modulation of membrane lipid composition exert any physiological impact? A major focus of this dissertation is investigating these two questions.

In this study, we have identified a nuclear receptor pathway that dynamically regulates the polyunsaturated phosphatidylcholine (PC) composition in cell membranes. Activation of liver X receptors (LXRs) preferentially drives the incorporation of polyunsaturated fatty acids, especially arachidonic acid, into phospholipids through induction of the remodeling enzyme lysophosphatidylcholine acyltransferase 3 (Lpcat3). Consistently, mice lacking Lpcat3 showed a dramatic and unique reduction in arachodonoyl-PC. We further demonstrated that the LXR-Lpcat3-mediated membrane PL remodeling plays important roles in different aspects of physiology in mice (Rong et al., 2013; Rong et al., 2015). In chapter 2, we showed that induction of Lpcat3 by LXRs reduces membrane saturation and counteracts saturated fatty acid-induced

endoplasmic reticulum (ER) stress. We also found that the LXR-Lpcat3 pathway suppresses hepatic inflammation by modulating c-Src-JNK activity and controls the availability of lipid inflammatory mediators (Rong et al., 2013). In chapter 3, we demonstrated that the Lpcat3-dependent production of arachidonoyl PC is required for efficient transportation of triglyceride to nascent very low-density lipoprotein (VLDL) (Rong et al., 2015). These studies highlight a previously unrecognized role for a specific membrane lipid class in ER stress, inflammation and triglyceride-rich lipoprotein production.

Besides the roles of Lpcat3 in liver and intestine physiology we discovered in this study, Lpcat3 is also reported to be essential for the incorporation of arachidonate into membranes in many other tissues, including brain, muscle, and spleen. Considering the fact that arachidonic acid has been associated to the biological function of these organs in various contexts, it is highly possible that Lpcat3 also plays physiological roles in these tissues. Tissue-specific Lpcat3 knockout mice will provide a unique and neat system to specifically study the function of arachidonoyl-PL and its derivatives in these tissues *in vivo*. Of broader interest, investigation of the metabolic regulation of the PL remodeling pathway will shed light on how cellular membrane lipids actively participate in biological processes and physiological functions.

Finally, aberrant cellular membrane lipid composition has been linked to several metabolic diseases. For example, lower amounts of polyunsaturated PLs have been observed in liver biopsies from nonalcoholic steatohepatitis patients (Puri et al., 2007), and cell membranes from patients with atherosclerotic disease tend to show decreased membrane fluidity (Chen et al., 1995). Although a causal relationship has not been established between abnormal membrane lipid composition and the pathogenesis of metabolic diseases, multiple lines of evidence, including this study, have demonstrated that alterations in membrane lipid composition affect

cellular ion balance, inflammation, ER stress, and lipid homeostasis, all of which are involved in the development of chronic metabolic diseases. These findings suggest that regulation of PL remodeling might represent a strategy for intervention in chronic metabolic diseases.

Reference:

Chen, M., Mason, R.P., and Tulenko, T.N. (1995). Atherosclerosis alters the composition, structure and function of arterial smooth muscle cell plasma membranes. Biochim Biophys Acta *1272*, 101-112.

Puri, P., Baillie, R.A., Wiest, M.M., Mirshahi, F., Choudhury, J., Cheung, O., Sargeant, C., Contos, M.J., and Sanyal, A.J. (2007). A lipidomic analysis of nonalcoholic fatty liver disease. Hepatology *46*, 1081-1090.

Rong, X., Albert, C.J., Hong, C., Duerr, M.A., Chamberlain, B.T., Tarling, E.J., Ito, A., Gao, J., Wang, B., Edwards, P.A., et al. (2013). LXRs regulate ER stress and inflammation through dynamic modulation of membrane phospholipid composition. Cell Metab *18*, 685-697.

Rong, X., Wang, B., Dunham, M.M., Hedde, P.N., Wong, J.S., Gratton, E., Young, S.G., Ford, D.A., and Tontonoz, P. (2015). Lpcat3-dependent production of arachidonoyl phospholipids is a key determinant of triglyceride secretion. Elife *4*.

Singer, S.J., and Nicolson, G.L. (1972). The fluid mosaic model of the structure of cell membranes. Science *175*, 720-731.